May 2015

contact: qualif@mercator-ocean.fr

QuO Va Dis?
Quarterly Ocean Validation Display #18

Validation bulletin for July-August-September (JAS) 2014

Edition:
Bruno Levier, Marie Drévillon, Charly Régnier, Charles Desportes, Coralie Perruche,
(MERCATOR OCEAN/Production Dep./Products Quality)

Contributions :
Eric Greiner (CLS)
Jean-Michel Lellouche, Olivier Le Galloudec (MERCATOR OCEAN/ Production Dep./R&D)

Credits for validation methodology and tools:
Eric Greiner, Mounir Benkiran, Nathalie Verbrugge, Hélène Etienne (CLS)
Fabrice Hernandez, Laurence Crosnier (MERCATOR OCEAN)
Nicolas Ferry, Gilles Garric, Jean-Michel Lellouche (MERCATOR OCEAN)
Stéphane Law Chune (Météo-France), Julien Paul (Links), Lionel Zawadzki (AS+)
Jean-Marc Molines (LGGE), Sébastien Theeten (Ifremer), Mélanie Juza (IMEDEA), the DRAKKAR and NEMO groups, the BCG group (Météo-France, CERFACS)
Bruno Blanke, Nicolas Grima, Rob Scott (LPO)

Information on input data:
Christine Boone, Gaël Nicolas (CLS/ARMOR team)

Abstract

*This bulletin gives an estimate of the accuracy of MERCATOR OCEAN's analyses and forecast for the season of **July-August-September 2014**. It also provides a summary of useful information on the context of the production for this period. Diagnostics will be displayed for the global 1/12° (PSY4), global ¼° (PSY3), the Atlantic and Mediterranean zoom at 1/12° (PSY2), and the Iberia-Biscay-Ireland (IBI) monitoring and forecasting systems currently producing daily 3D temperature, salinity and current products. Surface Chlorophyll concentrations from the BIOMER1 biogeochemical monitoring and forecasting system are also displayed and compared with simultaneous observations. Finally the new release of BIOMER at ¼° horizontal resolution is introduced. The BIOMER4 products, available since September 2014, are shortly evaluated against the BIOMER1 products.*

Table of contents

I Executive summary

T & S

The Mercator Ocean monitoring and forecasting systems are evaluated for the **period July-August-September 2014**. The 1/12° global system providing products for MyOcean V3 global MFC, and the other Mercator "off shore" systems (global ¼° and Atlantic+Mediterranean 1/12°) display similar performance in terms of water masses accuracy. The system's analysis of the **ocean water masses is very accurate on global average** and almost everywhere between the bottom and 200m. Between 0 and 500m departures from *in situ* observations **rarely exceed 1 °C and 0.2 psu** (mostly in high variability regions like the Gulf Stream or the Eastern Tropical Pacific). PSY4 is warmer (and less accurate) than PSY3 in the 0-800 m layer this quarter which could be due to spin up effects. The evolution of this difference between the global systems will be monitored in the next issues.

The temperature and salinity forecast have **significant skill** in many regions of the ocean in the 0-500m layer, but the signal is noisy.

Surface fields: SST, SSS, SSH, currents

A **warm SST bias** of 0.1 °C on global average is diagnosed this quarter, mainly due to the tropics and the ACC. The SST bias is cold in the mid latitudes and in the Arctic.

A **strong fresh bias is diagnosed in the tropics, especially in the high resolution products** in link with the overestimated convective precipitations in the ECMWF atmospheric fields.

The monitoring systems are generally very close to altimetric observations (global average of 6 cm residual RMS error). Biases persist locally that correspond to known uncertainties in the mean dynamic topography (for instance in the Indonesian region).

The **surface currents are underestimated in the mid latitudes and overestimated at the equator** with respect to *in situ* measurements of drifting buoys (drifter velocities are corrected of windage and slippage with a method developed by Mercator Océan). The underestimation ranges from 20% in strong currents up to 60% in weak currents. On the contrary the orientation of the current vectors is well represented**.** Lagrangian metrics show that after 1 day, 80% of the virtual drifters trajectories performed with Mercator Ocean forecast velocities stay within a 25 km distance of the actual drifters observed trajectories.

Regional North East Atlantic

The high resolution North East Atlantic at 1/36° (IBI36V1) with no data assimilation is accurate on average. **Tidal and residual sea surface elevations are well represented**. Zones of intense tidal mixing are less accurate. The mixed layer is too shallow in the Bay of Biscay (the thermocline is too diffusive). The upwelling along the Iberian coasts is underestimated.

Sea Ice

Sea ice observations are not yet assimilated, nevertheless sea ice concentrations are realistic. In JAS 2014 the sea ice melts too much in the Arctic, but the sea ice extent is still well diagnosed. In the Antarctic the sea ice cover is overestimated (too much ice during austral winter).

Biogeochemistry

The **large scale structures corresponding to specific biogeographic regions** (double-gyres, ACC, etc…) **are well reproduced** by the global biogeochemical model at 1° BIOMER1. However there are **serious discrepancies especially in the Tropical band** due to overestimated vertical velocities. The latter are the source of anomalous levels of nitrates in the equatorial surface layer. O2, however, is close to climatological estimations. The seasonal cycle is realistic in most parts of the ocean. However **the timing of the blooms is not yet in phase with observations**. This quarter, the North Atlantic bloom is still present in the observations while it has already disappeared in BIOMER1 (the bloom is between one and two months ahead of the observations and is shorter than in the observations).

II Status and evolutions of the systems

II.1. Short description and current status of the systems

A bit of history

PSY3V3 (global ¼°) and PSY2V4 (Altantic and Mediterranean 1/12°) systems have been operated at MERCATOR OCEAN since 2010 December, 15th. These systems provide the version 1 (PSY3V3*R1*/PSY2V4*R1, see QuOVaDis?* #2) and version 2 (PSY3V3*R1*/PSY2V4*R2, see QuOVaDis?* #5) products of the MyOcean global monitoring and forecasting centre. As reminded in table 1 (and illustrated for PSY2V2 in Figure 1) the atmospheric forcing is updated daily with the latest ECMWF analysis and forecast, and a new oceanic forecast is run every day for both PSY3V3R1 and PSY2V4R2.

The PSY3V3R1 system is started in October 2006 from a 3D climatology of temperature and salinity (World Ocean Atlas Levitus 2005) while the PSY2V4R2 is started in October 2009. After a short 3-month spin up of the model and data assimilation, the performance of PSY3V3R1 has been evaluated on the 2007-2009 period (MyOcean internal calibration report, which results are synthesised in *QuOVaDis?* #2).

The PSY4 system (global 1/12°) is delivering operational products since the beginning of 2010, and was developed in 2009. Its first version PSY4V1 did not benefit from the scientific improvements of PSY3V3R1 and PSY2V4R2, developed in 2010 and 2011. This system delivers 7-day forecast (and not 14-day like PSY3V3R1 and PSY2V4R2).

An upgrade of the data assimilation systems was performed in March 2012 in order to assimilate MyOcean V2 altimetric observations and in situ observations (instead of respectively AVISO and CORIOLIS observations, corresponding to MyOcean V0 observations). In consequence, more in situ observations are assimilated by all systems in the European seas since March 2012.

Current global systems

The whole Mercator Ocean global analysis and forecasting system (including PSY4, PSY2 and PSY3) has been updated in April 2013 (MyOcean products version 3). **The current versions names are PSY3V3R3, PSY2V4R4 and PSY4V2R2. Results from these current systems only**

will be described in this issue. For more simplicity they will be called PSY3, PSY2 and PSY4 in this document. A description of most updates, as well as the evaluation process, can be found in Lellouche et al (2013)[1]. With respect to this article, several additional modifications were made in order to stabilize the performance of the system (see table 1). A specific paragraph is dedicated to the evaluation of these new systems: in Quo Va Dis?#12.

North east Atlantic

The IBI36 system is described in QuOVaDis? #5 and #6 (see also table 1 and Figure 1). The nominal MyOcean production unit for IBI36 is Puertos Del Estado (Spain) while Mercator Océan produces the back up products. The Mercator Océan IBI36V1 system was officially operational in June 2011. The version IBI36V2 of the system was operated from December 2011 to April 2014 and was very similar to IBI36V1 except it used realistic river runoffs from SHMI and Prévimer instead of climatological runoffs. The version IBI36V4 of the system is operated since April 2014: the only difference with IBI36V2 is the switch of the NEMO code version, from 2.3 to 3.4. There are however minor code upgrades. The leapfrog time stepping scheme of 3d variables has been modified according to the work of Leclair and Madec (2009)[2]; this should have a small impact on the results. The computation of coriolis terms in the barotropic equations has been corrected in order to be fully compliant with the 3d calculation. The locally enhanced bottom friction in the Gulf of Cadiz implemented in IBI-V3 has been suppressed, since this leads to a relatively minor improvement of Mediterranean overflow.

[1] J.-M. Lellouche, O. Le Galloudec, M. Drévillon, C. Régnier, E. Greiner, G. Garric, N. Ferry, C. Desportes, C.-E. Testut, C. Bricaud, R. Bourdallé-Badie, B. Tranchant, M. Benkiran, Y. Drillet, A. Daudin, and C. De Nicola, Evaluation of global monitoring and forecasting systems at Mercator Océan, Ocean Sci., 9, 57-81, 2013, www.ocean-sci.net/9/57/2013/, doi:10.5194/os-9-57-2013

[2] M. Leclerc, G. Madec, A conservative Leap-Frog time stepping method, Ocean Modelling 30(2-3), 88-94, 2009, http://dx.doi.org/10.1016/j.ocemod.2009.06.006

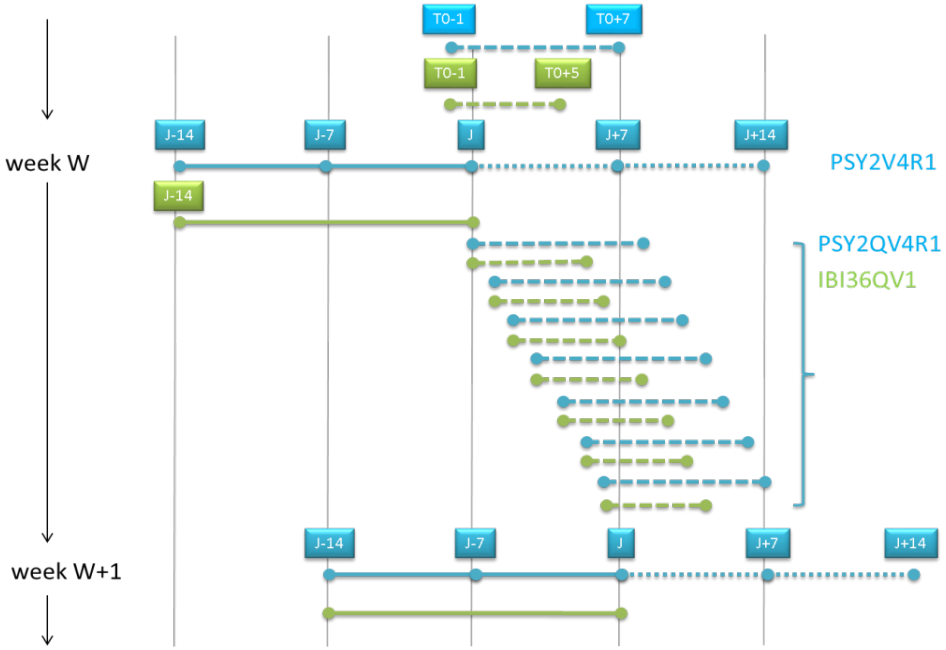

Figure 1: schematic of the operational forecast scenario for IBI36Q (green) and PSY2Q (blue). Solid lines are the PSY2 weekly hindcast and nowcast experiments, and the IBI36 spin up. Dotted lines are the weekly 14-day forecast, dashed lines are daily updates of the ocean forecast forced with the latest ECMWF atmospheric analysis and forecast. The operational scenario of PSY3, PSY4 and PSY3Q, PSY4Q is similar to PSY2's scenario. In the case of PSY4, only weekly hindcast, nowcast and 7-day forecast are performed.

Biogeochemistry

The BIOMER1 system is described in QuOVaDis? #6 (see also table 1 and Figure 2). It is a global hindcast biogeochemical model forced by physical ocean fields. The biogeochemical model used is PISCES. The coupling between ocean physics and biogeochemistry is performed offline. The physical fields from PSY3 are "degraded" to 1° horizontal resolution and 7-day time resolution.

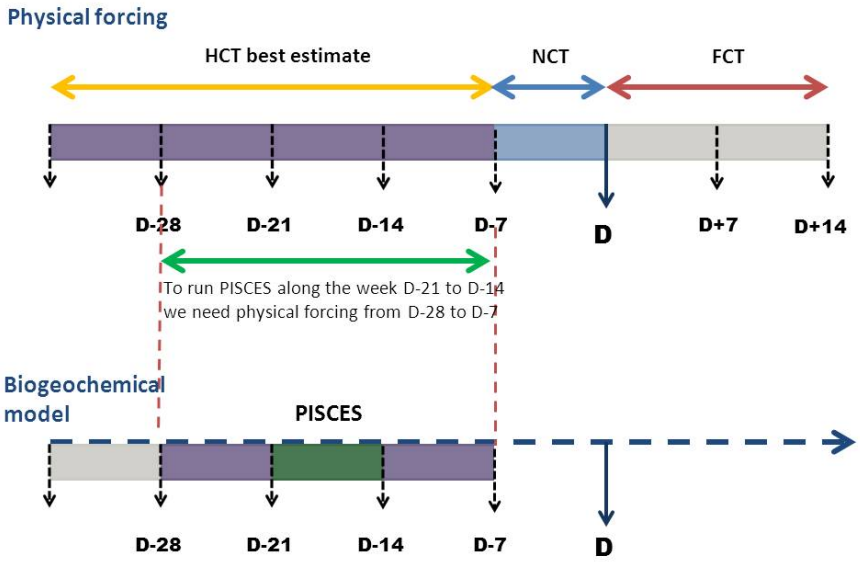

Figure 2: schematic of the operational forecast scenario for BIOMER..

System name	domain	resolution	Physical Model	Assimilation	Assimilated observations	Inter dependencies	Status of production
PSY4V1R3 (operational in JFM 2013) PSY4V2R2 (operational in AMJ 2013)	Global	1/12° on the horizontal, 50 levels on the vertical	ORCA12 LIM2 NEMO 1.09 Bulk CLIO 24-h atmospheric forcing LIM2 EVP NEMO 3.1 Bulk CORE 3-h atmospheric forcing mix, colour, iceberg, EMP init WOA09: oct 2012	SAM2V1 (SEEK) + IAU 3D-Var bias correction coast error, shelf error new MDT, radii Increase of Envisat error new QC, SST bulk corr	RTG-SST, MyOcean SLA along track, MyOcean T/S vertical profiles AVHRR-AMSR SST, new MDT Sea Mammals T/S profiles in CUTRR Black Sea SLA files		Weekly 7-day forecast Weekly 7-day forecast Daily update of atmospheric forcing for daily 7-day forecast
PSY3V3R1 (operational in JFM 2013) PSY3V3R2 (described in Lellouche et al, 2013) PSY3V3R3 (operational in AMJ 2013)	Global	1/4° on the horizontal, 50 levels on the vertical	ORCA025 LIM2 EVP NEMO 3.1 Bulk CORE 3-h atmospheric forcing mix, colour, iceberg, EMP flux corr no flux corr current in wind init WOA09:oct 2006	SAM2V1 (SEEK) + IAU 3D-Var bias correction coast error, shelf error MDT error adjusted first update of radii Increase of Envisat error new QC radii, SST bulk corr	RTG-SST, MyOcean SLA along track, MyOcean T/S vertical profiles AVHRR-AMSR SST, new MDT Sea Mammals T/S profiles in CUTRR Black Sea SLA files		Weekly 14-day forecast Daily update of atmospheric forcing for daily 7-day forecast
PSY2V4R2 (operational in JFM 2013) PSY2V4R3 (described in Lellouche et al., 2013) PSY2V4R4 (operational in AMJ 2013)	Tropical North Atlantic Mediterranean	1/12° on the horizontal, 50 levels on the vertical	NATL12 LIM2 EVP NEMO 3.1 Bulk CORE 3-h atmospheric forcing mix, colour flux corr no flux corr current in wind init WOA09:oct 2006	SAM2V1 (SEEK) + IAU 3D-3D-Var bias correction coast error, shelf error first update of radii Increase of Envisat error QC on T/S vertical profiles radii, SST bulk corr Larger weight of Bogus OBC on TSUV	AVHRR-AMSR SST, MyOcean SLA along track , MyOcean T/S vertical profiles new MDT Sea Mammals T/S profiles in CUTRR	OBC from PSY3V3R1 OBC and SMEMP from PSY3V3R2 OBC and SMEMP from PSY3V3R3	Weekly 14-day forecast Daily update of atmospheric forcing for daily 7-day forecast
BIOMER1 upgrade in AMJ 2013	Global	1° on the horizontal, 50 levels on the vertical	PISCES, NEMO 2.3, offline	none	none	Two weeks hindcast with PSY3V3R1 1° phy PSY3V3R3 1° phy	1-week average two weeks back in time.
IBI36V4 upgrade in AMJ 2014	North East Atlantic and West Mediterranean Sea (Iberian, Biscay and Ireland) region	1/36° on the horizontal, 50 levels on the vertical	NEATL36 NEMO 3.4 3-hourly atmospheric forcing from ECMWF, bulk CORE, tides, time-splitting, GLS vertical mixing, corrected bathymetry, river runoffs from SMHI & Prévimer	none	none	Two weeks spin up initialized with PSY2V4R4 and OBC from PSY2V4R4	Weekly spin up two weeks back in time. Daily update of atmospheric forcings for daily 5-day forecast IBI36QV1

Table 1: Main characteristics and latest updates of the Mercator Ocean global analysis and forecasting systems. The systems studied in Lellouche et al (2013) include the main characteristics (in black) plus the updates in blue. The 2013 systems (in red) include the main characteristics (in black) plus the updates in blue and red. In the legend below one can find a description of the updates referred to as "mix", "colour", etc…

Mix = New parameterization of vertical mixing
Colour = Taking into account ocean colour monthly climatology for depth of light extinction
Current in wind = taking 50 % of surface current for the computation of wind stress with bulk CORE
EMP = Adding seasonal cycle for surface mass budget
SMEMP = spatial mean EMP correction
Iceberg = Adding runoff for iceberg melting
Flux corr = Large scale correction to the downward radiative and precipitation fluxes
Coast error = Observation error s higher near the coast (SST and SLA)
Shelf error = Observation error s higher on continental shelves (SLA)

New MDT = MDT CNES/CLS09 adjusted with model solutions (bias corrected)
Radii = New correlation radii (minimum =130km)
New QC = additional QC on T/S vertical profiles computed from the innovations
SST bulk corr = Procedure to avoid the damping of SST increments via the bulk forcing function
OBC = Open Boundary Conditions
1° phy= physical forcings are "degraded" from ¼° horizontal resolution to 1° horizontal resolution, and weekly averaged.
CUTRR= Catch Up to Real Time Run, or calibration hindcast run (before 2013)

II.2. Incidents in the course of JAS 2014

Nothing to report.

III Summary of the availability and quality control of the input data

III.1. Observations available for data assimilation

III.1.1. In situ observations of T/S profiles

System	PSY3V3R3	PSY4V2R2	PSY2V4R4
Min/max number of T profiles per DA cycle	2600/3200	2600/3200	500/900
Min/max number of S profiles per DA cycle	2200/2600	2200/2600	500/600

Table 2: minimum and maximum number of observations (orders of magnitude of vertical profiles) of subsurface temperature and salinity assimilated weekly in JAS 2014 by the Mercator Ocean monitoring and forecasting systems.

The maximum number of in situ observations is displayed in Table 2. It is unchanged with respect to the previous quarter.

III.1.2. Sea Surface Temperature

System	PSY3V3R3	PSY4V2R2	PSY2V4R42
Min/max number (in 10^3) of SST observations	140/148	143/148	27/27

Table 3: minimum and maximum number (orders of magnitude in thousands) of SST observations (from Reynolds AVHRR ¼°) assimilated weekly in JAS 2014 by the Mercator Ocean monitoring and forecasting systems.

III.1.3. Sea level anomalies along track

As shown in Table 4 the data assimilated this JAS 2014 season come from Jason 2, Cryosat 2, SARAL/AltiKa and HY-2A.

system	PSY3V3R3	PSY4V2R2	PSY2V4R4
Min/max number (in 10^3) of Jason 2 SLA observations	159/164	160/165	29/31
Min/max number (in 10^3) of HY-2A SLA observations	37/154	37/156	7/29
Min/max number (in 10^3) of AltiKa SLA observations	156/159	157/161	30/31
Min/max number (in 10^3) of Cryosat 2 SLA observations	22/148	22/149	4/27

Table 4: minimum and maximum number (orders of magnitude in thousands) of SLA observations from Jason 2, Cryosat 2, AltiKa and HY-2A assimilated weekly in JAS 2014 by the Mercator Ocean monitoring and forecasting systems.

III.2. Observations available for validation

Both observational data and statistical combinations of observations are used for the real time validation of the products. All were available in real time during the JAS 2014 season:

- T/S profiles from CORIOLIS
- OSTIA SST from UKMO
- Arctic sea ice concentration and drift from CERSAT
- SURCOUF surface currents from CLS
- ARMOR-3D 3D temperature and salinity fields from CLS
- Drifters velocities from Météo-France reprocessed by CLS
- Tide gauges

Grodsky et al (GRL, May 2011) show that drifters' velocities overestimate current velocities in regions and periods of strong winds due to undetected undrogued drifters. This information will be taken into account for comparisons with Mercator Ocean currents.

IV Information on the large scale climatic conditions

Mercator Ocean participates in the monthly seasonal forecast expertise at Météo France. This chapter summarizes the state of the ocean and atmosphere during the JAS 2014 season, as discussed in the "Bulletin Climatique Global" of Météo France.

The equatorial pacific is still slightly warmer than normal. However, the ENSO conditions were neutral in JAS 2014. No significant kelvin wave propagation is diagnosed in the seasonal mean JAS 2014 as can be seen in **Figure 4**.

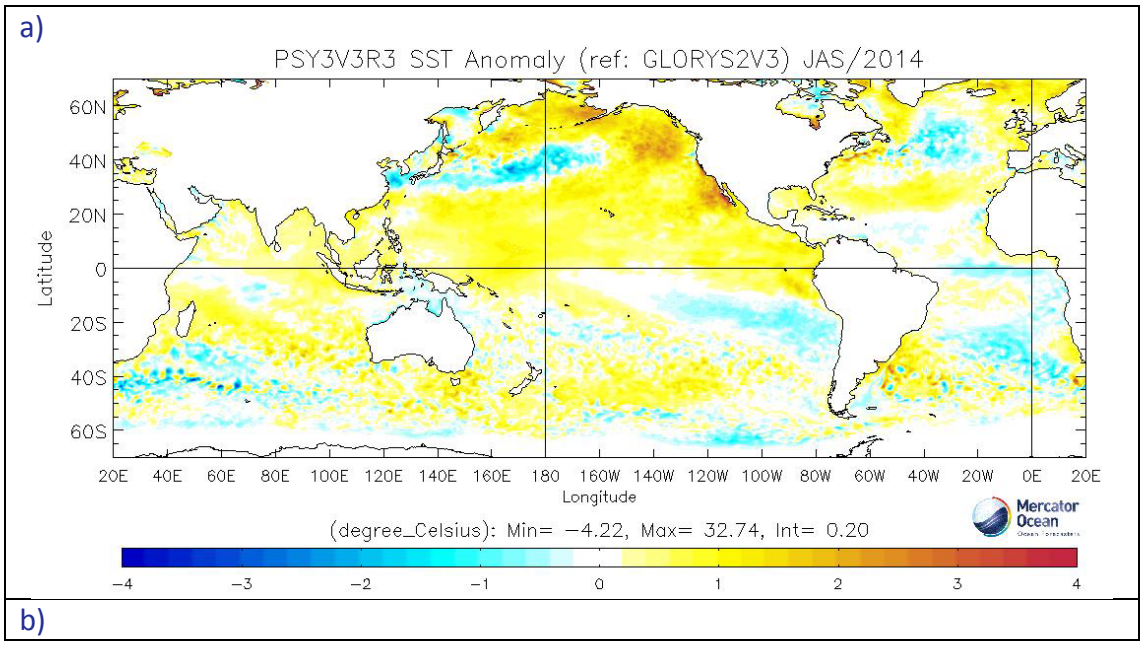

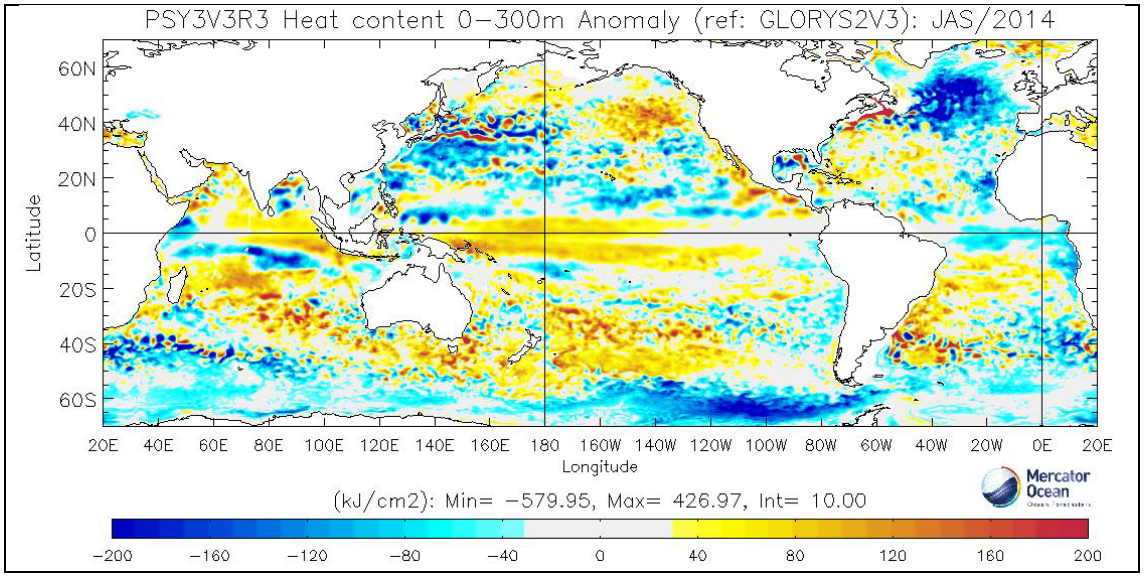

Figure 3: Seasonal JAS 2014 temperature anomalies with respect to GLORYS2V3 climatology (1993-2011). (a): SST anomaly (°C) at the global scale from the 1/4° ocean monitoring and forecasting system PSY3V3R3. (b): heat content anomaly ($\rho_0 C_p \Delta T$, with constant ρ_0=1020 kg/m3) from the surface to 300m.

In the North Atlantic, a warm anomaly dominates the Irminger and North Sea. Between the subpolar gyre and the subtropical gyre, a cold anomaly persists throughout the season crossing the Atlantic from Newfoundland to the Bay of Biscay, which is well marked in the upper ocean heat content. The subtropical gyre is warmer than normal while the tropical North Atlantic is colder than normal. The atmospheric circulation in the North Atlantic was dominated alternatively by the Scandinavian blocking pattern, negative NAO and East Atlantic West Russia patterns during this JAS season. These circulation patterns are consistent with the persistence of warm anomalies in the northern sub basins of the Atlantic (Labrador Sea, North Sea).

The signature of the positive phase of the PDO is well marked in the North Pacific basin, with large positive anomalies along the west coast of the US, coincident with severe heat and droughts in this area.

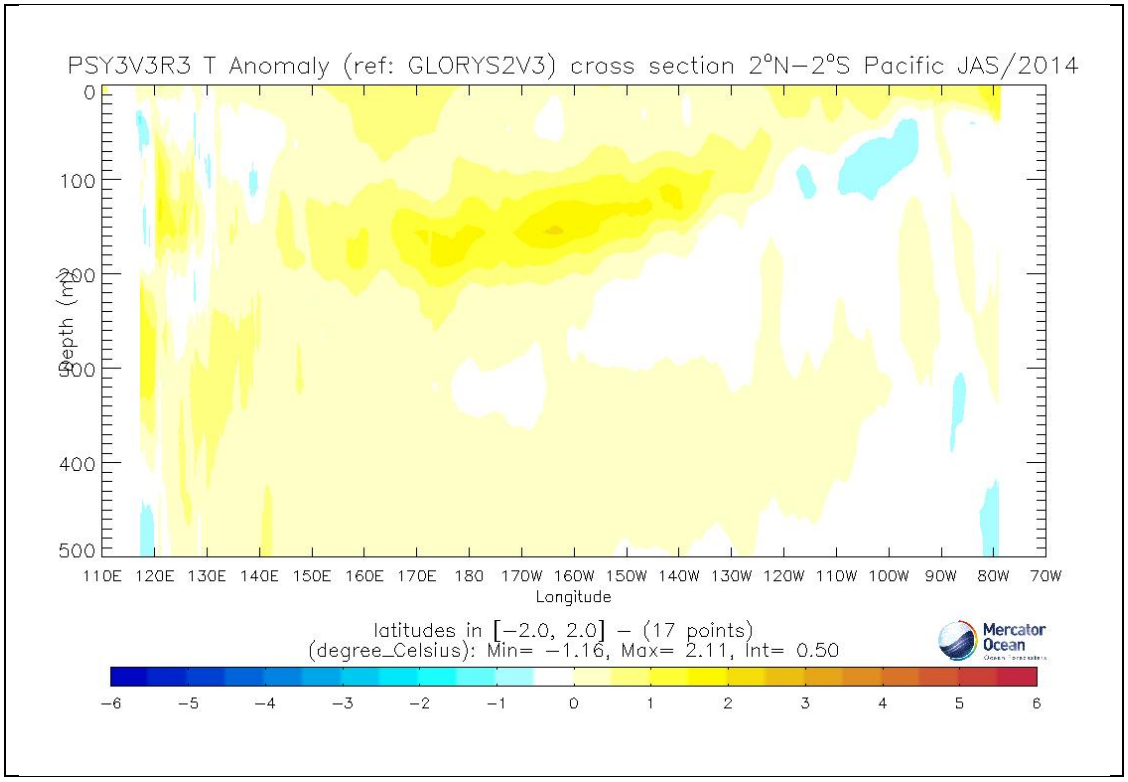

Figure 4: Seasonal JAS 2014 temperature anomaly (°C) with respect to GLORYS2V3 climatology (1993-2011), vertical section 2°S-2°N mean, Pacific Ocean, PSY3V3R3.

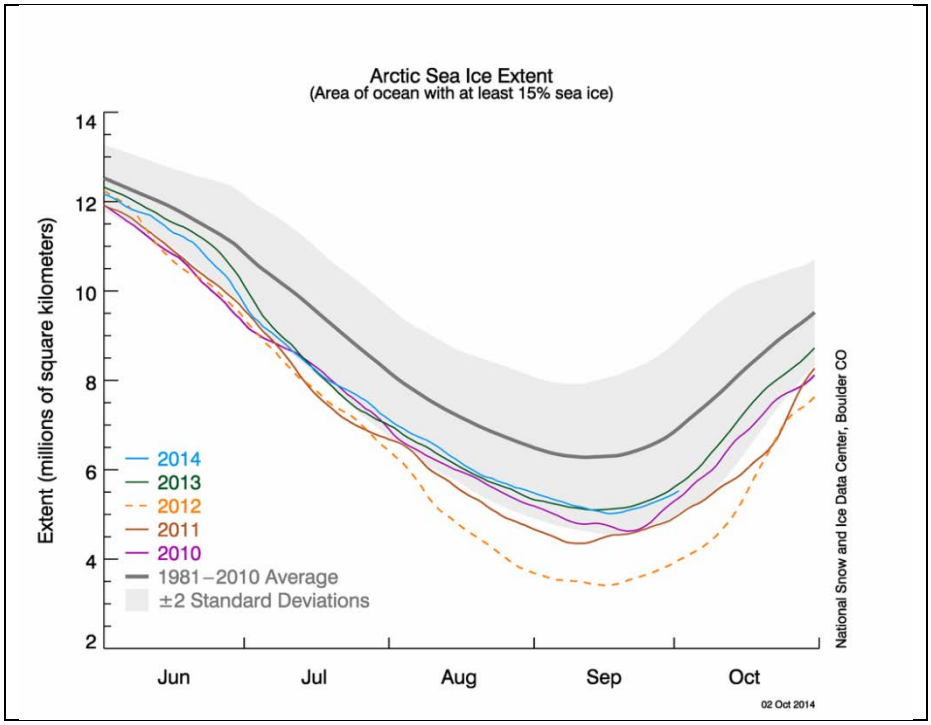

Figure 5 : Arctic sea ice extent from the NSIDC, available at http://nsidc.org/arcticseaicenews/2014/10/

As can be seen in Figure 5, the Arctic sea ice minimum in JAS 2014 is lower than that of 2013, but does not reach the lowest extent measured in 2012. The seasonal ice loss of 2014 is the 9th largest of satellite records, according to NSIDC.

V Accuracy of the products

V.1. Data assimilation performance

V.1.1. Sea surface height

V.1.1.1. Basin scale statistics (GODAE metrics)

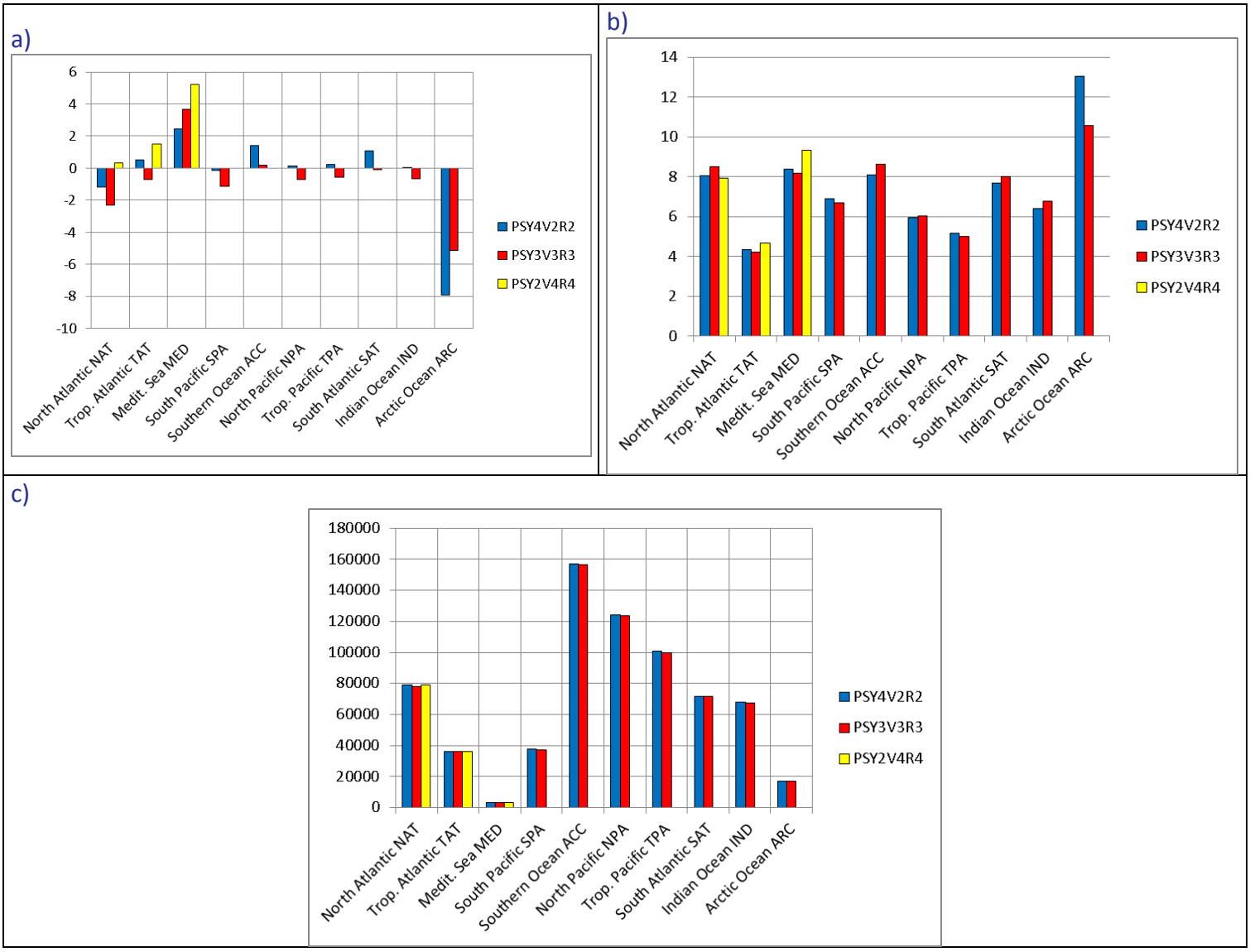

Figure 6 : Comparison between SLA data assimilation scores (a: average misfit in cm, b: RMS misfit in cm, c: number of observations) for all available Mercator Ocean systems in JAS 2014. The scores are averaged for all available satellite along track data (Saral/altiKa, Jason 2, Cryosat 2, HY-2a). For each region the bars refer to PSY2V4R4 (yellow), PSY3V3R3 (red), and PSY4V2R2 (blue).

SLA assimilation scores for PSY4, PSY3, and PSY2 in JAS 2014 are displayed in Figure 6. The different systems reach similar levels of performance on average. The basin scale SLA bias does not exceed 2 cm except in the Mediterranean Sea and in the Arctic where it can reach 8 cm (Figure 6 a). The Arctic SSH undergoes large uncertainties (MSSH, measurement errors, sea ice limit). In the Mediterranean Sea this quarter, the global systems (PSY4 and PSY3) are less biased than the regional system (PSY2). The RMS error (Figure 6 b) is of the order of 8-9 cm in the Mediterranean Sea, in the Atlantic and the Southern Oceans (more than 10 cm in the Arctic). It is of the order of 6-7 cm in the Indian and Pacific oceans, and it is close

to 4 cm in the Tropical Atlantic Ocean and 5 cm in the Tropical Pacific Ocean. The error amplitude is proportional to the region's internal variability.

V.1.1.2. North Atlantic Ocean and Mediterranean Sea in all systems

The SLA assimilation scores for PSY4, PSY3, and PSY2 in JAS 2014 are displayed for sub-regions of the Tropical and North Atlantic Ocean in Figure 7. The different systems reach identical levels of performance on average. The biases are generally small (less than 2 cm) during the summer season and do not exceed 3 cm in JAS 2014.

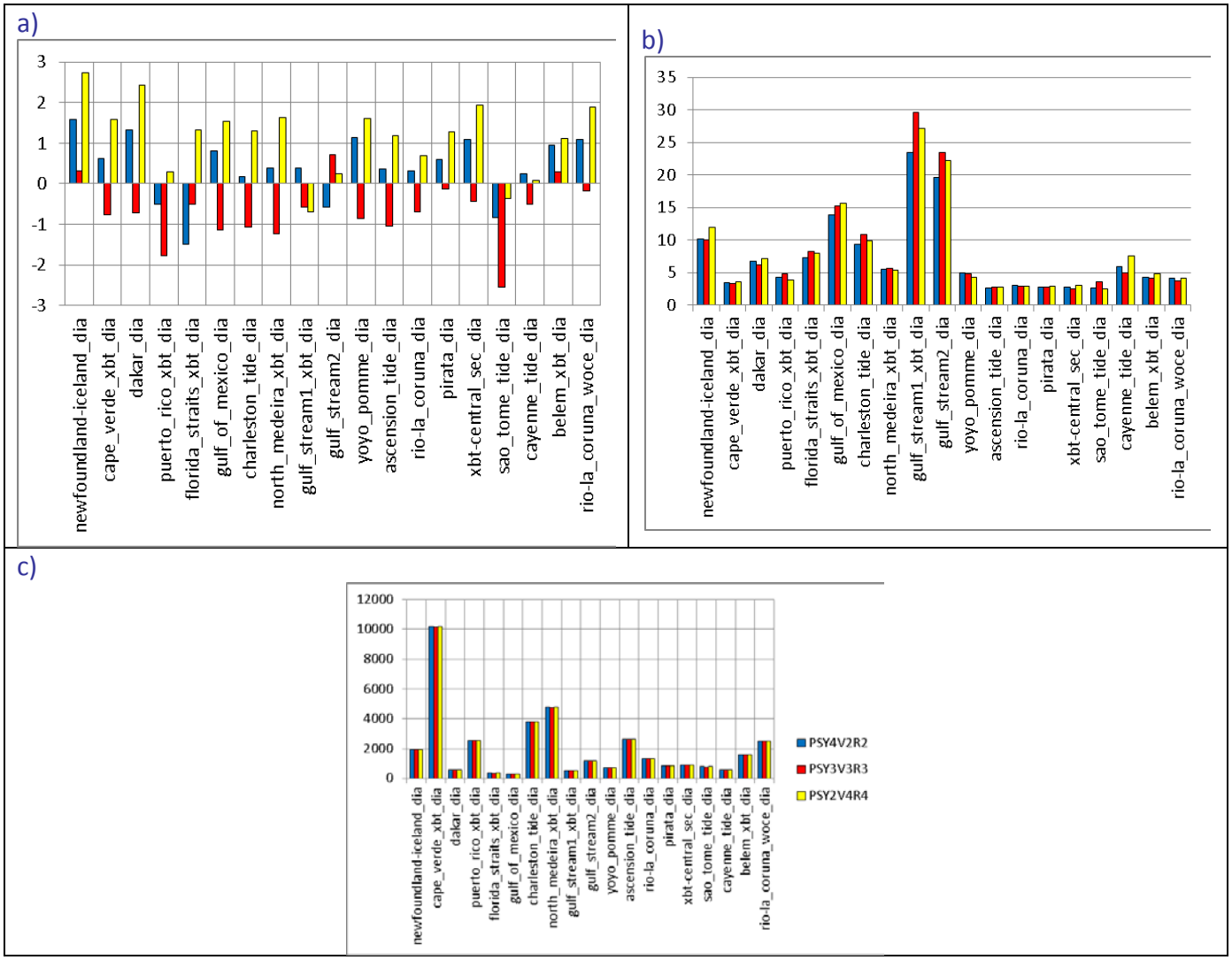

Figure 7: Comparison between SLA data assimilation scores (a: average misfit in cm, b: RMS misfit in cm, c: number of observations) for all available Mercator Ocean systems in JAS 2014 in sub-regions of the Tropical Atlantic (TAT) and North Atlantic (NAT). The scores are averaged for all available satellite along track data (SARAL/Altika, Jason 2, Cryosat 2, HY-2a). For each region the bars refer respectively to PSY2V4R4 (yellow), PSY3V3R3 (red), and PSY4V2R2 (blue).

The RMS errors are almost identical in all systems, and stay below 10 cm in most regions, except regions of high mesoscale variability (Gulf Stream) and in the gulf of Mexico. This JAS 2014 season, the RMS error in the Gulf Stream regions is larger in PSY3 than in the other systems PSY2 and PSY4. PSY2 and PSY4 biases are small but positive in nearly all regions, meaning that PSY2 and PSY4 are slightly lower than the observations on average over the basin, consistently with Figure 6. On the contrary, PSY3 biases are negative in nearly all regions.

In the Mediterranean Sea (Figure 8), significant positive biases (the model is lower than the observations) appear in summer. PSY2 displays biases of 4 to 10 cm, while the global systems PSY3 and PSY4 present smaller biases of 1 to 6 cm. A bias of 10 cm is present in PSY2 in the Aegean Sea (it was nearly 12 cm in JAS 2013). The Mediterranean sub-regions are circled by coasts, and consequently few observations are assimilated. Figure 8 c gives the number of observations taken into account by the system, but the observation error that is applied reduces strongly the influence of observations within a 50 km distance of the coast.

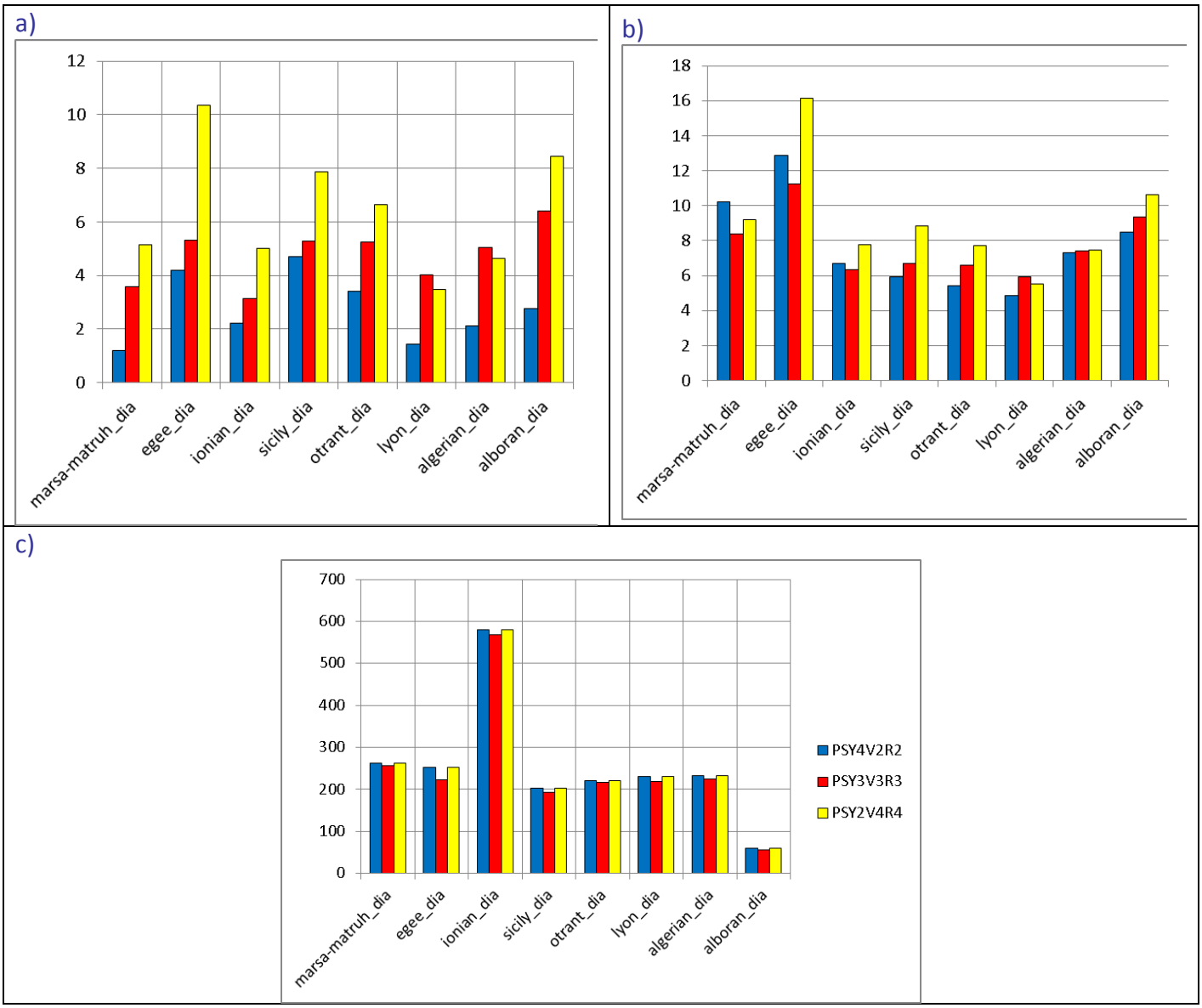

Figure 8: Comparison between SLA data assimilation scores (a: average misfit in cm, b: RMS misfit in cm, c: number of observations) for all available Mercator Ocean systems in JAS 2014 in the Mediterranean Sea MED sub-regions: PSY2V4R4 (yellow), PSY3V3R3 (red) and PSY4V2R2 (blue). The scores are averaged for all available satellite along track data (SARAL/Altika, Jason 2, Cryosat 2, HY-2a). See annex B for geographical location of regions.

One can also note that the variability in the Aegean Sea is difficult to model because of the presence of many islands. PSY4 may perform better in this region due to the presence of the Black sea in the global configuration PSY4, which is not present in PSY2. Except in the Aegean Sea, the RMS of the innovation (misfit) is generally less than 10 cm for all systems.

V.1.1.3. Performance at global scale in PSY3 (1/4°) and PSY4 (1/12°)

Figure 9: Comparison between SLA data assimilation scores (a: average misfit in cm, b: RMS misfit in cm, c: number of observations) for all available global Mercator Ocean systems in JAS 2014 in sub-regions of the SAT, IND, NPA, SPA, TPA, and ACC basins: PSY3V3R3 (red) and PSY4V2R2 (blue). The scores are averaged for all available along track satellite data (SARAL/Altika, Jason 2, Cryosat 2, HY-2a). The geographical location of regions is displayed in annex B.

As can be seen in Figure 9 the performance of intermediate resolution global PSY3 and the performance of high resolution global PSY4 in terms of SLA assimilation are of the same order of magnitude. A small positive bias (less than 2 cm) is present in many regions in PSY4. A strong bias of around 10 cm persists in the "Nino 5" box centred on the Banda Sea in Indonesia, which corresponds to a MDT problem. The RMS error reaches its highest values in the Agulhas current where the variability is high (and in the Niño 5 box because of the strong bias). Other regions with high variability (eastern Australia, Southern Ocean) consistently display RMS errors of more than 8 cm.

V.1.2. Sea surface temperature

V.1.2.1. Basin scale statistics (GODAE metrics)

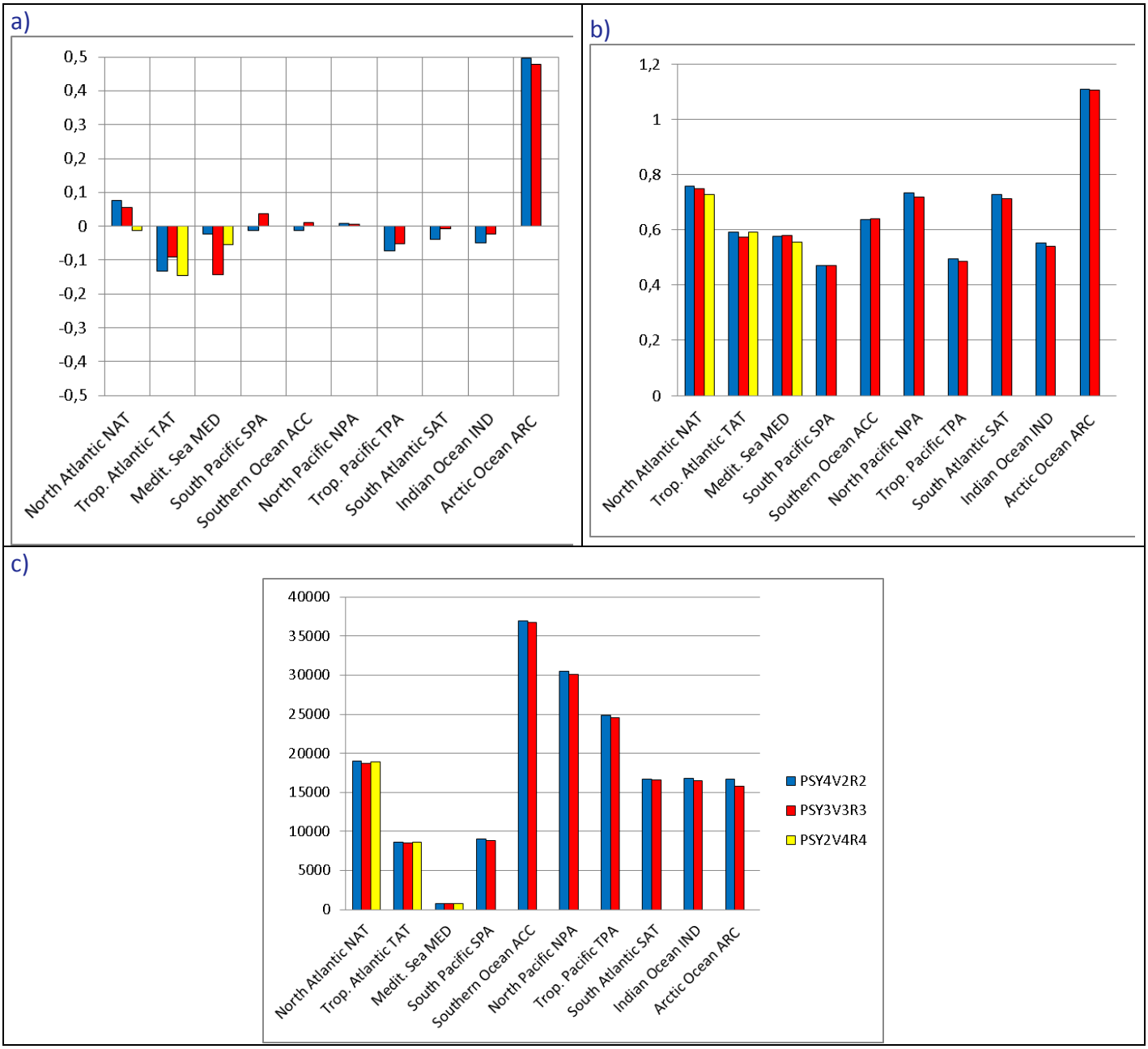

Figure 10: Comparison between Reynolds ¼°AVHRR-data assimilation scores (a: average misfit in °C, b: RMS misfit in °C, c: number of observations) for all available Mercator Ocean systems in JAS 2014: PSY4V2R2 (blue), PSY3V3R3 (red), and PSY2V4R4 (yellow).

This JAS season, a warm bias persists in all systems in most of the regions (Figure 10), except in the Arctic Ocean (colder (0.5 °C) than the observations) and in the North Atlantic. It is known that not enough Atlantic (warm) waters enter the Arctic in both PSY3 and PSY4. In parallel there is too much sea ice melting in the Arctic this summer season (see Figure 41 and Figure 42). The Mediterranean is warmer than the observations on average over the basin (0.1°C). The RMS error is lower than 0.8 °C except in the Arctic Ocean, where it reaches 1.1°C on average (due to the strong bias).

V.1.2.2. North and Tropical Atlantic Ocean and Mediterranean Sea

Figure 11: Comparison between Reynolds ¼°AVHRR SST data assimilation scores (a: average misfit in °C, b: RMS misfit in °C, c: number of observations) for all available Mercator Ocean systems in JAS 2014 in sub-regions of the Tropical Atlantic (TAT) and of the North Atlantic (NAT): PSY4V2R2 (blue), PSY3V3R3 (red) and PSY2V4R4 (yellow). The geographical location of regions is displayed in annex B.

In the Atlantic the three systems display consistent regional behaviours in terms of SST bias as illustrated in Figure 11. In most regions the bias stays below 0.3 °C. A warm bias of around 0.3 to 0.5°C is diagnosed in the Tropical Atlantic (Dakar, Gulf of Mexico, Florida straits, Sao Tome). In the Dakar region, the upwelling is underestimated by all systems. Note that as for SLA, prescribed SST errors are higher within 50km off the coast. The RMS error reaches 1°C in the Gulf Stream regions, and in the Newfoundland Iceland region.

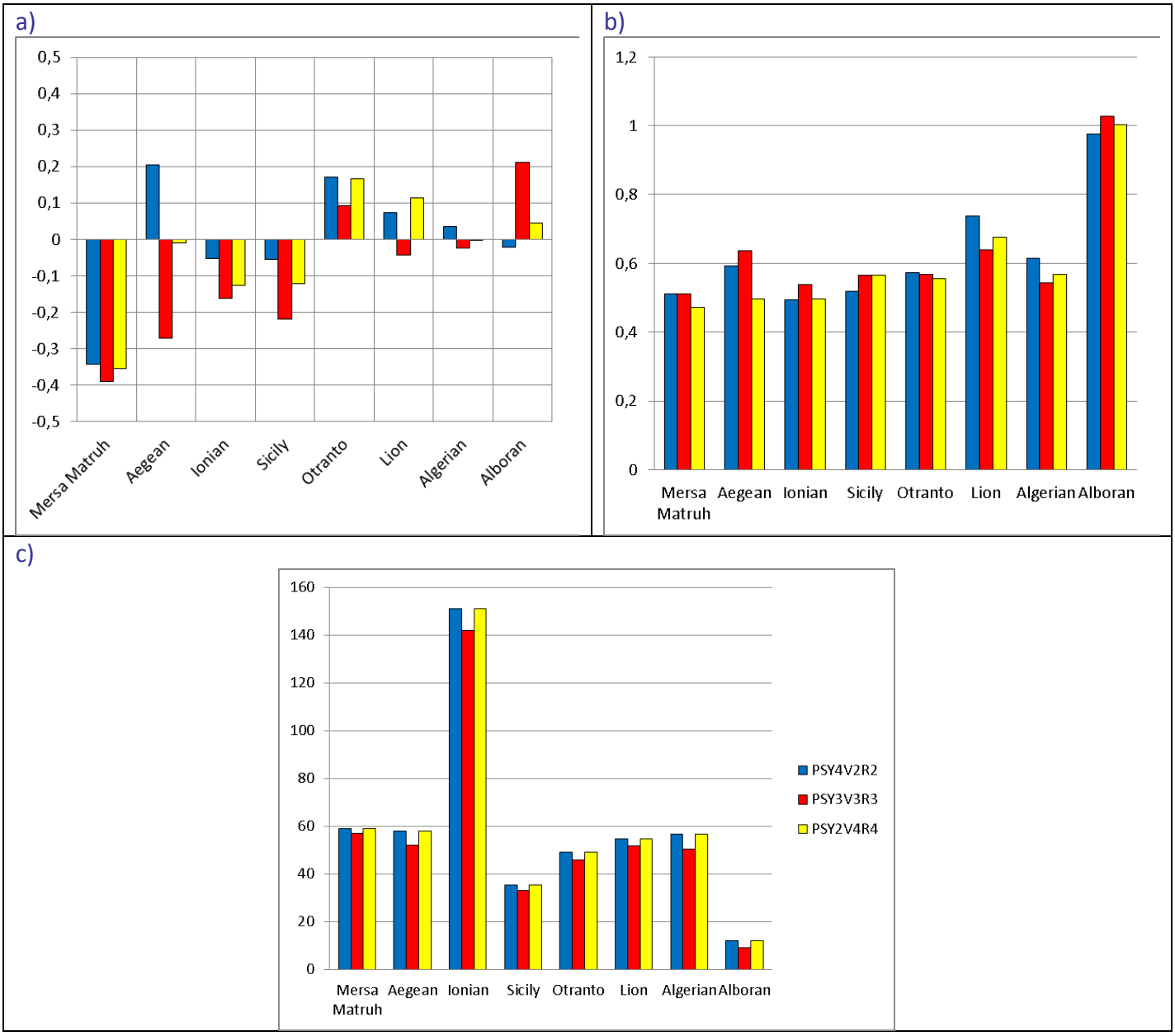

Figure 12: Comparison between Reynolds ¼° AVHRR SST data assimilation scores (a: average misfit in °C, b: RMS misfit in °C, c: number of observations) for all available Mercator Ocean systems in JAS 2014 in the Mediterranean Sea: PSY4V2R2 (blue), PSY3V3R3 (red) and PSY2V4R4 (yellow). The geographical location of regions is displayed in annex B.

This JAS 2014 season (Figure 12) is different from JAS 2013 (not shown). The maximum bias is found in the Mersa Matruth region (between 0.3 and 0.4°C). In the Aegan Sea PSY3 and PSY4 display opposite bias (the Black Sea is present in PSY4 and not in PSY3 which can explain this result). The RMS error is generally of the order of 0.5-0.7°. As in SLA, the performance of the systems is lower in the Aegean Sea. Errors are also higher in the Alboran Sea but one can note that not many observations are available in this small region.

V.1.2.3. Performance at global scale in PSY3 (1/4°) and PSY4 (1/12°)

Figure 13: Comparison between Reynolds ¼° AVHRR SST data assimilation scores (a: average misfit in °C, b: RMS misfit in °C, c: number of observations) for all available global Mercator Ocean systems in JAS 2014 in the SAT, NPA, TPA, SPA, IND and ACC basins: PSY3V3R3 (red) and PSY4V2R2 (blue). See annex B for geographical location of regions.

The global products exhibit a warm surface bias in most regions this JAS 2014 season (Figure 13), of magnitude 0.1°C to 0.3°C. This warm bias is stronger in (small) coastal regions: in the cold waters of the California current or in the Angola upwelling. In JAS, a cold bias (0.4°C) is diagnosed in the North Pacific region. PSY3 and PSY4 exhibit the same levels of performance. The warm bias is generally stronger in PSY4 than in PSY3 by 0.05°C, and so is the RMS error, meaning that the variability is at least as well represented in PSY4 than in PSY3. The RMS error stands between 0.4°C in the tropical Pacific, and 1°C in the Agulhas current.

V.1.3. Temperature and salinity profiles

V.1.3.1. Methodology

All systems innovation (**observation – model first guess**) profiles from the **hindcast or "best analysis" week (J-14 to J-7)** are systematically inter-compared in all regions given in annex B. In the following, intercomparison results are shown on the main regions of interest for Mercator Ocean users in JAS 2014. Some more regions are shown when interesting differences take place, or when the regional statistics illustrate the large scale behaviour of the systems.

V.1.3.1.1. Basin scale statistics (GODAE metrics)

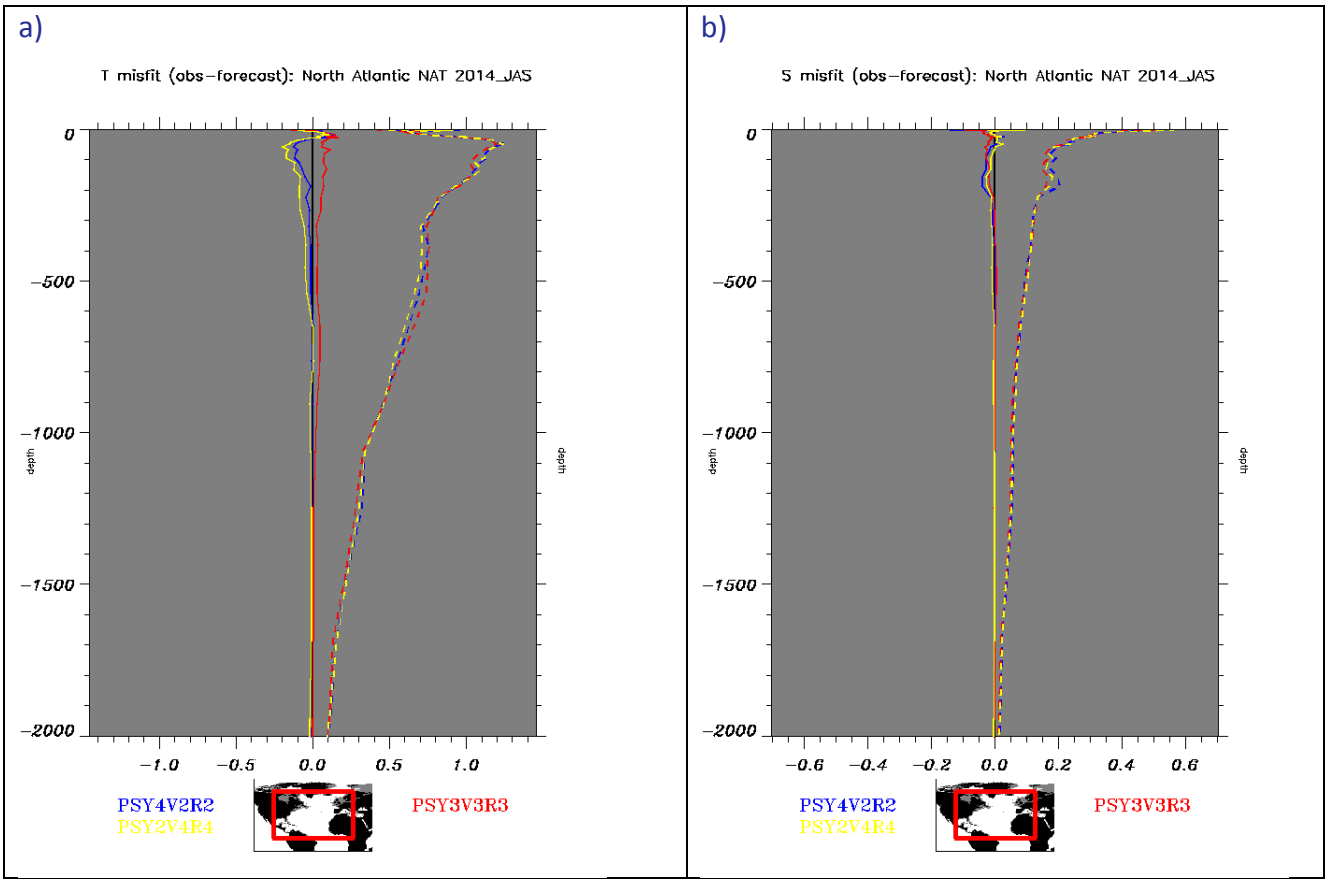

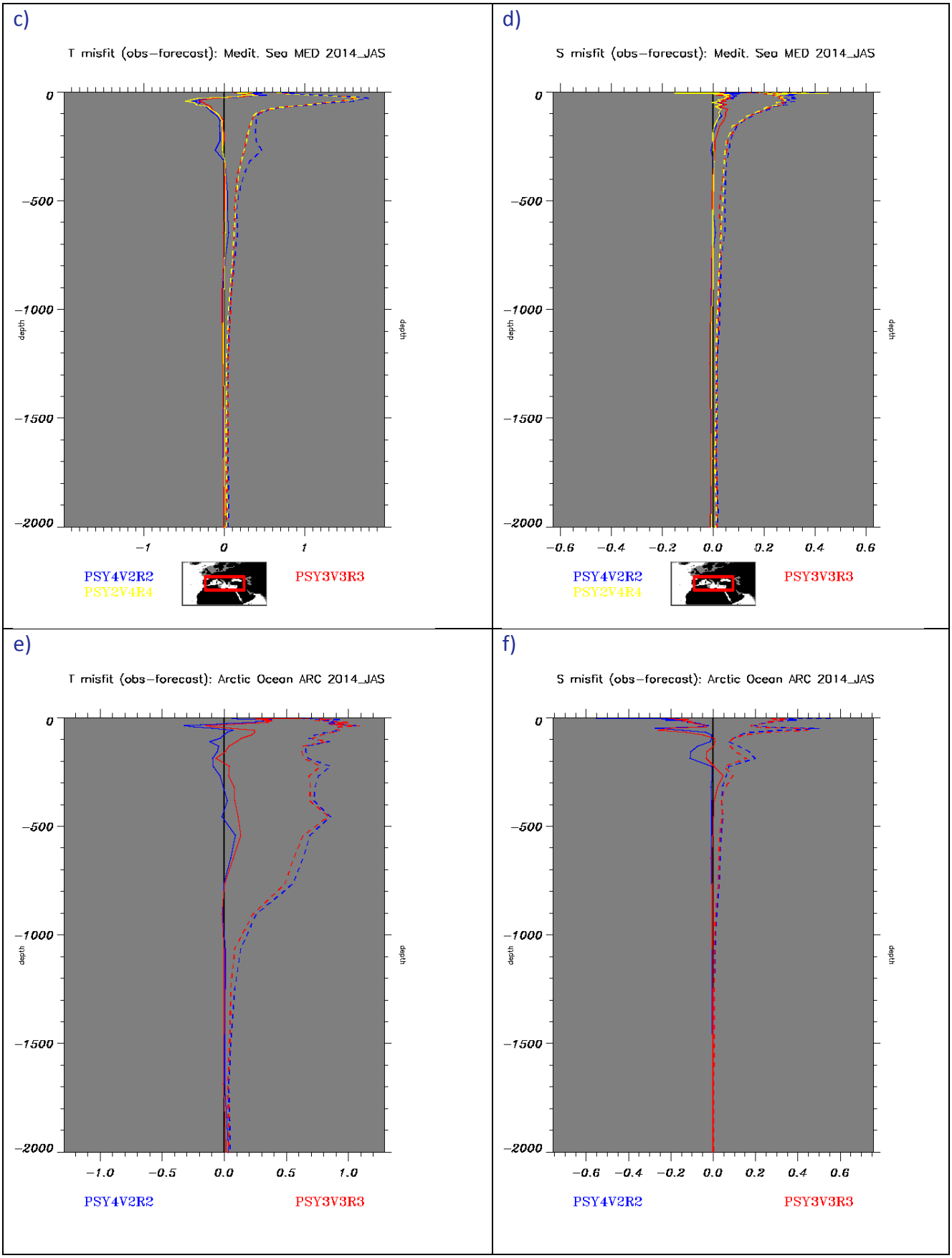

Figure 14: Profiles of JAS 2014 innovations of temperature (°C, left column) and salinity (psu, right column), mean (solid line) and RMS (dashed line) for PSY3V3R3 (red), PSY2V4R4 (yellow) and PSY4V1R3 (blue) in the North Atlantic NAT (a and b), Mediterranean Sea MED (c and d) and Arctic Ocean ARC (e and f, the region starts of north of 67°N). Basin masks are applied to keep only the main basin of interest (no Mediterranean in the Atlantic NAT, no Black Sea in the Mediterranean MED, etc…).

On average over the North Atlantic, PSY2 displays a warm bias from 50 m to 600 m (Figure 14). In PSY4 the warm bias is also present but with less amplitude. PSY3 displays a slightly cold bias between 50 m and 300 m. In the mean time, the salinity bias is very small in all systems. On average over the Mediterranean Sea, all systems display the same behaviour, with a cold and salty bias at the surface and a warm and fresh bias between 50 m and 200 m. In the Artic PSY3 displays a cold bias from 50 m to 800 m. In PSY4, the temperature bias is warm from 50 m to 400 m, and cold from 400 m to 800 m. PSY3 and PSY4 display a salty bias between surface and 300 m.

On average over the Tropical Atlantic basin the high resolution systems exhibit warm (0.1°C to 0.2°C) and salty (around 0.1 psu) biases in the 0-300m layer (Figure 15). No significant temperature or salinity biases appear underneath the surface layer. PSY3 performs slightly better in this region.
PSY3 is less biased than PSY4 as well in the South Atlantic Basin, where PSY4 is too warm in the 0-800 m layer (and PSY3 slightly too cold), and is too fresh at the surface. In the Indian Ocean PSY3 exhibits a cold bias from the surface to 1000 m (up to 0.2°C near 100 m depth) that is restricted to the surface layer (0-100m) in the case of PSY4. The surface layer from 0 to 200 m is too salty in both systems (0.02 psu).

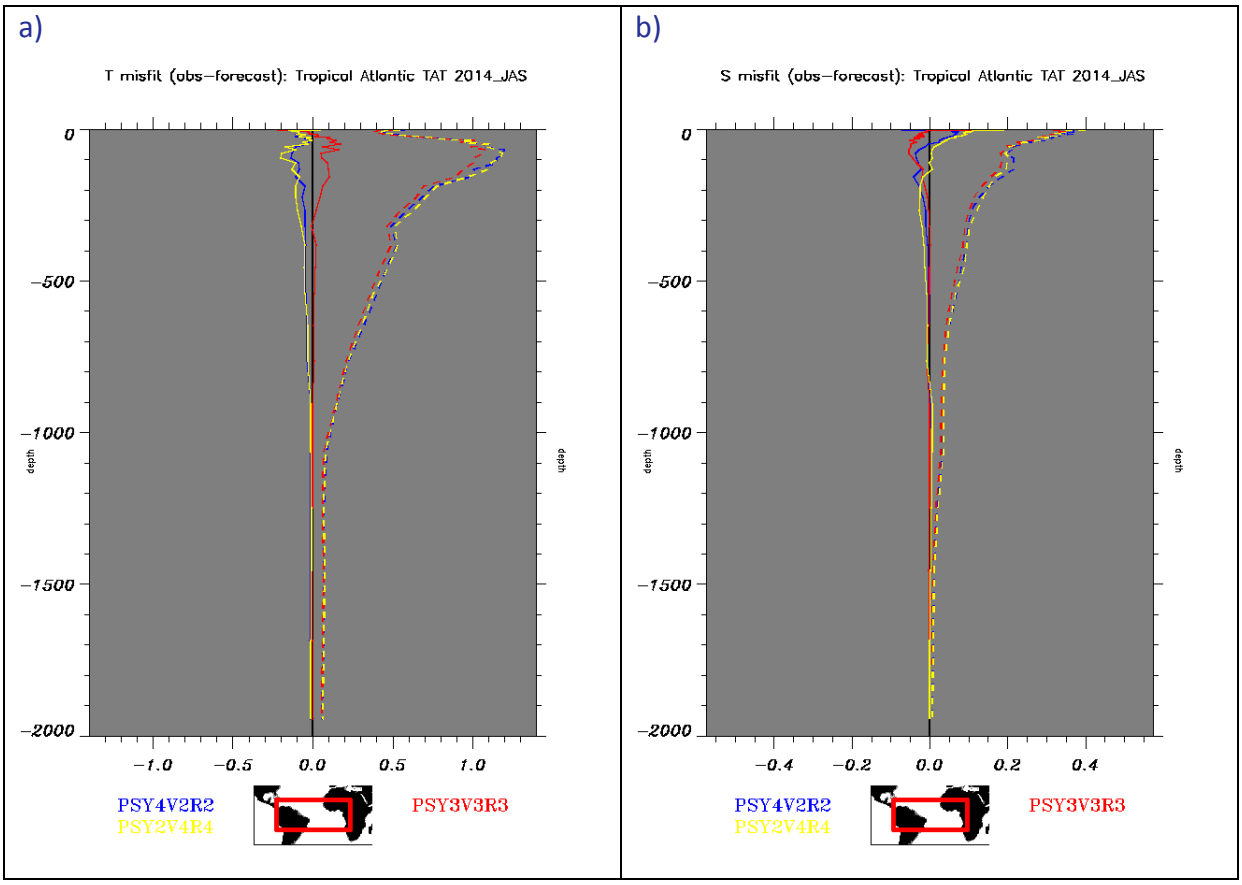

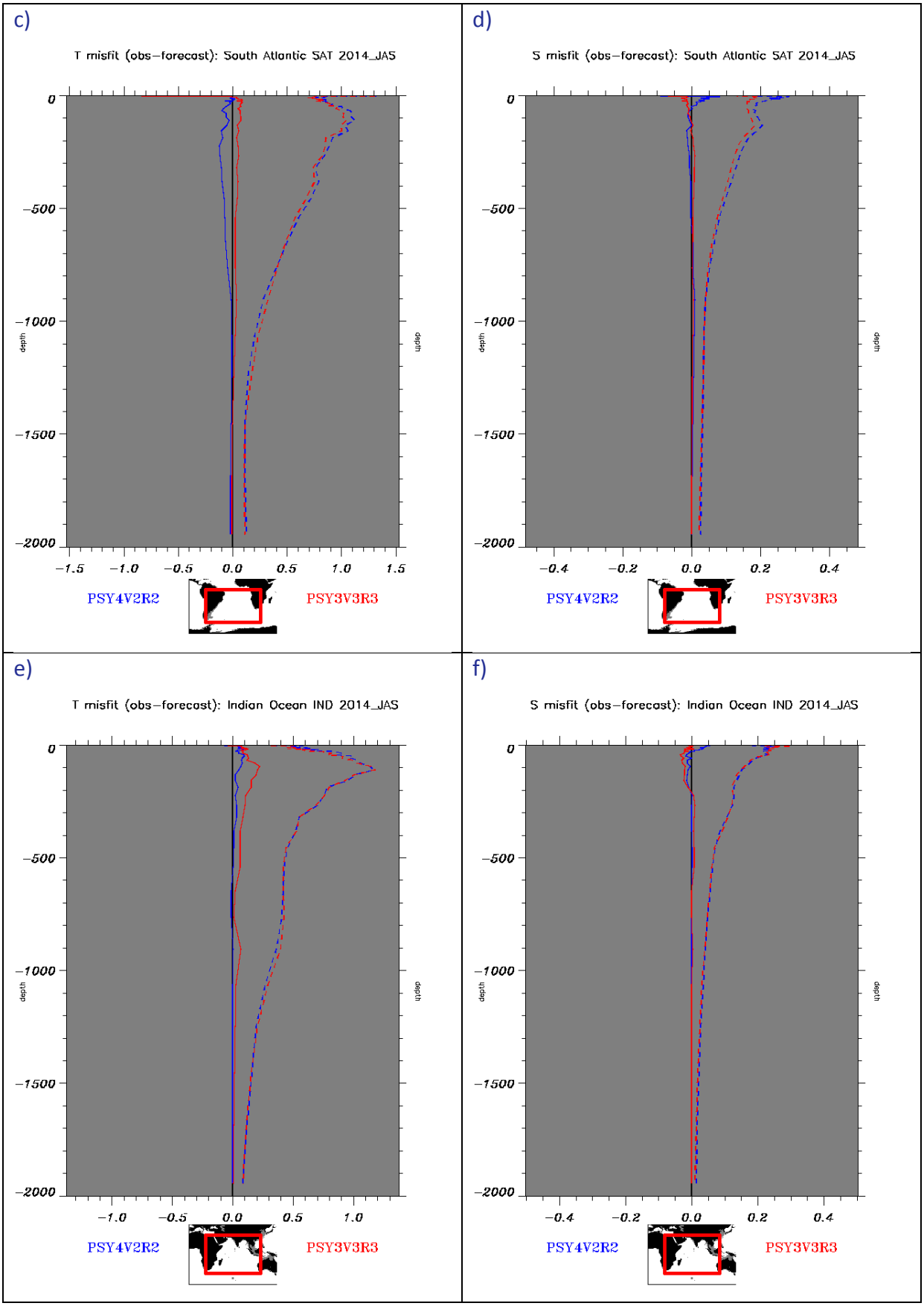

Figure 15: As Figure 14 in the Tropical Atlantic TAT (a and b), South Atlantic SAT (c and d) and Indian IND (e and f) basins.

On average over the Pacific Ocean (Figure 16), PSY4 is warmer (less than 0.1 °C) than the observations, and PSY3 colder (more than 0.1°C), from the surface to 700 m.

a)

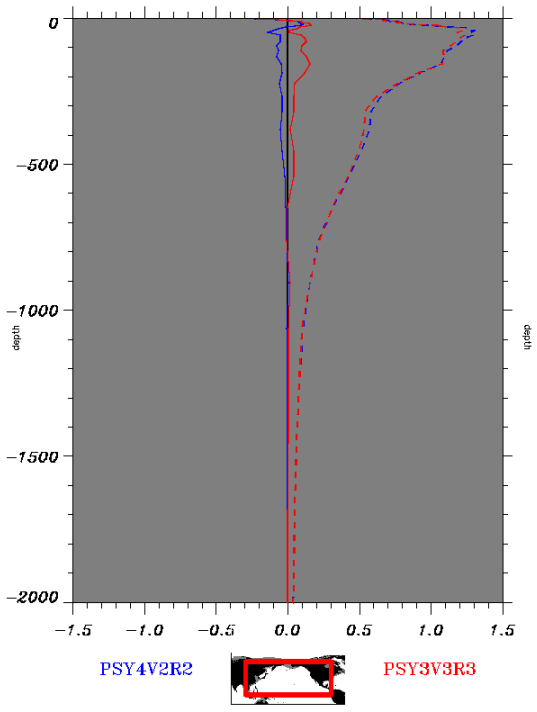
T misfit (obs−forecast): North Pacific NPA 2014_JAS
0
−500
−1000
−1500
−2000
depth
−1.5
−1.0
−0.5
0.0
0.5
1.0
1.5
PSY4V2R2
PSY3V3R3

b)

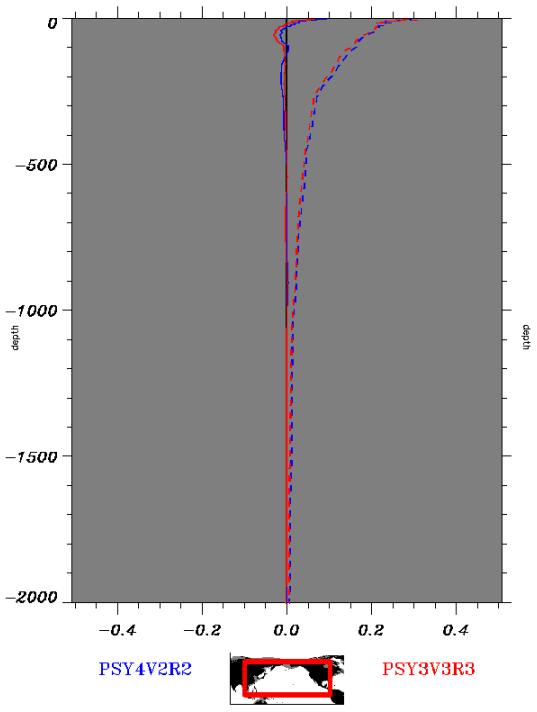
S misfit (obs−forecast): North Pacific NPA 2014_JAS
0
−500
−1000
−1500
−2000
depth
−0.4
−0.2
0.0
0.2
0.4
PSY4V2R2
PSY3V3R3

c)

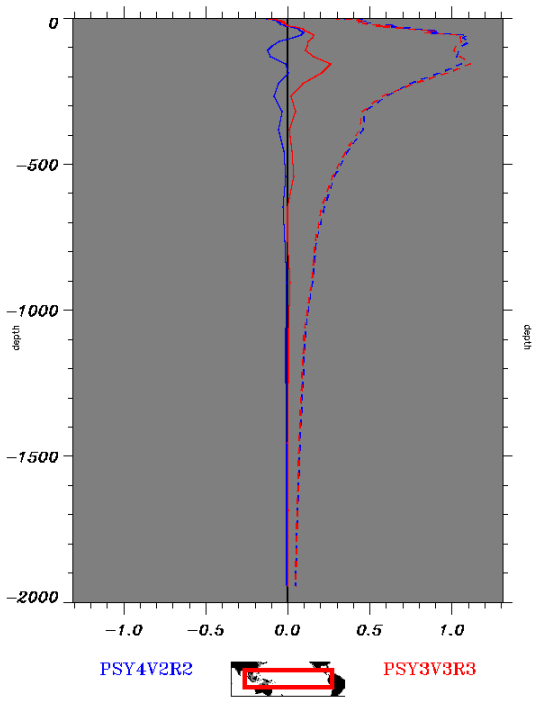
T misfit (obs−forecast): Trop. Pacific TPA 2014_JAS
0
−500
−1000
−1500
−2000
depth
−1.0
−0.5
0.0
0.5
1.0
PSY4V2R2
PSY3V3R3

d)

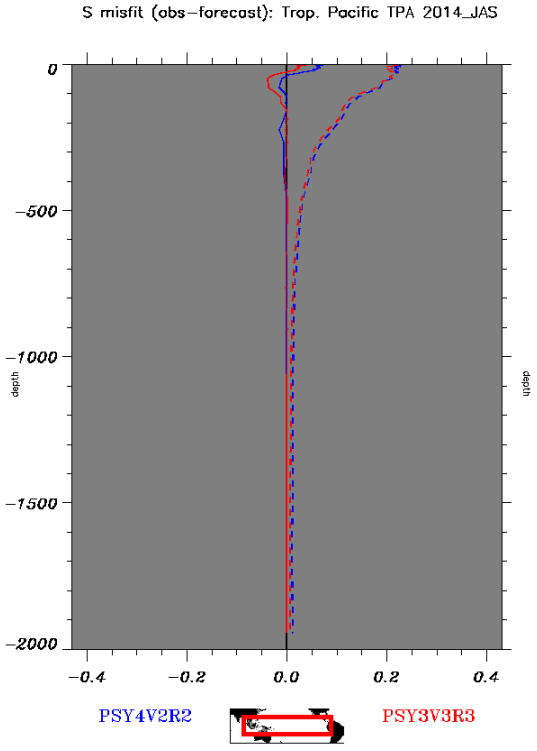
S misfit (obs−forecast): Trop. Pacific TPA 2014_JAS
0
−500
−1000
−1500
−2000
depth
−0.4
−0.2
0.0
0.2
0.4
PSY4V2R2
PSY3V3R3

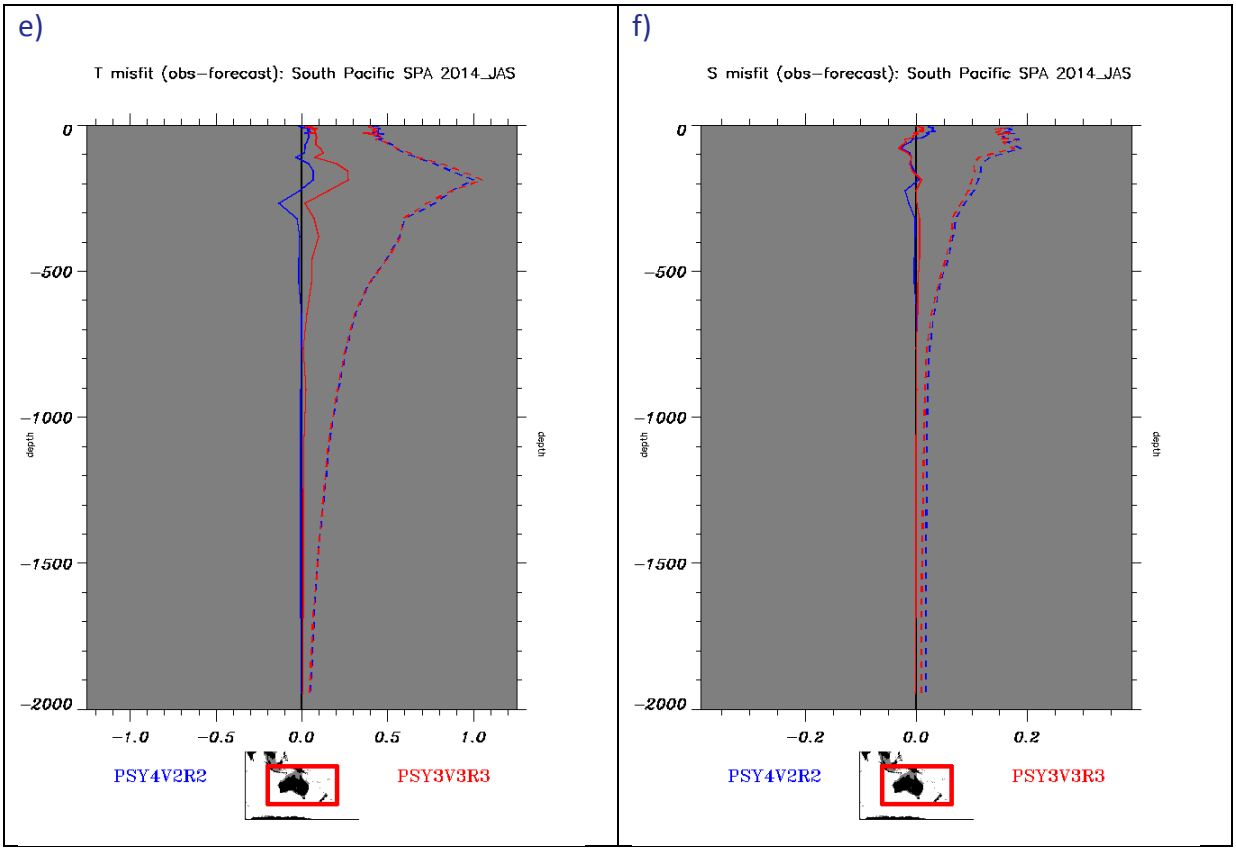

Figure 16: As Figure 14 in the North Pacific NPA (a and b), Tropical Pacific TPA (c and d) and South Pacific SPA (e and f).

For both PSY3 and PSY4 the salinity bias vertical structure is similar, and its amplitude is small (less than 0.05 psu). A salty bias is diagnosed near 100 m over the whole Pacific Ocean (higher for PSY3 than for PSY4), and a second salty bias appears in PSY4 near 200m in the Tropical and South Pacific. The temperature and salinity RMS errors of PSY3 and PSY4 are identical.

In the Southern Ocean in Figure 17, a warm temperature bias is observed again in PSY4 (up to 0.2 °C near 200m) while PSY3 is nearly unbiased, except for a warm (0.1 °C) and salty (0.02 psu) bias maximum near 200m.

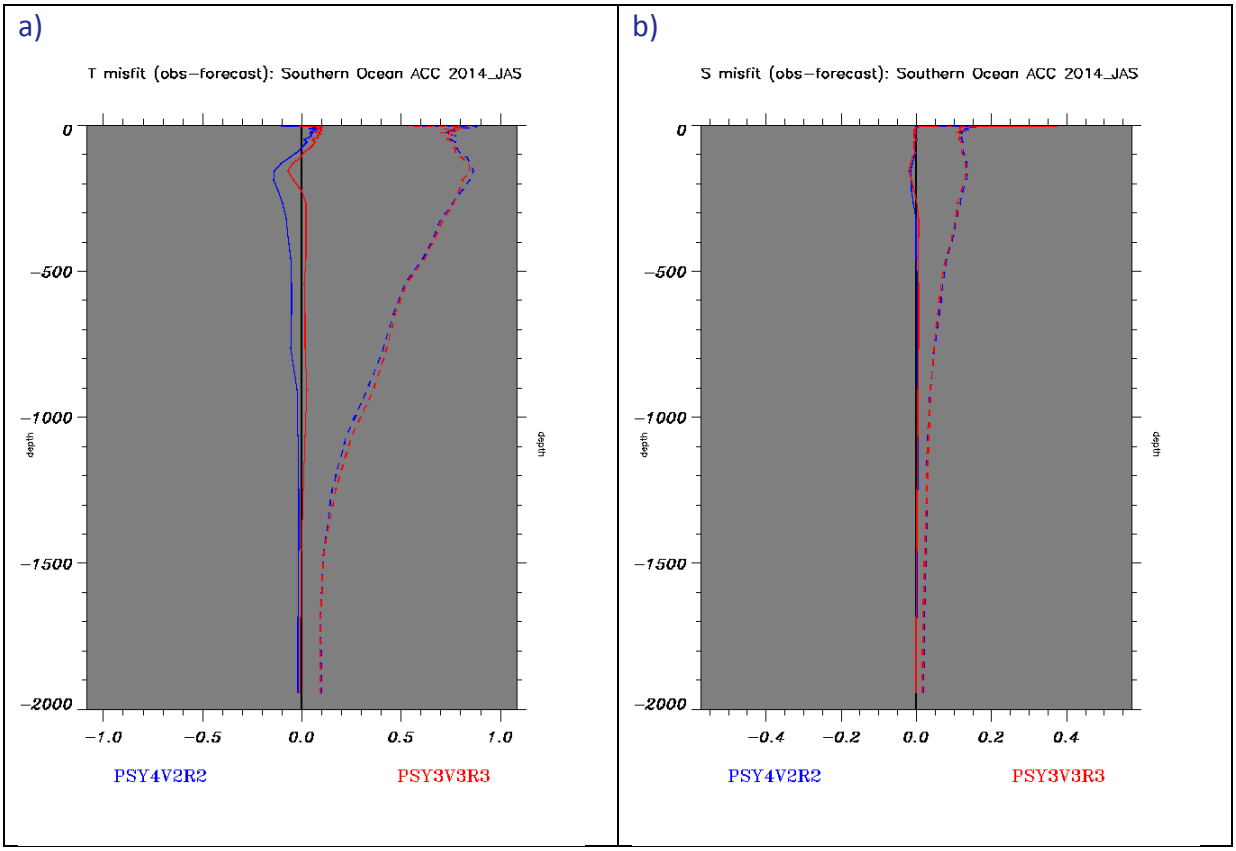

Figure 17: As Figure 14 in the ACC Southern Ocean basin (from 35°S).

V.1.3.1.2. Atlantic sub-regions

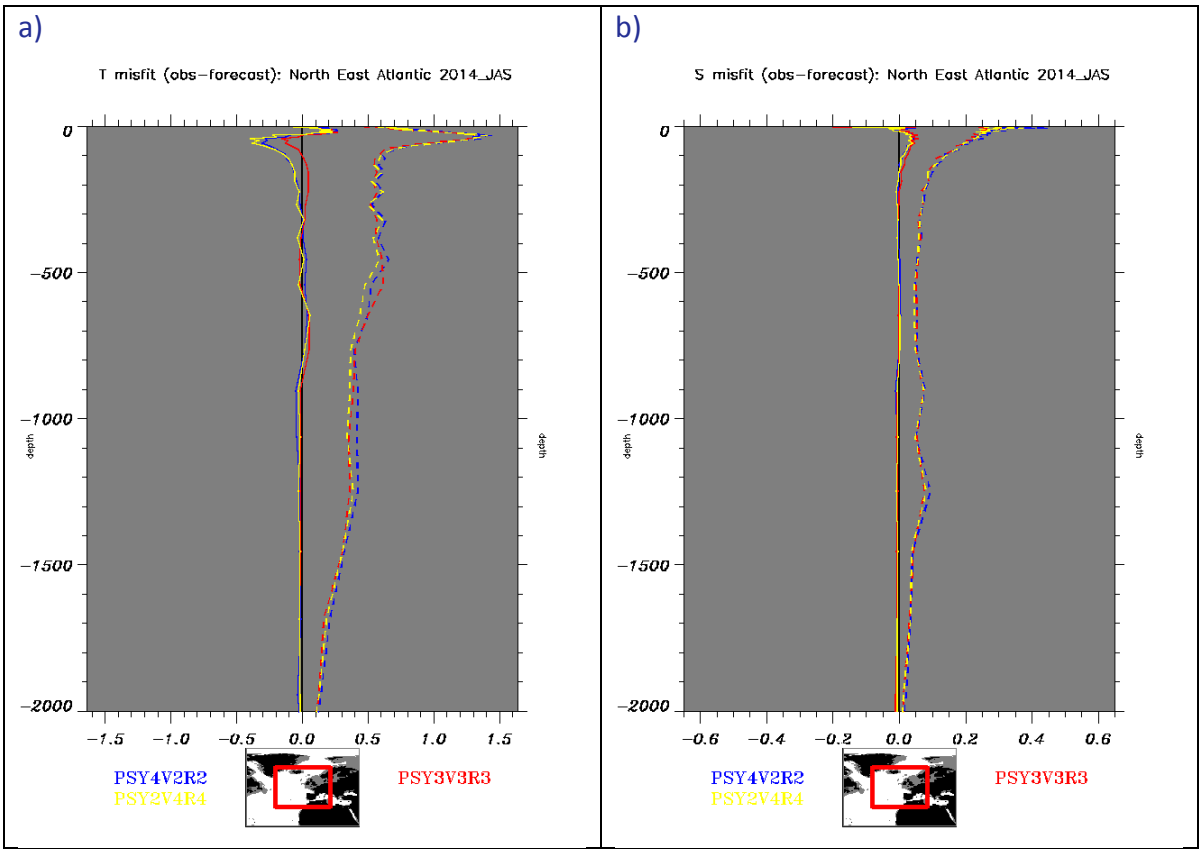

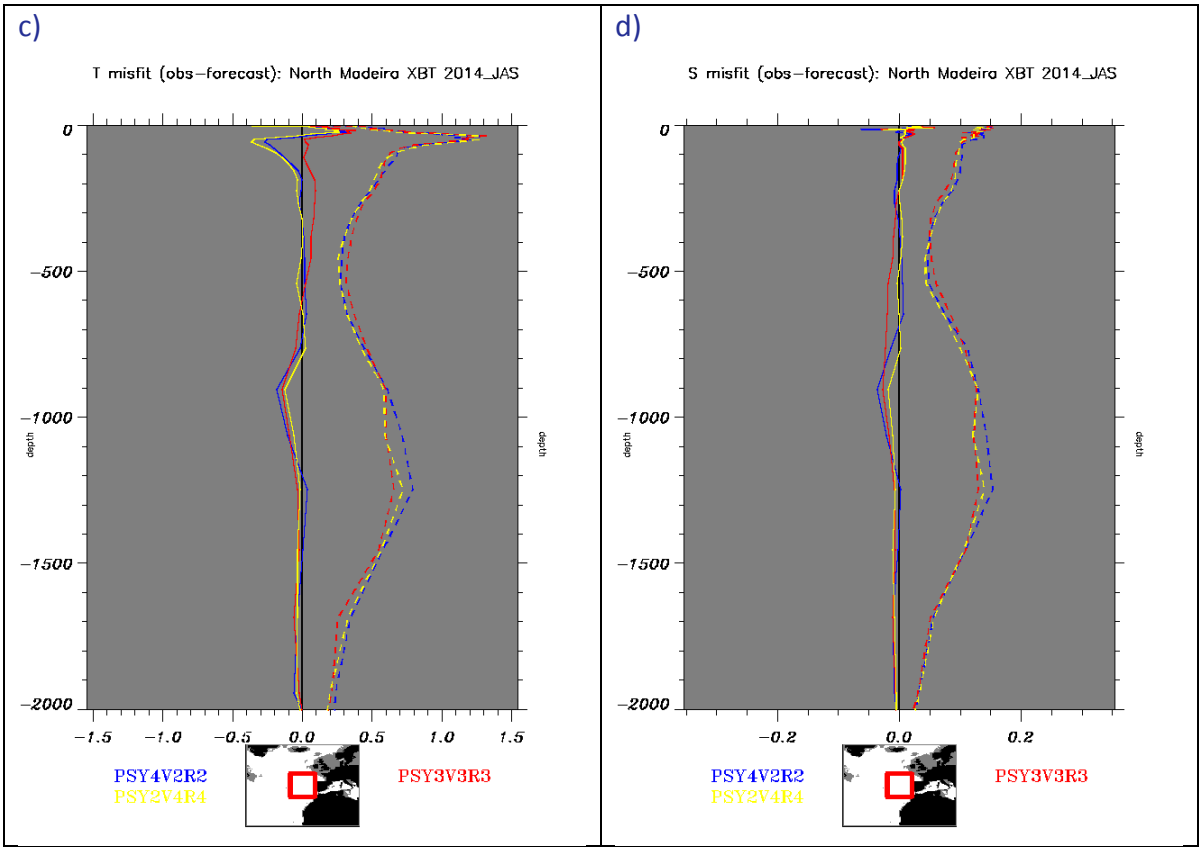

Figure 18: As Figure 14 in the North East Atlantic (IBI) and the North Madeira XBT regions.

The previous general comments apply also in smaller regions of the North East Atlantic Ocean, as shown in Figure 18. The signature of the Mediterranean waters is clear in the T and S RMS error for all systems (Figure 18 c and d). This quarter is characterized by the warm bias in both high resolution systems PSY2 and PSY4 in the 50-500 m layer.

In sub-regions of the Tropical Atlantic and in the Gulf Stream (Figure 19), the vertical structure of the biases is more complex. It reflects the underestimation of the upwelling in the Dakar region, and the errors in the vertical structure of the currents. In the Gulf of Mexico the systems are too cold. In the Gulf Stream, the three systems are too warm in the 100-800m layer, especially PSY4 (1°C) near 500 m. The systems are also too salty in the 100-800m layer (0.2 psu for PSY3 and PSY4, 0.1 psu for PSY2).

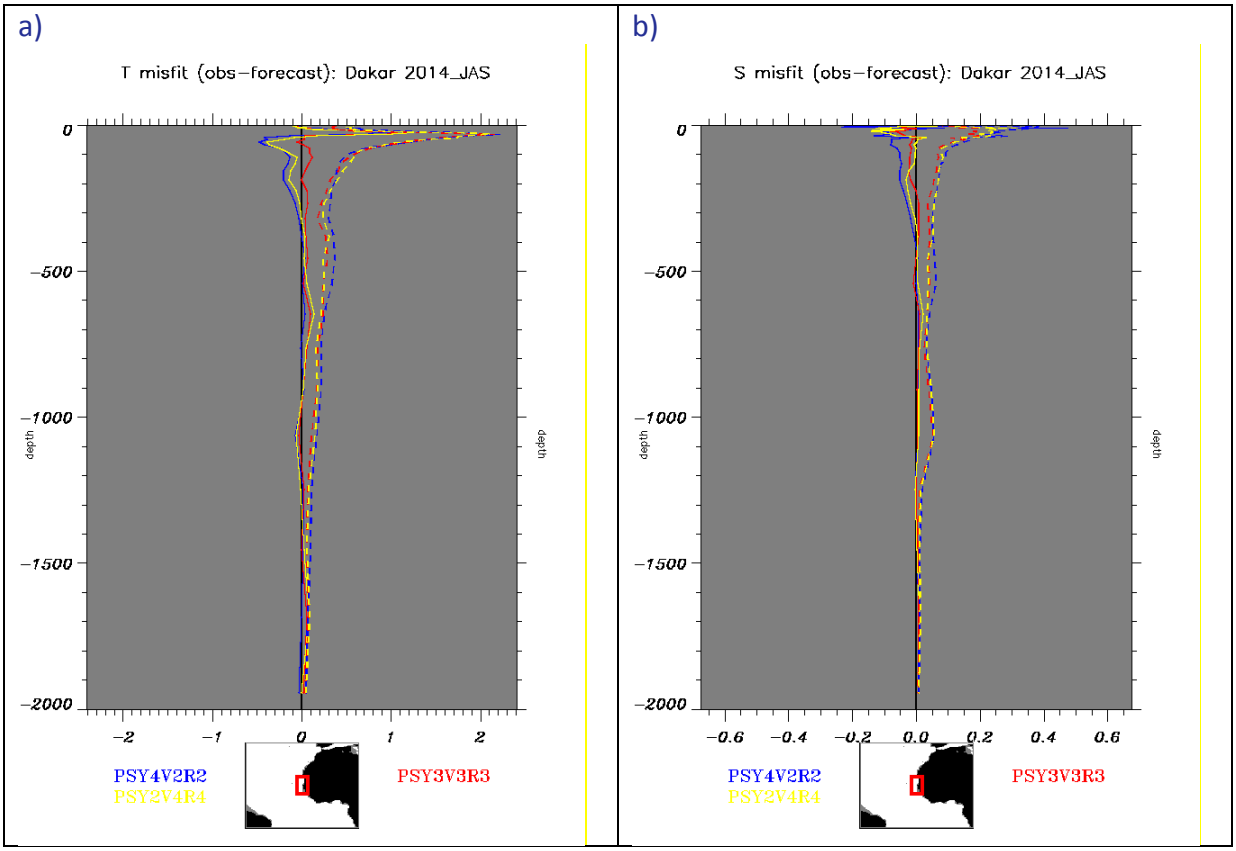

Figure 19: As Figure 14 in the Dakar region.

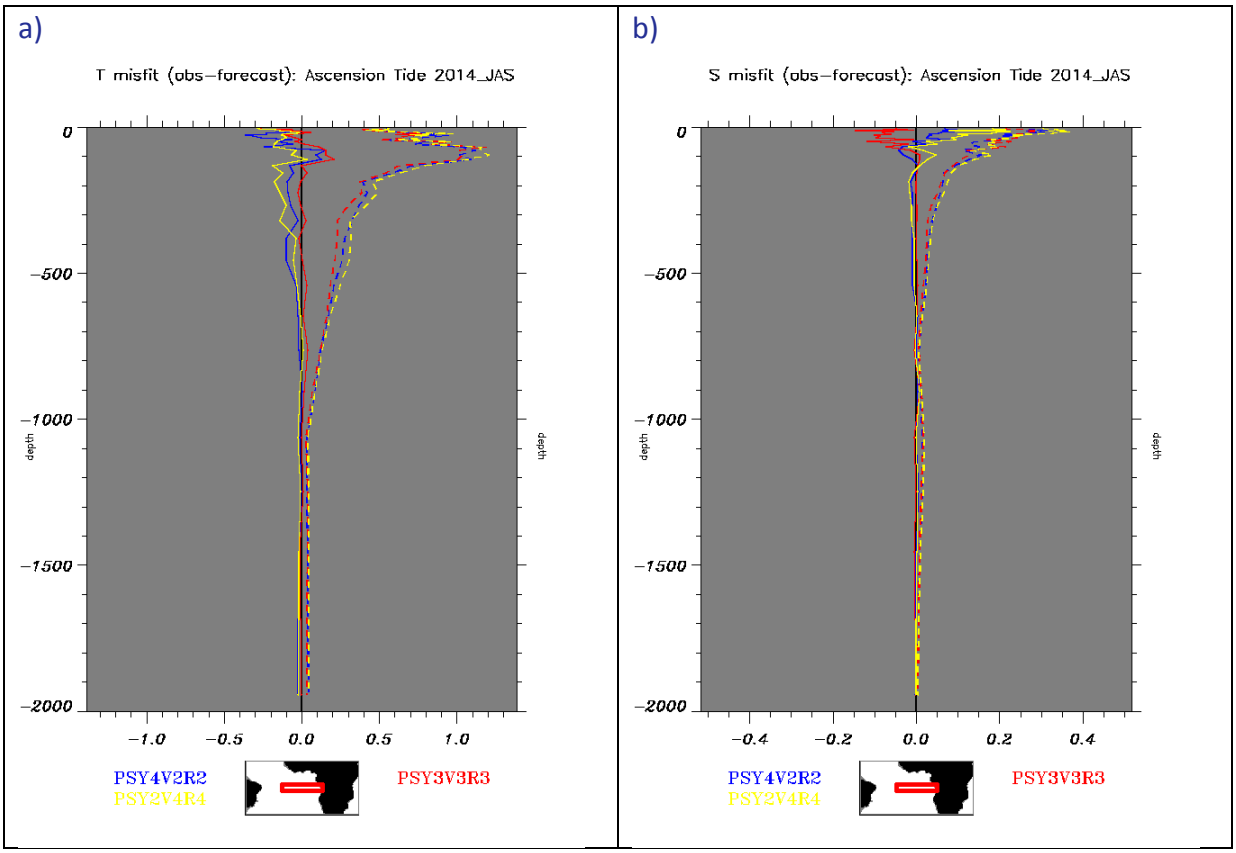

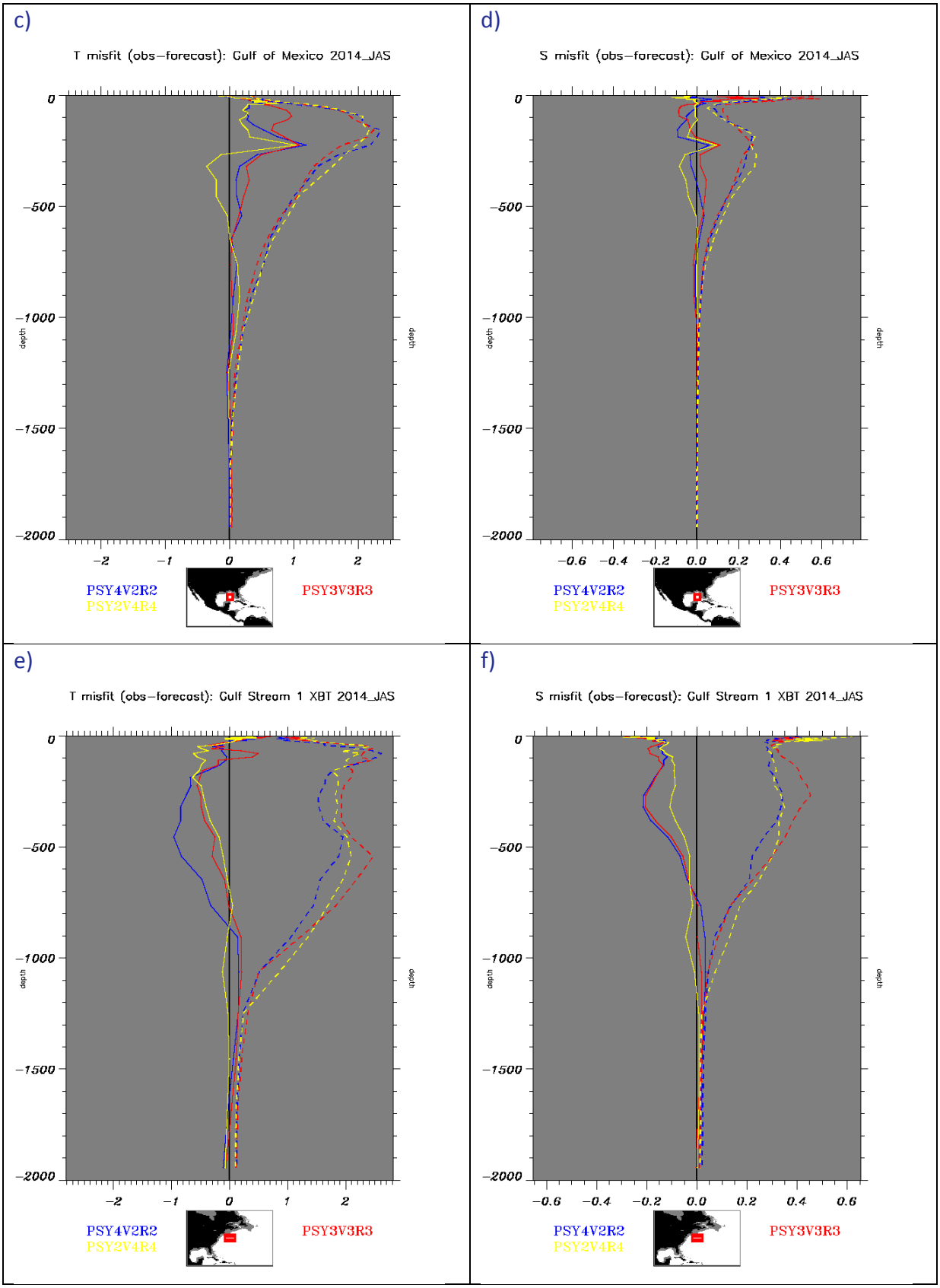

Figure 20: As Figure 14 in the Ascension tide (a and b), the Gulf of Mexico (c and d) and the Gulf Stream 1 regions (e and f)

However, one must keep in mind that the smallest sub-regions contain only a few data per assimilation cycle and that in this case the statistics may not be representative of the whole period, see for instance in Figure 21.

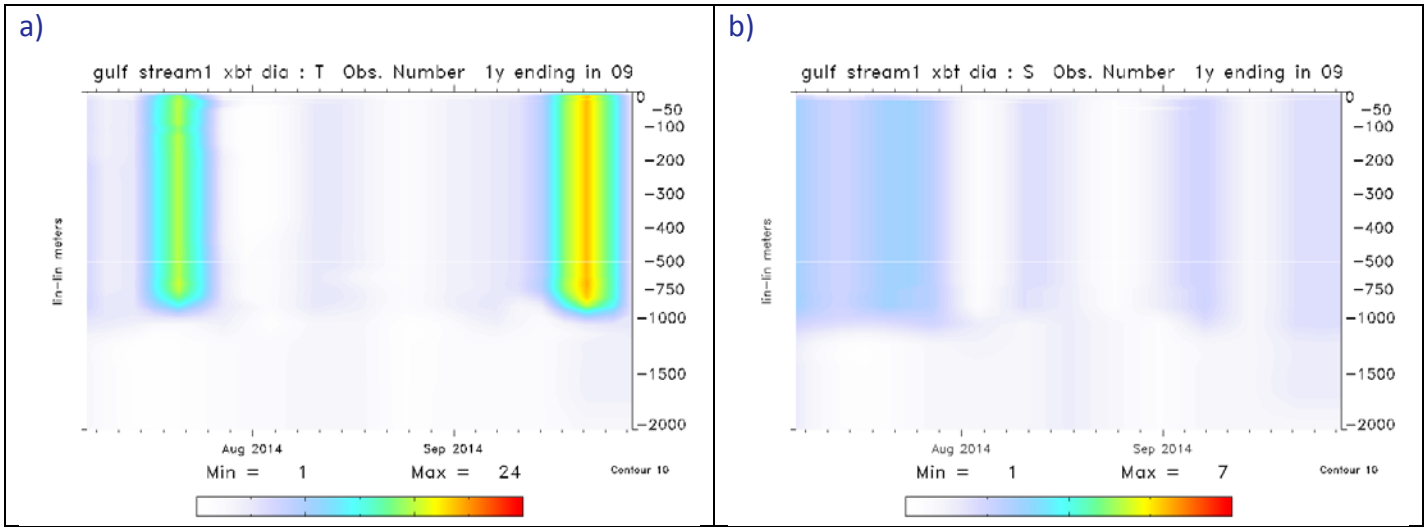

Figure 21: number of observations of T (a) and S (b) assimilated in PSY4V2R2 in the Gulf Stream 1 region during the JAS 2014 quarter.

V.1.3.1.3. Mediterranean Sea sub-regions

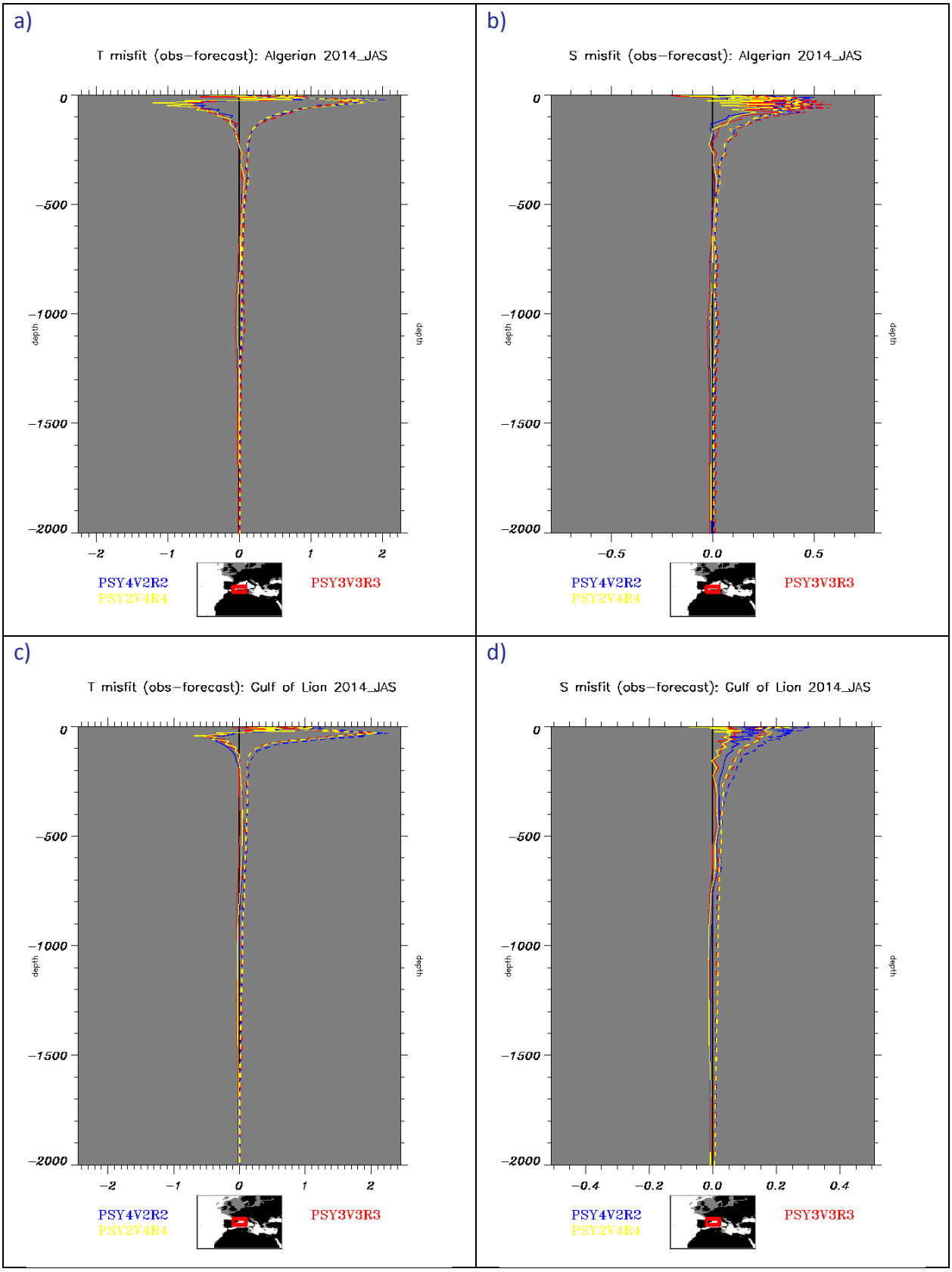

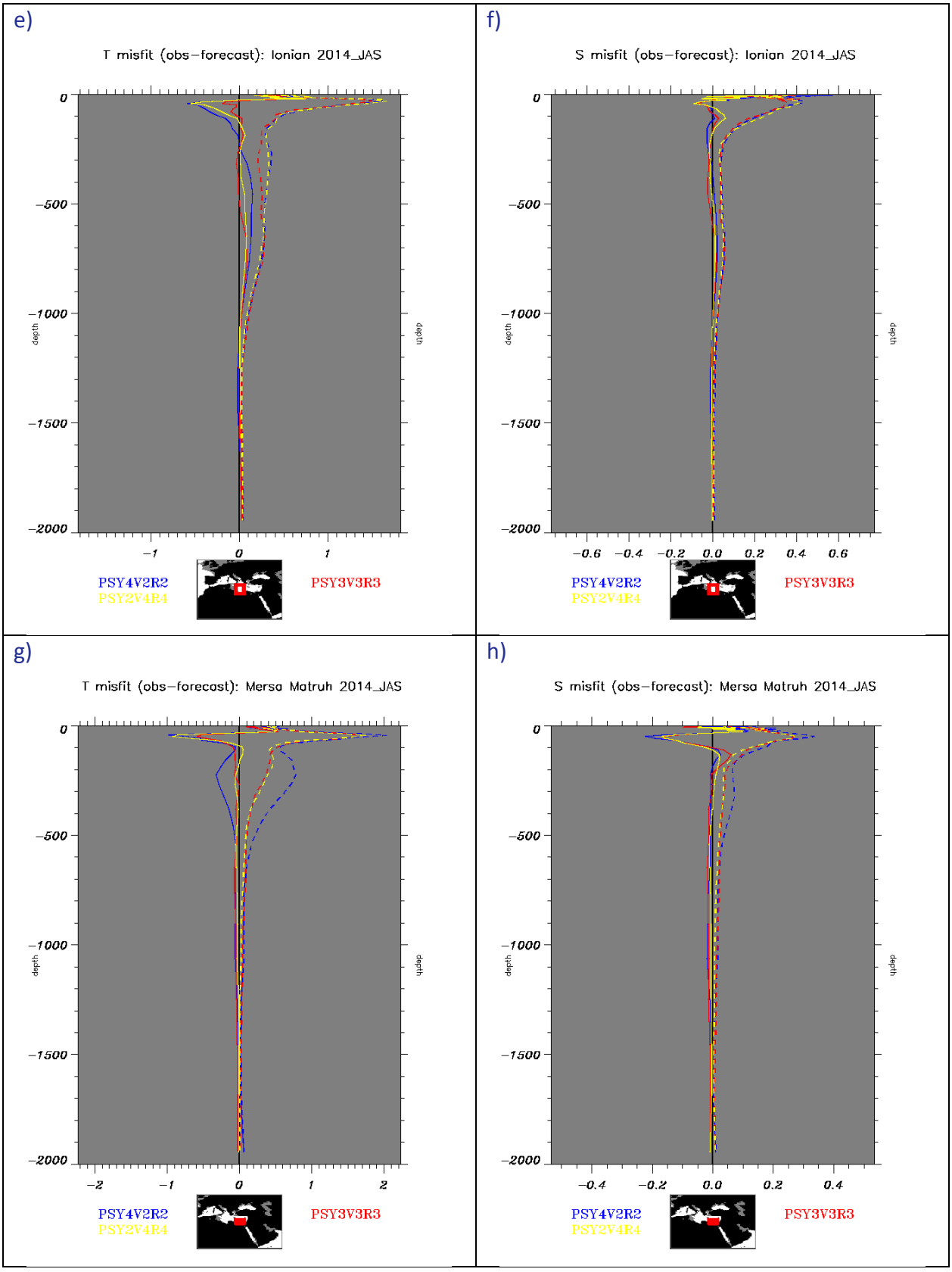

Figure 22: As Figure 14 in the Algerian (a and b), the gulf of Lion (c and d), the Ionian (e and f) and the Mersa Matruh (g and h) regions.

Figure 22 shows the T and S error profiles in sub-regions of the Mediterranean Sea. In the Western part of the basin, all systems seem to display a stratification bias. A cold and fresh bias is diagnosed at the surface, and a warm and fresh bias appears near 50 m. In the South eastern part of the basin, the bias maximum is

located near 100 m. The systems are consistent with one another in average. The rms difference and bias is higher for PSY4 in the Mersa Matruh region.

V.1.3.1.4. Indian Ocean sub-regions

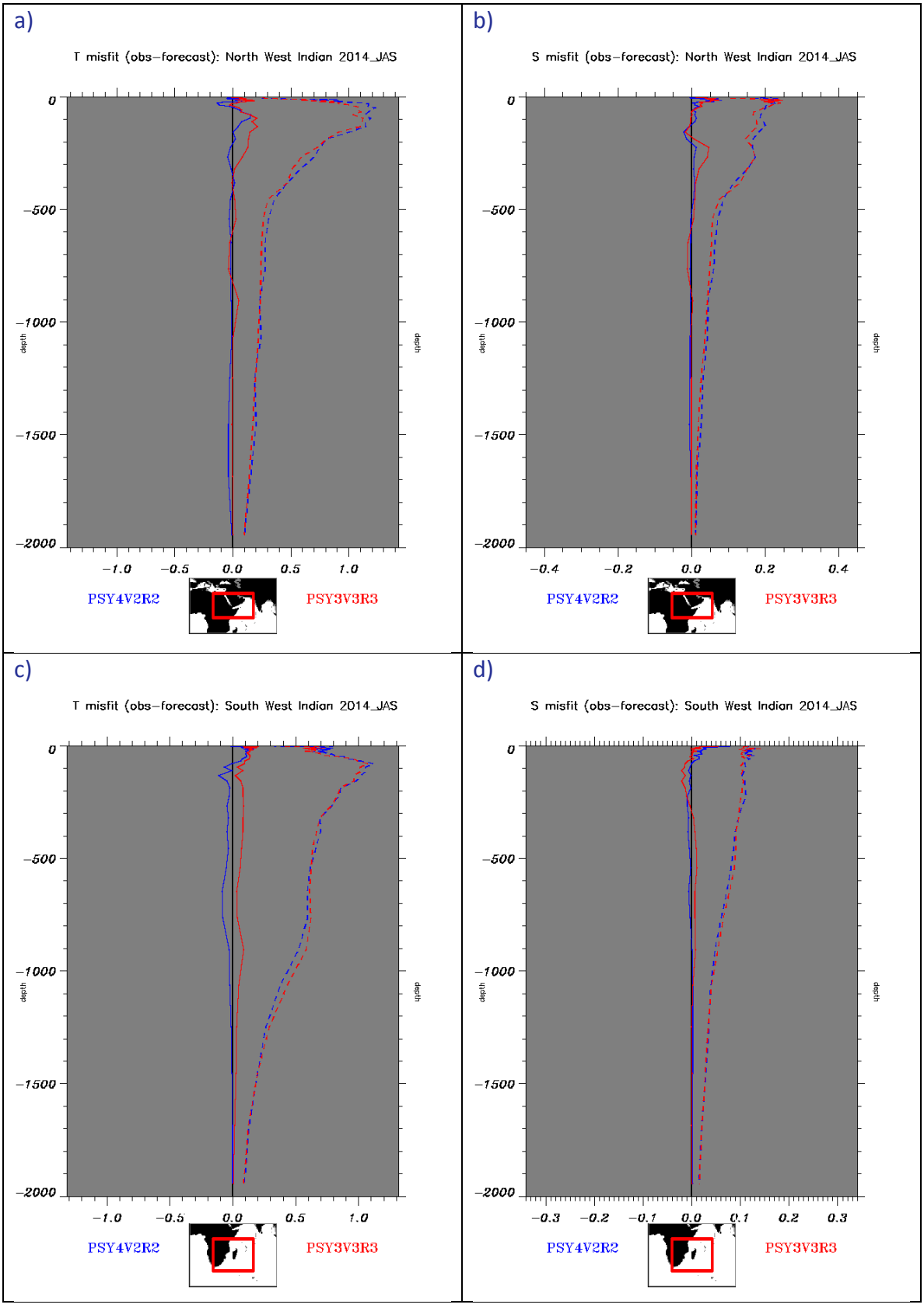

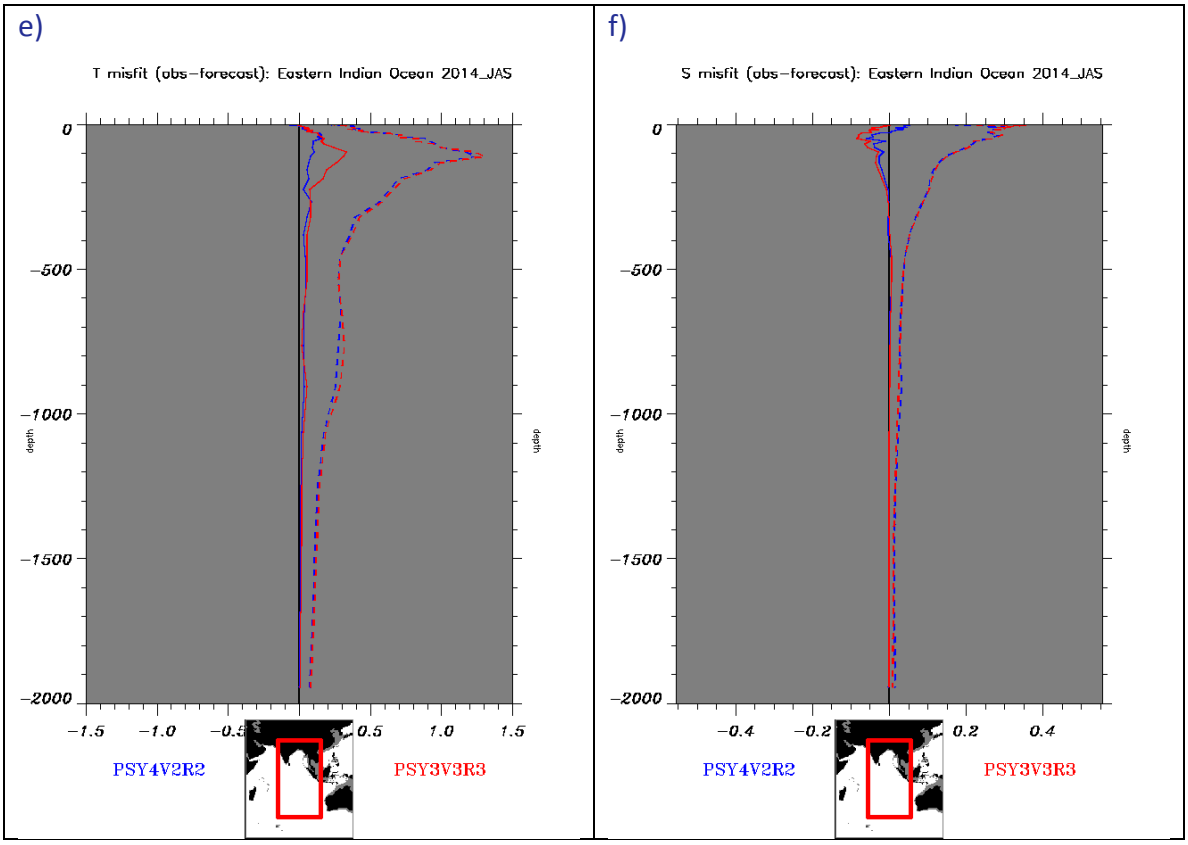

Figure 23: As Figure 14 in the North West Indian (a and b), the South West Indian (c and d) and the East Indian (e and f) regions

The analysis of the sub-regions of the Indian basin (Figure 23) shows that PSY3 displays a cold bias mainly in the south western part of the Basin. PSY4 being warmer than PSY3, it is less biased this season with respect to the in situ temperature observations. On average over the Indian Ocean, PSY4 performs as well and is even less biased than PSY3 on the whole water column.

SUMMARY: Starting in April 2013, the PSY2, PSY3 and PSY4 systems converge in terms of model version and parameterizations. The data assimilation method and tunings are the same, and so do the data sets assimilated by the three systems. In consequence **the three Mercator Ocean systems display consistent data assimilation statistics** for the quarter JAS 2014. **The systems are close to the observations**, and misfits lie within the prescribed error (most of the time misfit in T is less than 0.1 °C, misfit in S less then 0.05 psu, misfit in SLA less than 7 cm). **The average and RMS errors are larger in regions of high spatial and/or temporal variability** (thermocline, regions of high mesoscale activity, upwelling, fronts, etc…). **PSY4 displays a warm bias in the 0-800m layer** mainly due to the initialization of the system as already explained in previous QVD. **Coastal regions are weakly constrained in all systems**, and consistent biases appear in SLA and SST (warm and high, or cold and low). There are still many uncertainties in the MDT, mainly near the coasts and in the Polar Regions. The systems do not use the SLA misfit information in coastal regions, but problems can appear in open ocean regions where there are still errors in the MDT. A warm bias is diagnosed in SST this quarter. **There is still too much mixing in the surface layer inducing a cold bias in the surface layer (0-50 m) and warm bias in subsurface (50-150 m).** This is particularly clear in the Atlantic and Mediterranean Sea in JAS 2014. This bias is intensifying with the summer stratification and the winter mixing episodes reduce the bias. The bias correction is not as efficient on reducing seasonal biases as it is on reducing long term systematic biases. No precipitation correction is applied in the systems, and uncertainties (overestimation) of the convective precipitations induce **large fresh biases in the tropical oceans**.

V.2. Accuracy of the daily average products with respect to observations

V.2.1. T/S profiles observations

V.2.1.1. Global statistics for JAS 2014

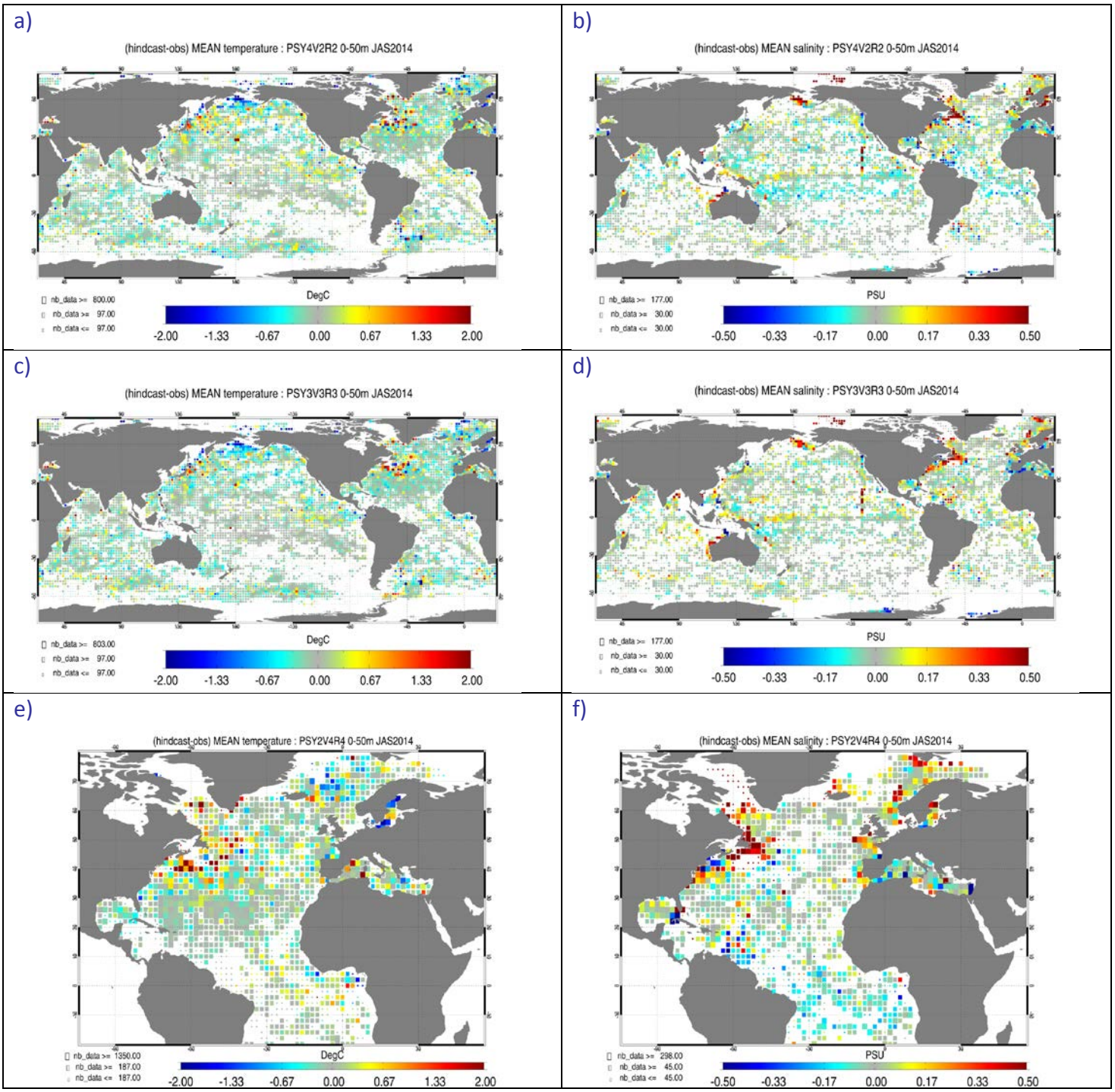

Figure 24: Average difference MODEL-OBSERVATION of temperature (a, c, and e, in °C) and salinity (b, d, and f, in psu) in JAS 2014 between the daily average hindcast PSY4V2R2 (a and b), PSY3V3R3 (c and d) and PSY2V4R4 (e and f) hindcast products and all available T/S observations from the Coriolis database. The Mercator hindcast products are taken at the time and location of the observations. Averages are performed in the 0-50m layer. The size of the pixel is proportional to the number of observations used to compute the RMS in 2°x2° boxes.

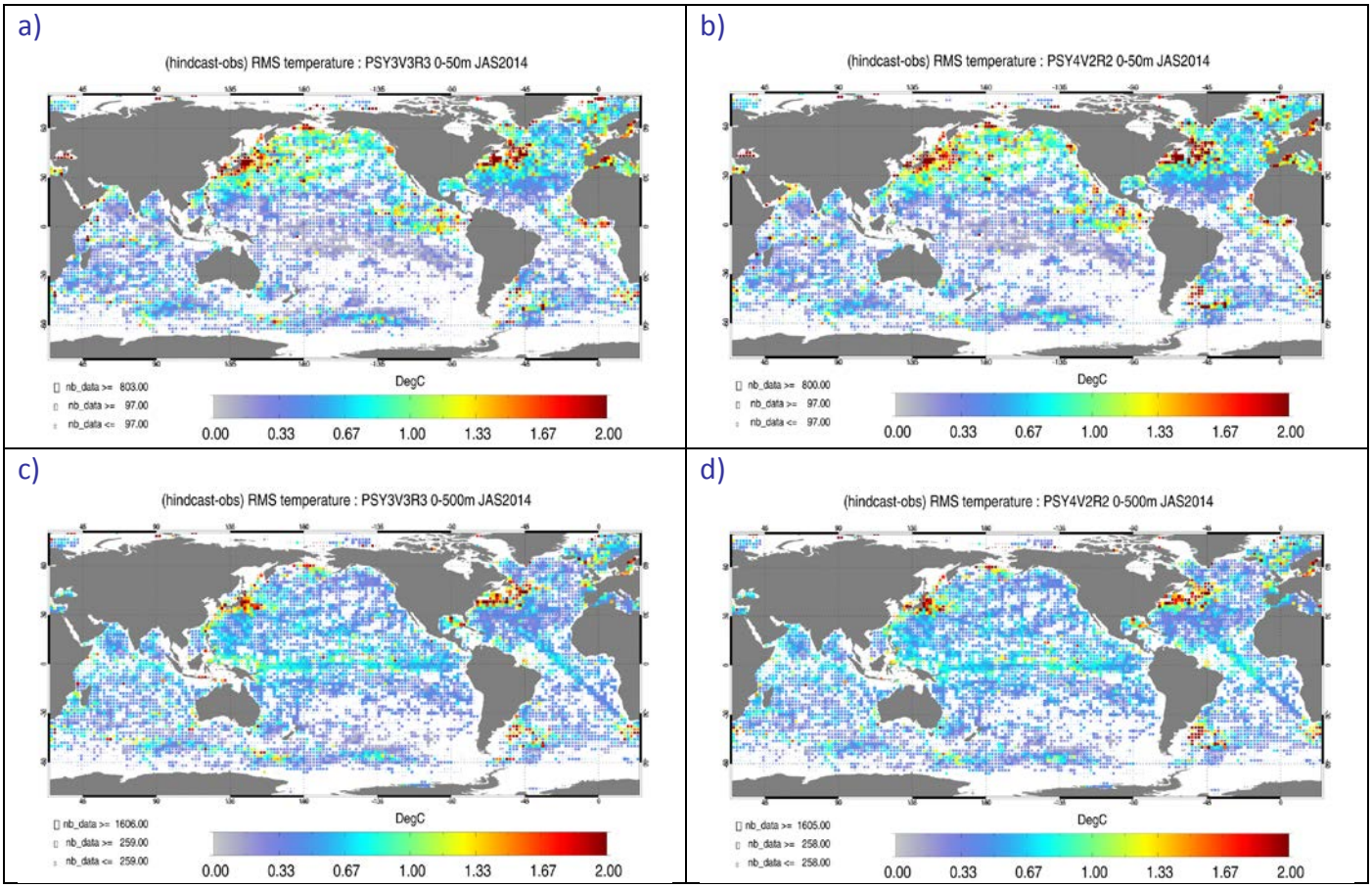

Figure 25: RMS temperature (°C) difference (model-observation) in JAS 2014 between all available T/S observations from the Coriolis database and the daily average hindcast PSY3V3R3 products on the left and hindcast PSY4V2R2 on the right column colocalised with the observations. Averages are performed in the 0-50m layer (a and b) and in the 0-500m layer (c and d). The size of the pixel is proportional to the number of observations used to compute the RMS in 2°x2° boxes.

Consistently with the data assimilation statistics the three systems PSY3, PSY4 and PSY2 are slightly warmer (~0.1°C) than the observations at the global scale in the surface layer (0-50m) as can be seen in Figure 24. Fresh biases also appear, mainly in the tropics, linked with overestimated convective precipitations in the ECMWF analyses, and also to the climatological runoffs that are prescribed.

As can be seen in Figure 25, in both PSY3 and PSY4 temperature errors in the 0-500m layer have similar amplitude and spatial patterns, and stand between 0.5 and 1°C in most regions of the globe. RMS errors in the tropical thermocline can reach 1°C. Regions of high mesoscale activity (Kuroshio, Gulf Stream, Agulhas current) and regions of upwelling in the tropical Atlantic and Tropical Pacific display higher errors (up to 3°C).

The salinity RMS errors (Figure 26) are usually less than 0.2 psu but can reach higher values in regions of high runoff (Amazon, Sea Ice limit) or precipitations (ITCZ, SPCZ, Gulf of Bengal), and in regions of high mesoscale variability. RMS errors of around 0.2 psu in the Tropics in the 0-50m layer correspond to the fresh bias linked with overestimated precipitation.

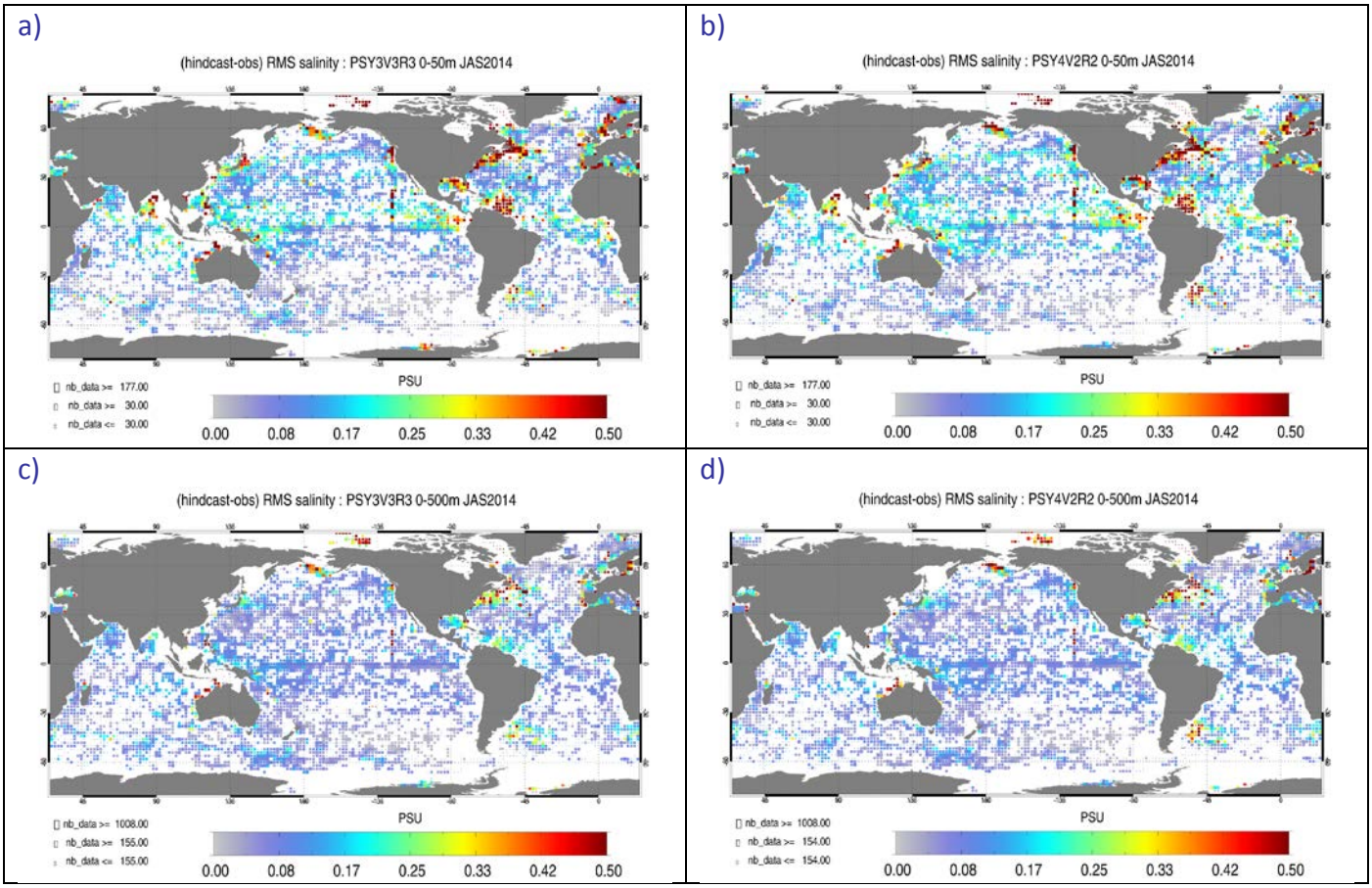

Figure 26: RMS salinity (psu) difference (model-observation) in JAS 2014 between all available T/S observations from the Coriolis database and the daily average hindcast PSY3V3R3 products (a and c) and hindcast PSY4V2R2 (b and d), colocalised with the observations. Averages are performed in the 0-50m layer (a and b) and in the 0-500m layer (c and d). The size of the pixel is proportional to the number of observations used to compute the RMS in 2°x2° boxes.

As can be seen in Figure 27, the intermediate resolution model (PSY3) and the high resolution model (PSY4) display comparable temperature and salinity RMS difference. PSY4 displays a global average fresh bias (0.015 psu) at the surface, while PSY3 and PSY4 are saltier than the observations (0.01 psu) on global average between 5 m and 300 m. PSY3 is too cold on the whole water column (except in the 2000-5000 m layer). PSY4 is slightly warmer at the surface and slightly colder in the 5-800 m layer, and closer to the observations than PSY3 on average over the whole global domain. Both systems are more accurate than the WOA09 climatology (Levitus 2009).

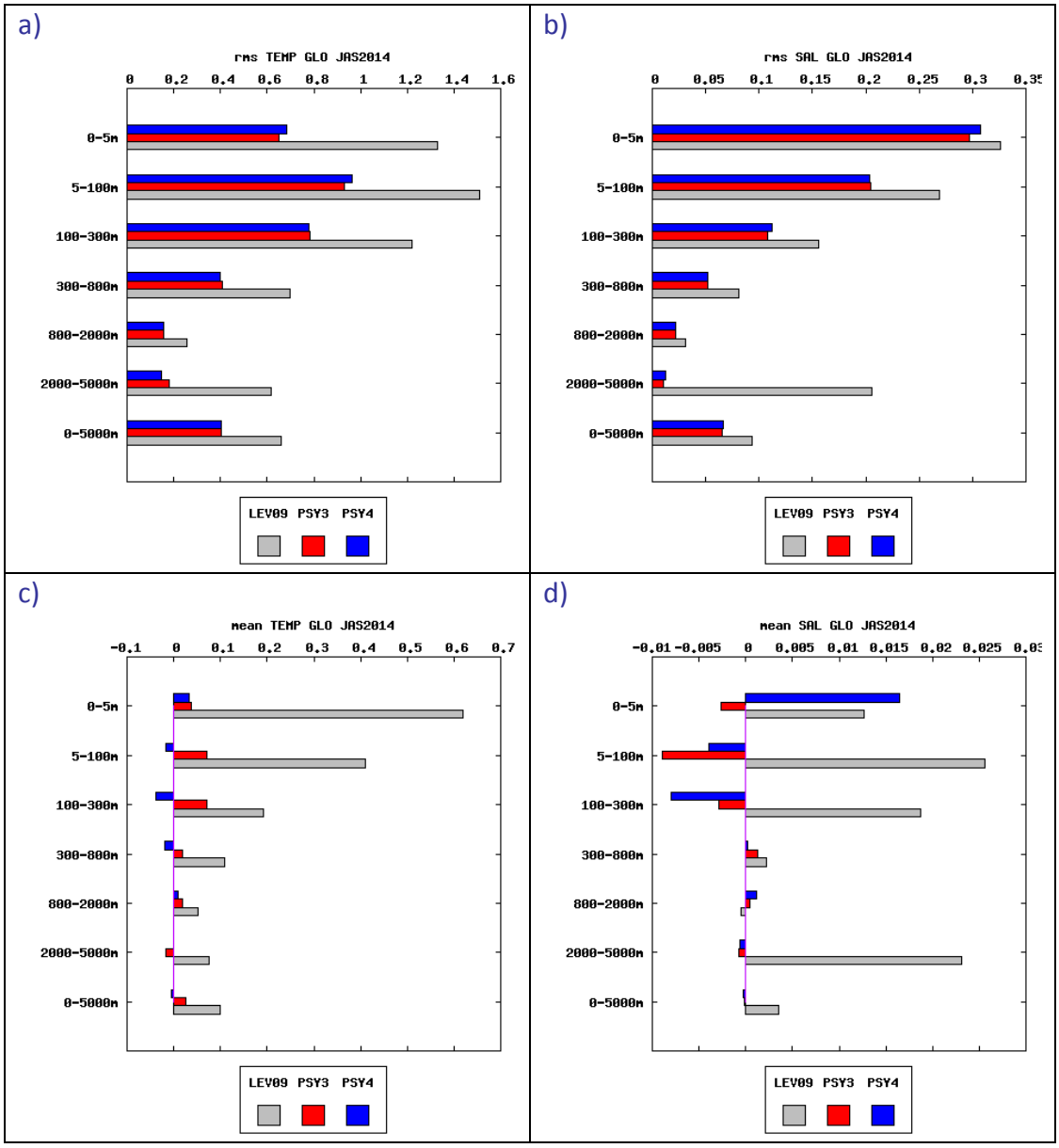

Figure 27 : JAS 2014 global statistics of temperature (°C, a and c) and salinity (psu, b and d) averaged in 6 consecutive layers from 0 to 5000m. RMS difference (a and b) and mean difference (observation-model, c and d) between all available T/S observations from the CORIOLIS database and the daily average hindcast products PSY3V3R3 (red), PSY4V2R2 (blue) and WOA09 climatology (grey) colocalised with the observations. NB: average on model levels is performed as an intermediate step which reduces the artefacts of inhomogeneous density of observations on the vertical.

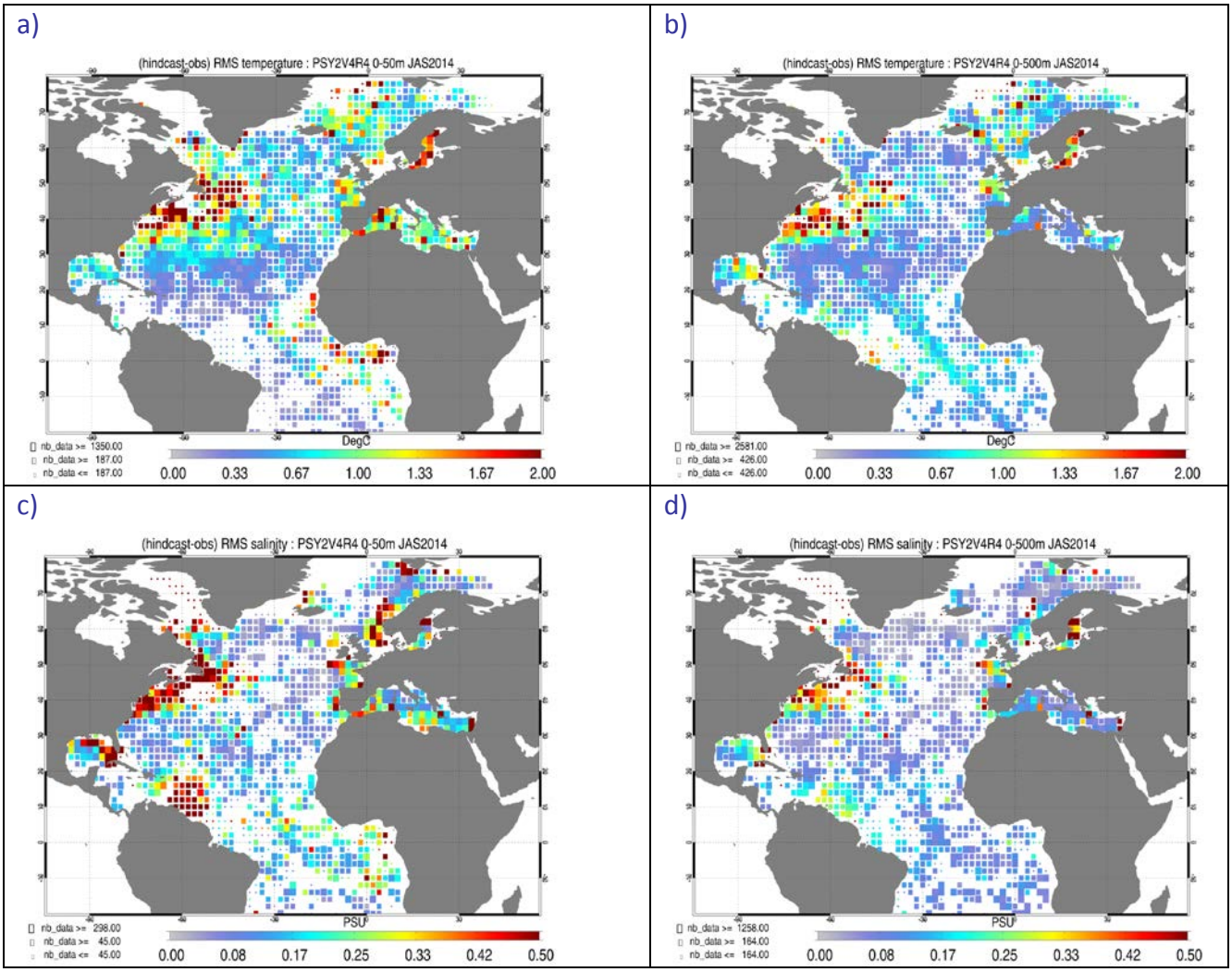

Figure 28: RMS difference (model-observation) of temperature (a and b, °C) and salinity (c and d, psu) in JAS 2014 between all available T/S observations from the Coriolis database and the daily average PSY2V4R4 hindcast products colocalised with the observations in the 0-50m layer (a and c) and 0-500m layer (b and d)

The general performance of PSY2 (departures from observations in the 0-500m layer) is less than 0.3°C and 0.05 psu in many regions of the Atlantic and Mediterranean (Figure 28). The strongest departures from temperature and salinity observations are always observed in the Gulf Stream and the tropical Atlantic. Near surface salinity biases appear in the Alboran Sea, the Gulf of Guinea, the Caribbean Sea, the Labrador Sea and the Gulf of Mexico (see also Figure 24). In the tropical Atlantic biases concentrate in the 0-50m layer (cold and fresh bias). This is consistent with the bias correction not being at work in the mixed layer.

V.2.1.2. Water masses diagnostics

a)

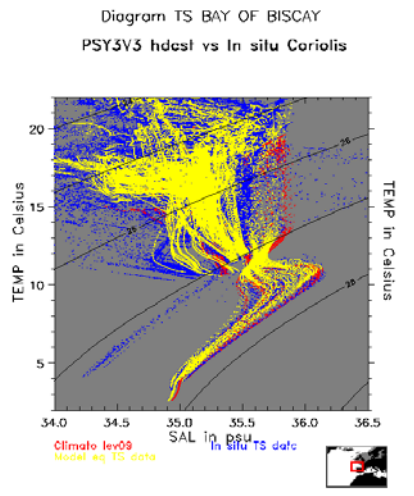

b)

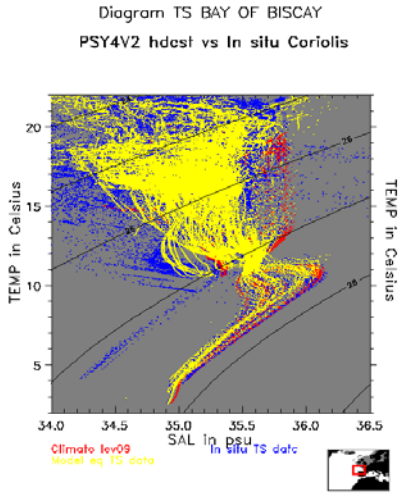

c)

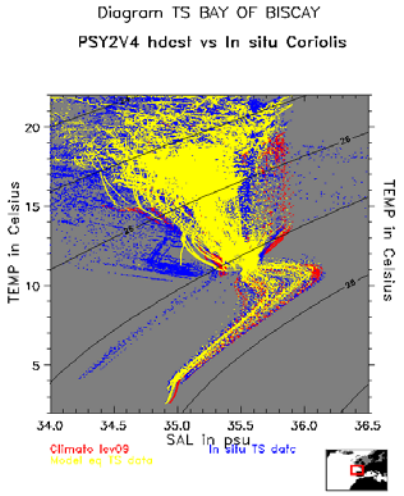

d)

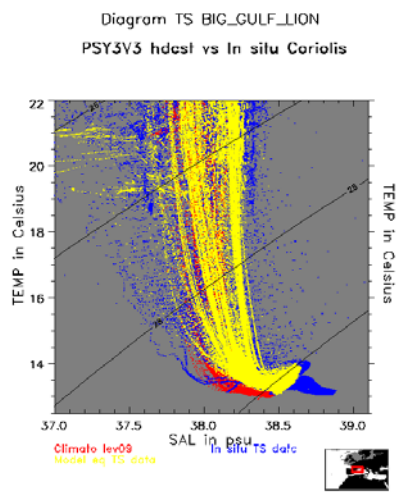

e)

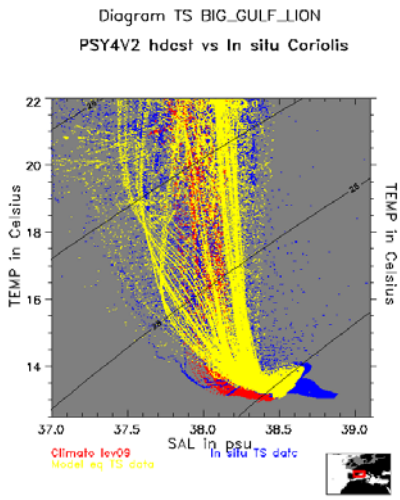

f)

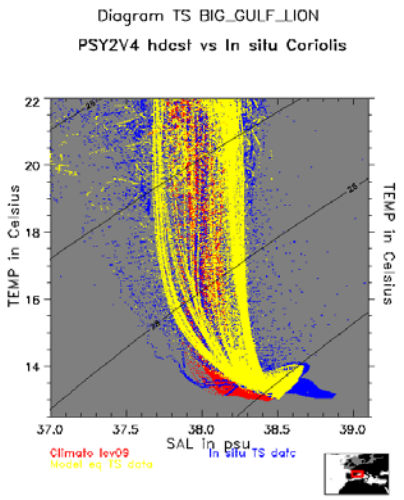

g)

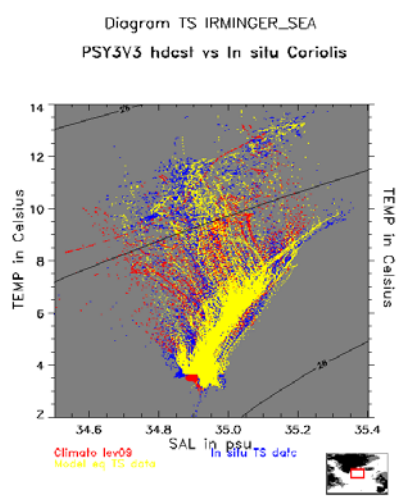

h)

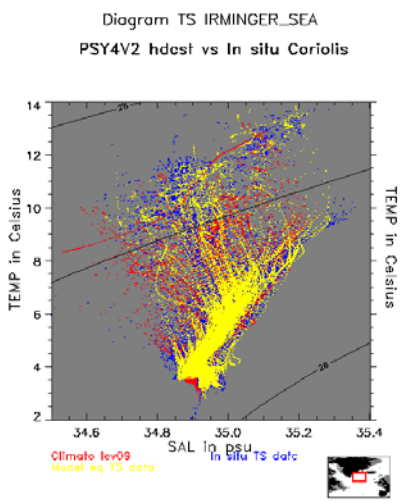

i)

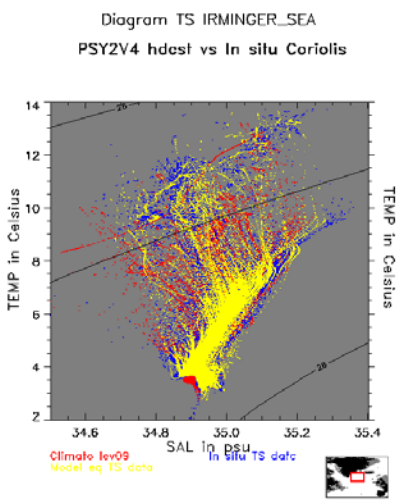

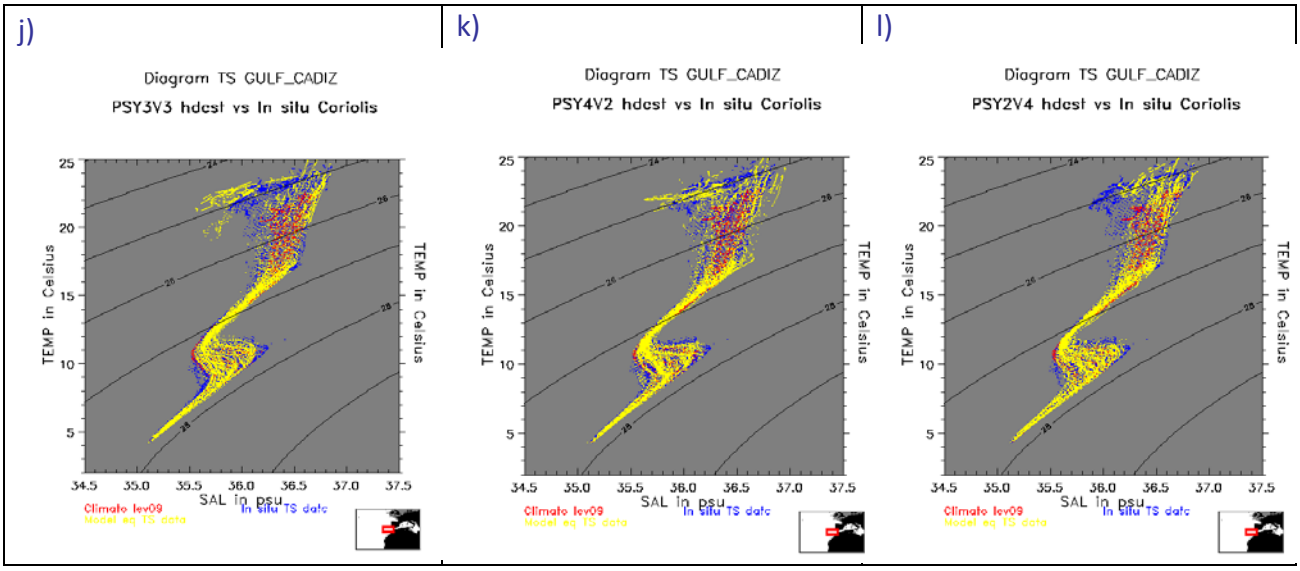

Figure 29: : Water masses (Theta, S) diagrams in JAS 2014 in the Bay of Biscay (a to c), Gulf of Lion (d to f), Irminger Sea (g to i) and Gulf of Cadiz (j to l), comparison between PSY3V3R3 (a, d, g, j), PSY4V2R2 (b, e, h, k) and PSY2V4R4 (c, f, I, and l) in JAS 2014. PSY2, PSY3 and PSY4: yellow dots; Levitus WOA09 climatology: red dots; in situ observations: blue dots.

In Figure 29 the daily products (analyses) are collocated with the T/S profiles in order to draw "Theta, S" diagrams. The water masses characteristics of the three systems are nearly similar, PSY4 being locally slightly better than PSY3 and PSY2 (Mediterranean waters)

In the Bay of Biscay the Eastern North Atlantic Central Water, Mediterranean and Labrador Sea Water can be identified on the diagram.

- Between 11°C and 15°C, 35 and 36 psu, warm and relatively salty Eastern North Atlantic Central Water gets mixed with the shelf water masses. The saltiest ENACW waters are slightly better captured by PSY4 than by PSY2 and PSY3 during this JAS 2014 season. PSY3 and PSY4 capture also better the minimum of salinity of ENACW.
- The Mediterranean Waters are characterized by high salinities (Salinities near 36 psu) and relatively high temperatures (Temperatures near 10°C).
- The Labrador Sea waters appear between 4°C and 7°C, 35.0 and 35.5 psu

In the Gulf of Lion:

- The Levantine Intermediate Water (salinity higher than 38.5 psu) is too fresh in all systems this JAS 2014 season.
- The lower salinities (lower than 37.7 psu) are slighty better reproduced by PSY4.

In the Irminger Sea:

- The Irminger Sea Water (≈ 4°C and 35 psu) and the North Atlantic water (at the surface) are well represented by the systems.

In the Gulf of Cadiz:

- The Mediterranean outflow waters (T around 10°C) are well represented. PSY4 better captures the spread of temperature and salinity at surface (Atlantic Surface waters).

In the western tropical Atlantic the three systems represent well the water masses.

In the eastern tropical Atlantic the three systems represent well the water masses. PSY2 (and to a lesser extent PSY4) displays fresh waters near the surface that are not present in the observations.

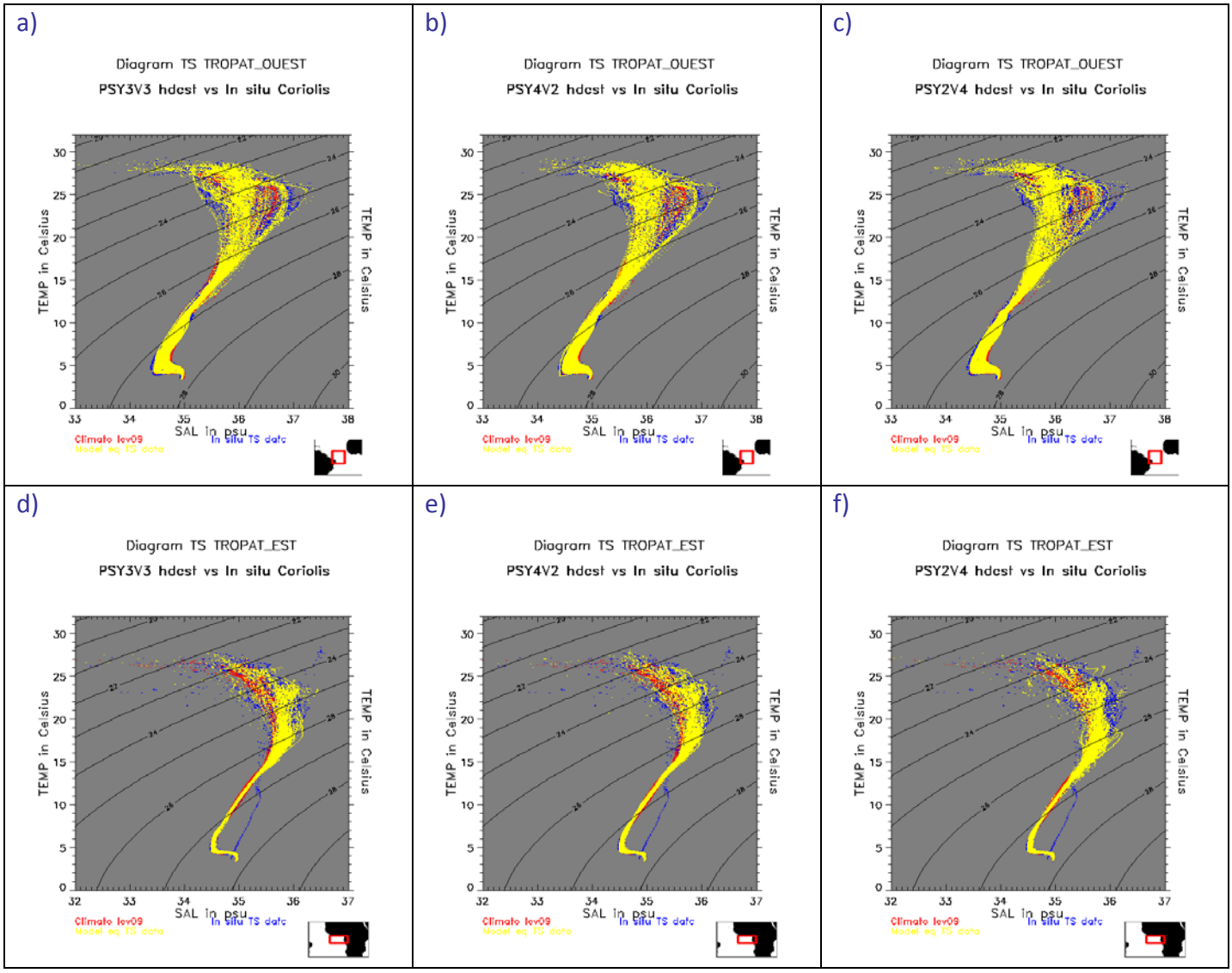

Figure 30 : Water masses (T, S) diagrams in the Western Tropical Atlantic (a to c) and in the Eastern Tropical Atlantic (d to f) in JAS 2014: for PSY3V3R3 (a, d); PSY4V2R2 (b, e); and PSY2V4R4 (c, f). PSY2, PSY3 and PSY4: yellow dots; Levitus WOA09 climatology; red dots, in situ observations: blue dots.

In the Agulhas current (Figure 31) PSY3 and PSY4 give a realistic description of water masses. The deep waters characteristics are slightly more realistic in PSY4 than in PSY3. In the Kuroshio region the North Pacific Intermediate waters (NPIW) are better represented in PSY4 than in PSY3 (too salty). At the surface in the highly energetic regions of the Agulhas and of the Gulf Stream, the water masses characteristics display a wider spread in the high resolution 1/12° than in the ¼°, which is more consistent with T and S observations. In the Gulf Stream region, PSY4 is fresher than PSY3 in the North Atlantic Central Waters (NACW), which is more consistent with the in situ observations of the quarter JAS 2014. The saltiest waters near the surface (North Atlantic Subtropical Waters, NASW) are only captured by PSY4.

a)

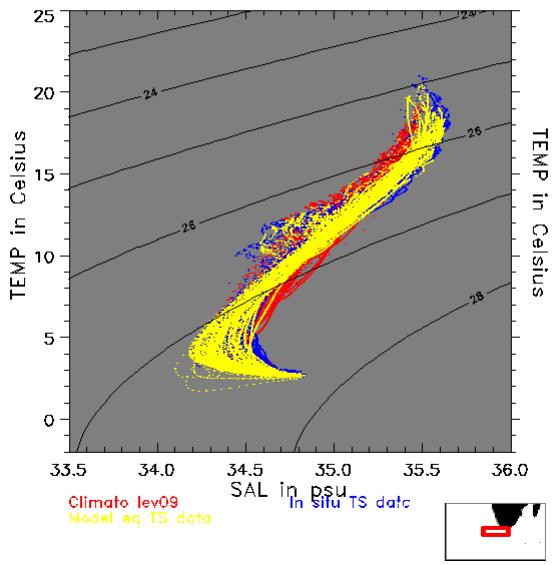
Diagram TS SOUTH_AFRICA
PSY3V3 hdcst vs In situ Coriolis
TEMP in Celsius
SAL in psu
Climato lev09
Model eq TS data
In situ TS data

b)

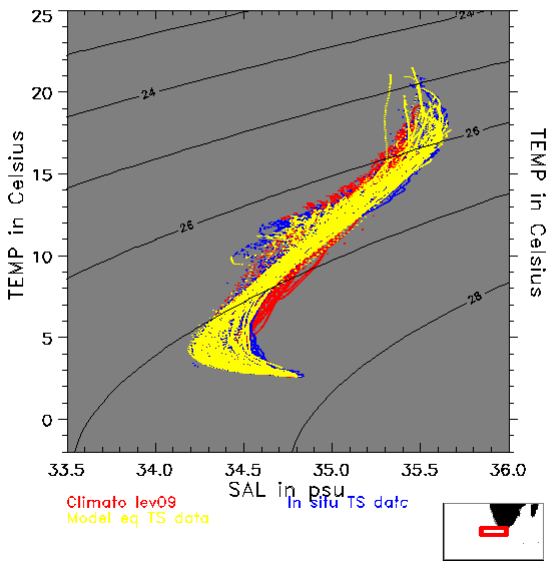
Diagram TS SOUTH_AFRICA
PSY4V2 hdcst vs In situ Coriolis
TEMP in Celsius
SAL in psu
Climato lev09
Model eq TS data
In situ TS data

c)

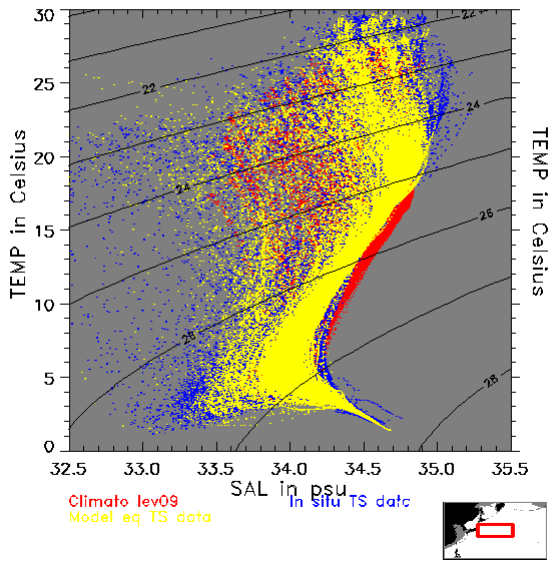
Diagram TS KUROSHIO
PSY3V3 hdcst vs In situ Coriolis
TEMP in Celsius
SAL in psu
Climato lev09
Model eq TS data
In situ TS data

d)

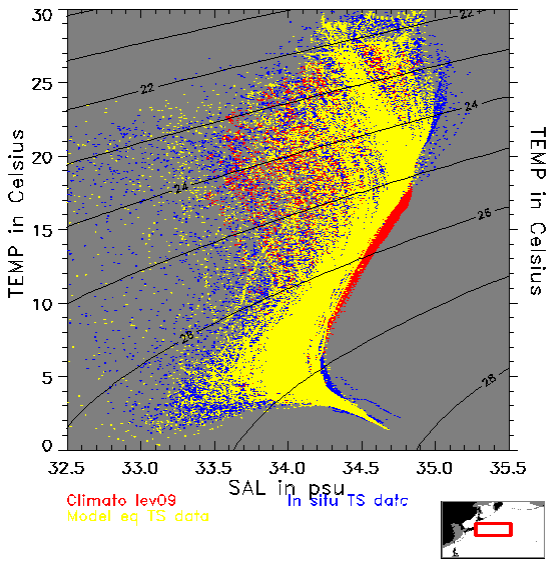
Diagram TS KUROSHIO
PSY4V2 hdcst vs In situ Coriolis
TEMP in Celsius
SAL in psu
Climato lev09
Model eq TS data
In situ TS data

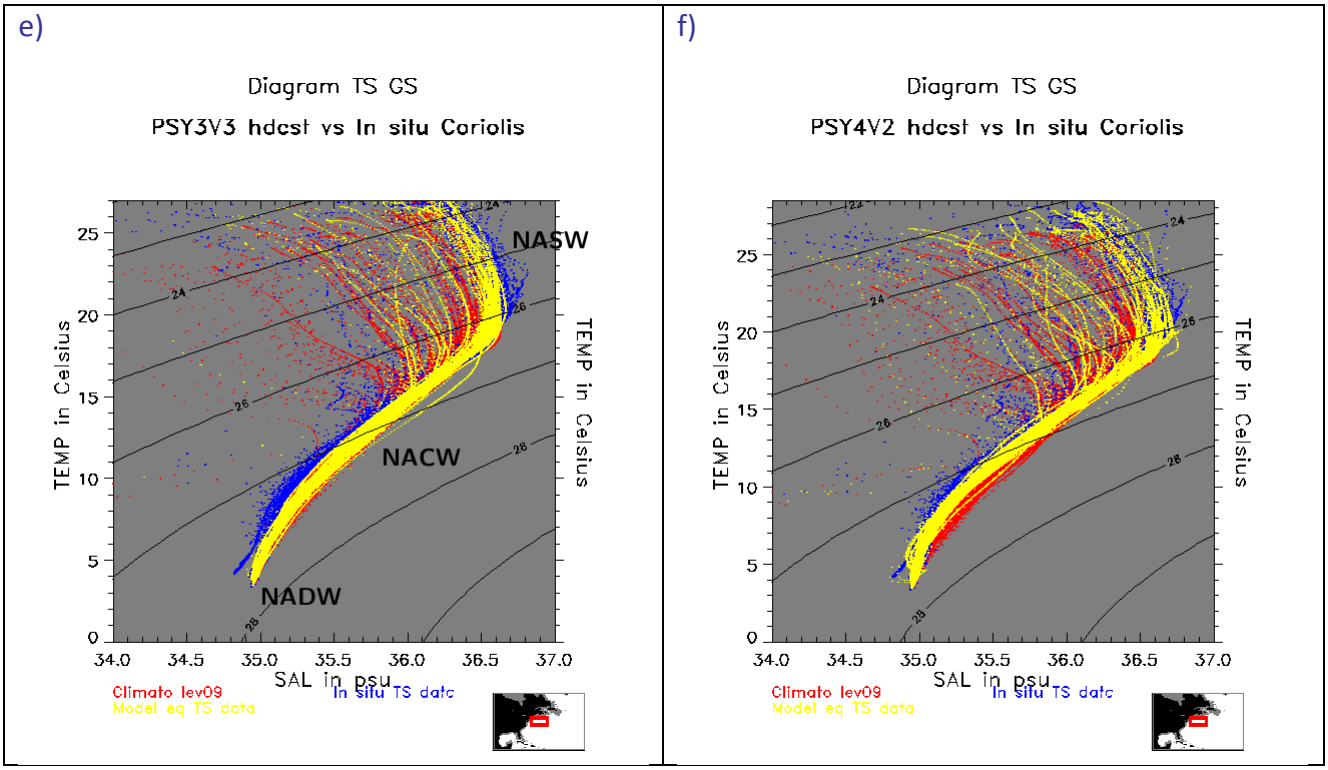

Figure 31: Water masses (T, S) diagrams in South Africa (a and b), Kuroshio (c and d), and Gulf Stream region (e and f): for PSY3V3R3 (a, c and e); PSY4V2R2 (b, d and f) in JAS 2014. PSY3 and PSY4: yellow dots; Levitus WOA09 climatology: red dots; in situ observations: blue dots.

V.2.1.2.1. Focus on Greenland Sea

We plot a section in the Greenland Sea with data coming from the NAOOS project. The Figure 32 below shows the positions of the in situ profiles between the 20140723 and the 20140930.

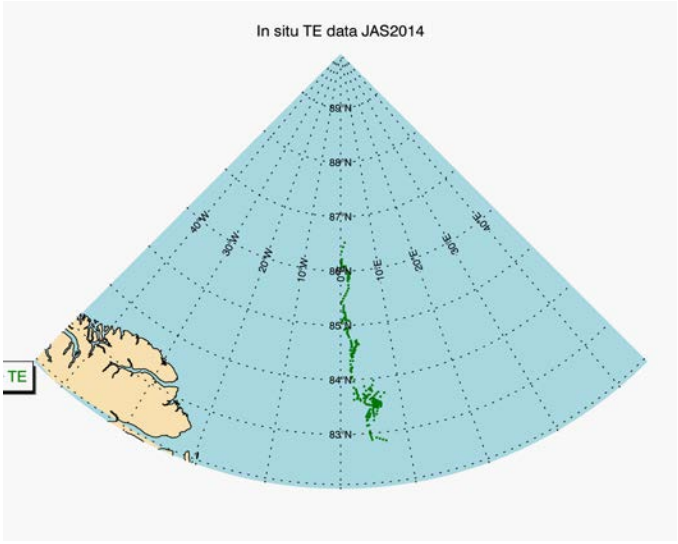

Figure 32 : Positions of In Situ TE profiles between the 23 July and 30 the September 2014

We compute a mean profiles each 0.1° to avoid multiple profiles in the same location and we plot the sections along latitude and longitude for the variables temperature and salinity (cf figures below)

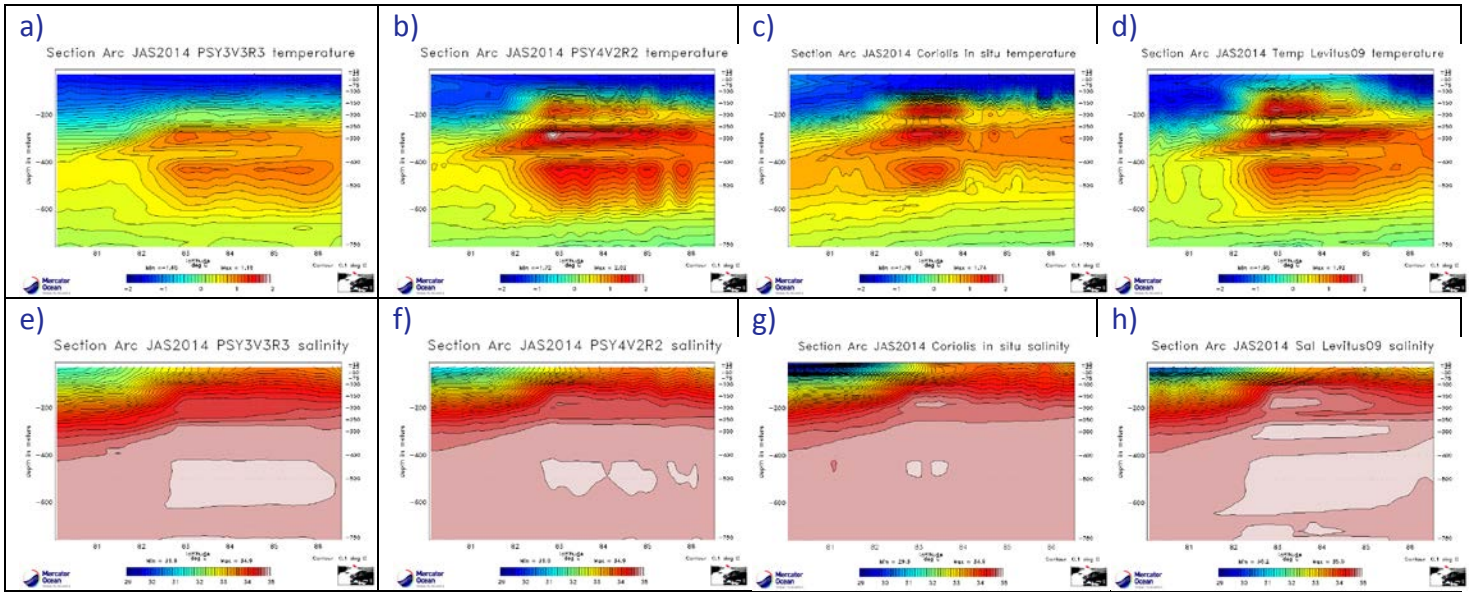

Figure 33 : Latitude/Depth Sections for temperature (a),b),c),d)) and salinity (e),f),g),h)) for PSY4V2R2 b),f), In situ data c),g), PSY3V3R3 a),e), and climatology WOA09 d),h). The region is situated in the Greenland Sea between 80°N and 87°N and 0 and 800m.

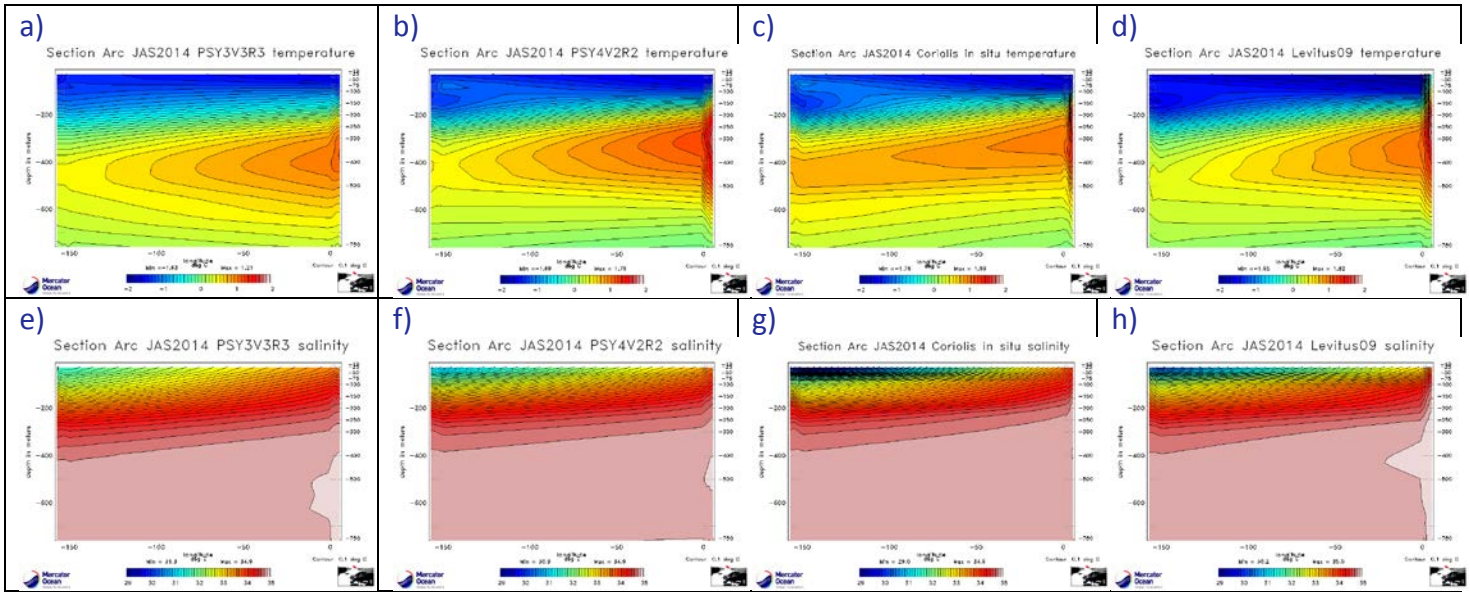

Figure 34 : Longitude/Depth Sections for temperature (a),b),c),d)) and salinity (e),f),g),h)) for PSY4V2R2 b),f), In situ data c),g), PSY3V3R3 a),e), and climatology WOA09 d),h). The region is situated in the Greenland Sea between 80°N and 87°N and 0 and 800m.

The Latitude/Depth diagrams show that the PSY4 and PSY3 systems are close to the observations in the South of the section even if the observations are fresher near the surface between 80 and 82°N. The subsurface Atlantic water appears in the observations between 100 and 500m seems to be too hot in PSY4 system but more realistic than PSY3: he is too cold in subsurface. The three core structure between 82°N and 84°N is probably an artifact of the data sampling. We can notice that the WOA09 climatology sticks the observations but appears too hot at the surface around 84°N.

The Longitude/Depth diagrams show the core of the Atlantic Water, it appears slightly hot for PSY4 and good for PSY3. The surface waters in the North of the section are too salty for the two systems**. Even if the systems don't assimilate these data the operational systems stay close to the observations**.

V.2.2. SST Comparisons

Quarterly average SST differences with OSTIA analyses show that the systems' SST is close to OSTIA, with difference values staying below the observation error of 0.5 °C on average. High RMS difference values (Figure 35) are encountered in high spatial and temporal variability regions such as the Gulf Stream, the Kuroshio or the Agulhas current. The error is also high (more than 2°C locally) in marginal seas of the Arctic Ocean where the sea ice limit increases the SST errors and the SST contrasts. This JAS 2014 season, the RMS difference is also high in the eastern tropical part of the Pacific Ocean.

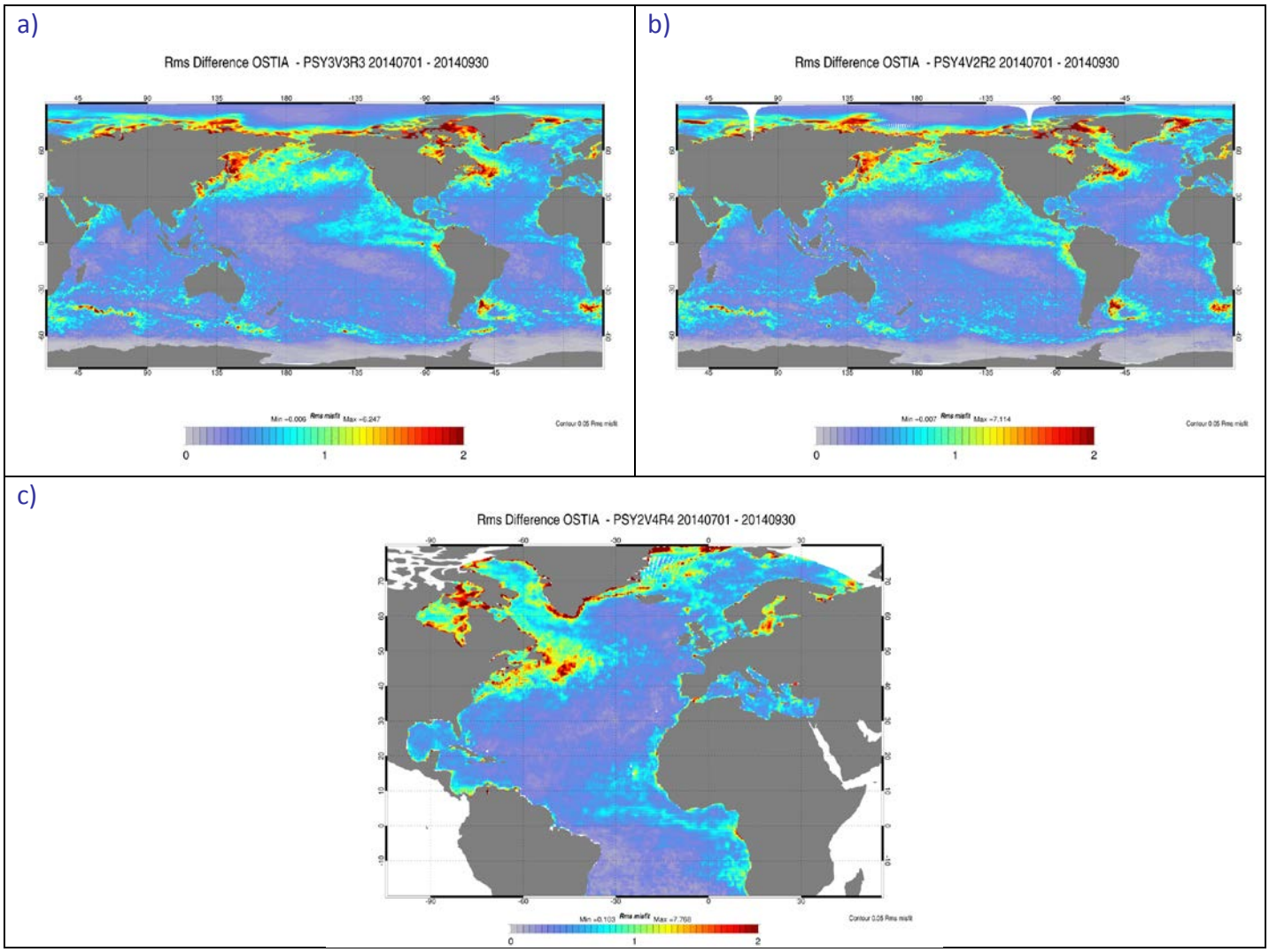

Figure 35 : RMS temperature (°C) differences between OSTIA daily analyses and PSY3V3R3 daily analyses (a); between OSTIA and PSY4V2R2 (b), between OSTIA and PSY2V4R4 (c) in JAS 2014. The Mercator Océan analyses are colocalised with the satellite observations analyses.

The systems' tropical oceans are warmer than OSTIA especially in the East Pacific Ocean (Figure 36), as do the south high latitudes (especially in the ACC this austral winter). In the South Indian Ocean and east of Australia, the systems are colder than OSTIA on average, as in the closed or semi-enclosed seas: the Sea of Okhotsk, the Mediterranean Sea; the North Sea; the Baltic Sea; the Labrador Sea and the Hudson Bay.

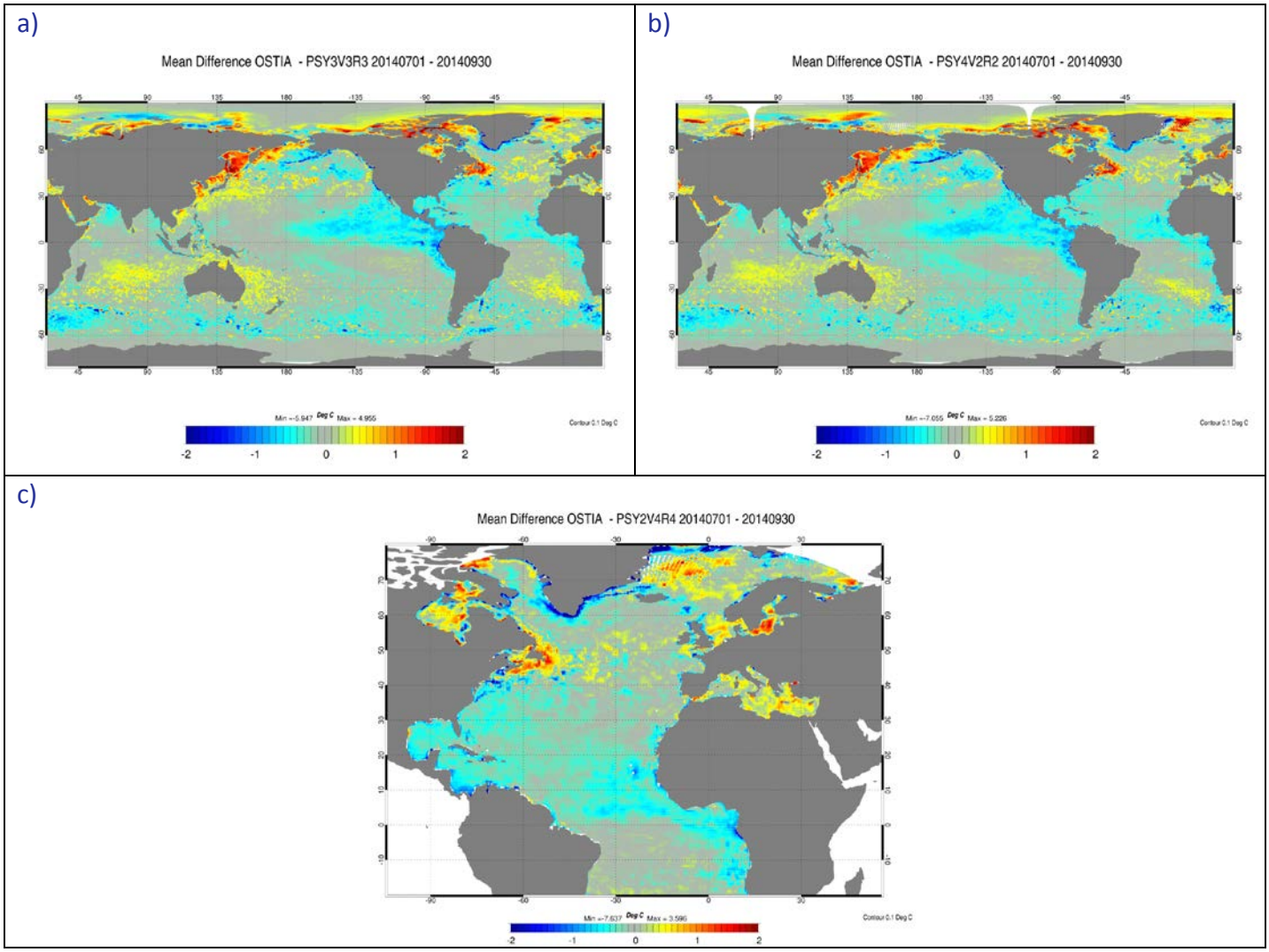

Figure 36: Mean SST (°C) daily differences inJAS 2014 between OSTIA daily analyses and PSY3V3R3 daily analyses (a), between OSTIA and PSY4V2R2 (b) and between OSTIA and PSY2V4R4 daily analyses (c).

V.2.3. Drifting buoys velocity measurements

Recent studies (*Law Chune, 2012*[3] , *Drévillon et al, 2012*[4]) - in the context of Search-And-Rescue and drift applications – focus on the need for accurate surface currents in ocean forecasting systems. *In situ* currents are not yet assimilated in the Mercator Ocean operational systems, as this innovation requires a better characterization of the surface currents biases.

The comparison of Mercator analyses and forecast with AOML network drifters velocities combines two methods based on Eulerian and Lagrangian approaches.

[3] Law Chune, 2012 : Apport de l'océanographie opérationnelle à l'amélioration de la prévision de la dérive océanique dans le cadre d'opérations de recherche et de sauvetage en mer et de lutte contre les pollutions marines

[4] Drévillon et al, 2012 : A Strategy for producing refined currents in the Equatorial Atlantic in the context of the search of the AF447 wreckage (Ocean Dynamics, Nov. 2012)

V.2.3.1. Eulerian Quality control

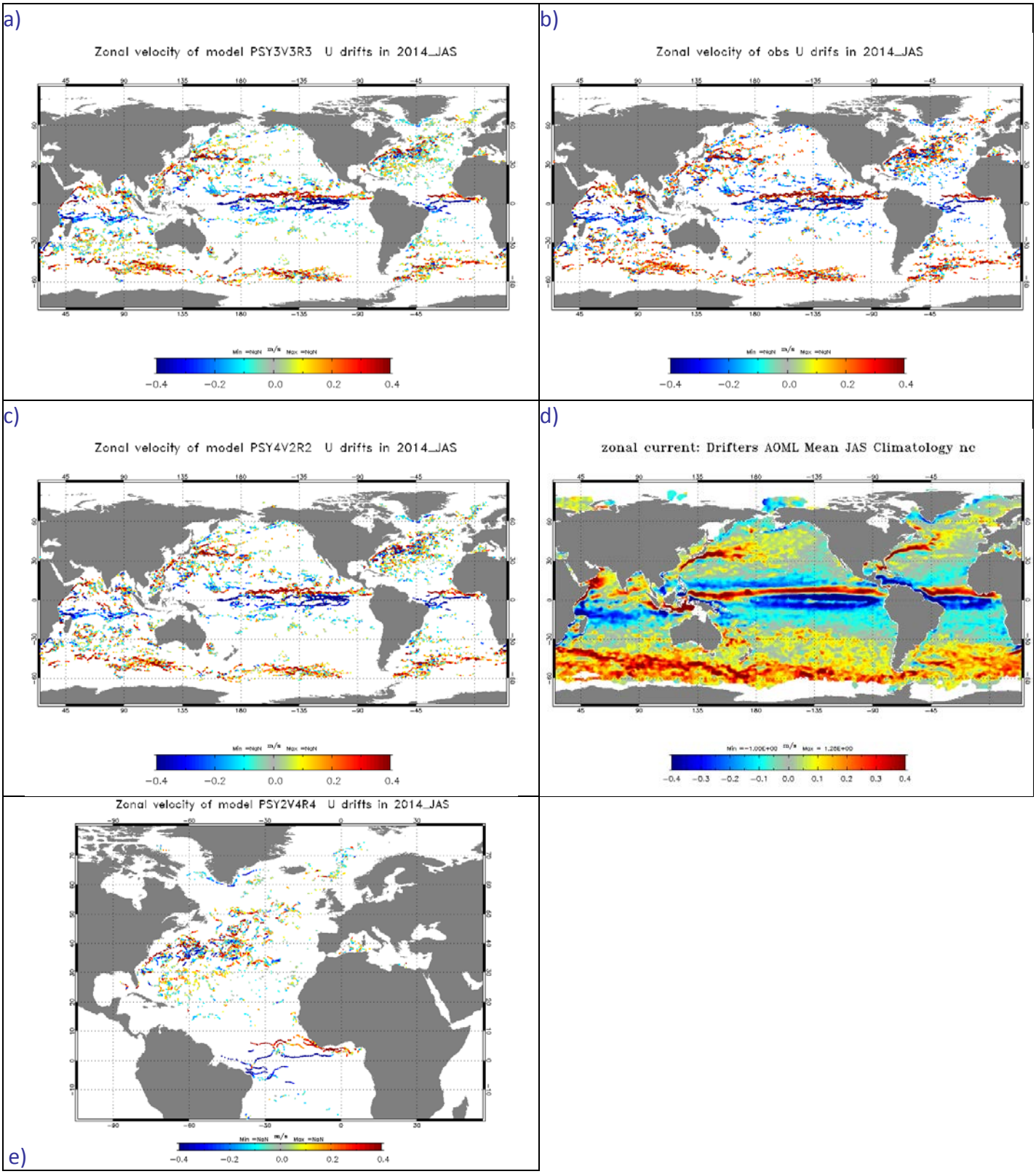

Figure 37: Near surface (15m) zonal current (m/s) comparison between the Mercator systems analyses and observed velocities from drifters. In the left column: velocities collocated with drifter positions in JAS 2014 for PSY3V3R3 (a), PSY4V2R2 (c) and PSY2V4R4 (e). In the right column, zonal current from drifters in JAS 2014 (b) at global scale, AOML drifter climatology for JAS with new drogue correction from Lumpkin & al, in preparation (d) and observed zonal current in JAS 2014 (b) over PSY2's domain.

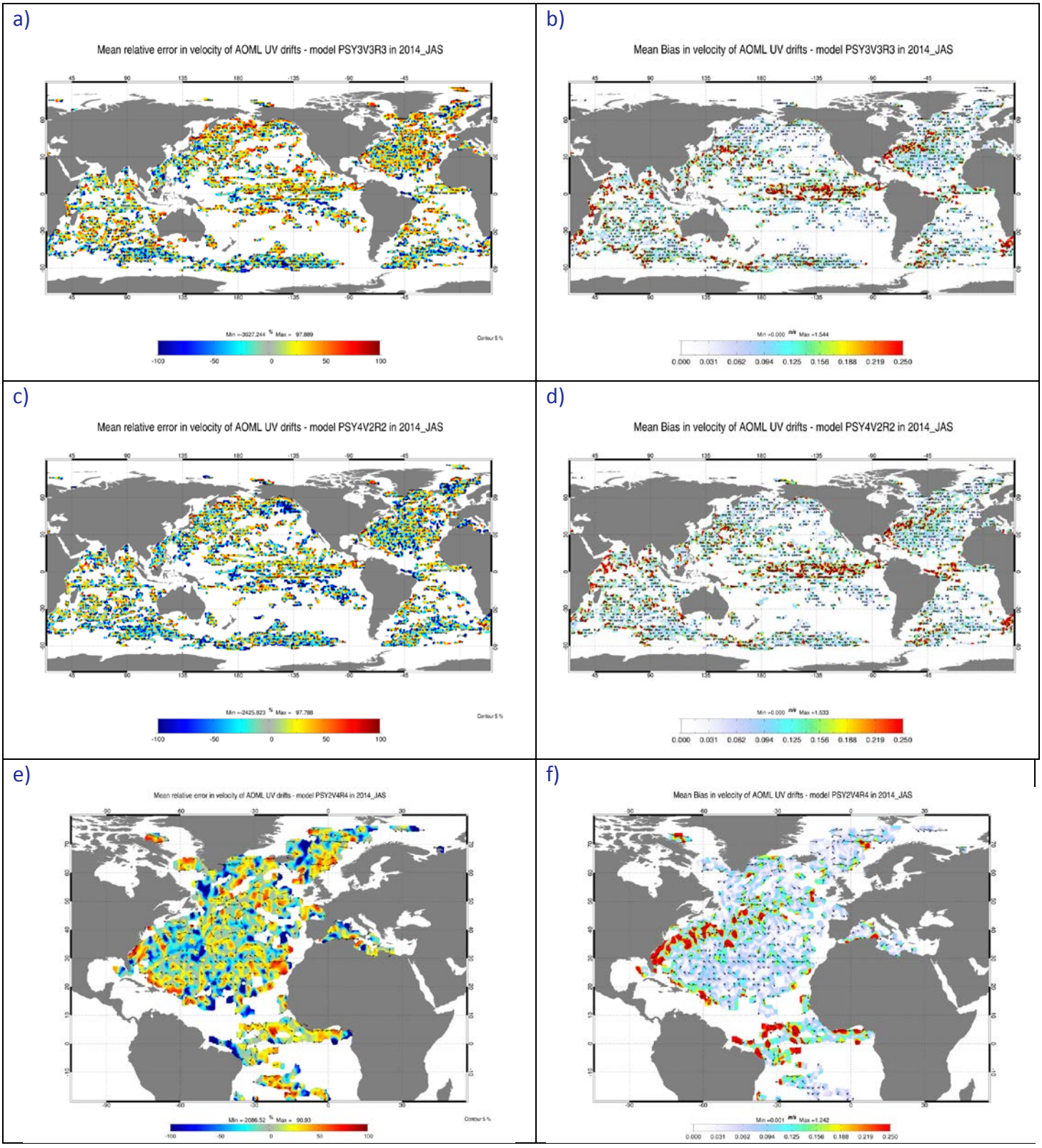

Figure 38 : In JAS 2014, comparison of the mean relative velocity error between in situ AOML drifters and model data (a, c and e) and mean zonal velocity bias between in situ AOML drifters with Mercator Océan correction (see text) and model data (b, d and f). a and b: PSY3V3R3, c and d: PSY4V2R2, e and f: PSY2V4R4. NB: zoom at 500% in order to see the arrows.

The fact that velocities estimated by the drifters happen to be biased towards high velocities is taken into account, applying slippage and windage corrections (cf *QuO Va Dis?* #5 and Annex C). Once this so called "Mercator Océan" correction is applied to the drifter observations, the zonal velocity of the model (Figure

37 and Figure 38) at 15 m depth and the meridional velocity (not shown) are more consistent with the observations for the JAS 2014 period.

On average over long periods, the usual behaviour compared to drifters' velocities is that the systems underestimate the surface velocity in the mid-latitudes. All systems overestimate the Equatorial currents and the southern part of the North Brazil Current (NBC).
For all systems the largest direction errors are local (not shown) and generally correspond to ill positioned strong current structures in high variability regions (Gulf Stream, Kurioshio, North Brazil Current, Zapiola eddy, Agulhas current, Florida current, East African Coast current, Equatorial Pacific Countercurrent).

The differences between the systems mainly appear in the North Atlantic and North Pacific Oceans on Figure 38, in the relative error. In these regions PSY3 underestimates on average the eastward currents, which is a bit less pronounced in the high resolution systems PSY4 and PSY2. On the contrary the systems overestimate the equatorial westward currents on average, and this bias is less pronounced in PSY3 than in PSY4. 50% of the ocean current feedbacks on the wind stress in PSY2 and PSY3, which slows the surface currents with respect to PSY4.

V.2.3.2. Lagrangian Quality control

The aim of the Lagrangian approach is to compare the observed buoy trajectory with virtual trajectories obtained with hindcast velocities, starting from the same observed initial location. The virtual trajectories are computed with the ARIANE software[5] (see annex III.2). The metric shown here (Figure 39) is the distance between the trajectories after 1, 3 and 5 days, displayed at each trajectory initial point.

a)

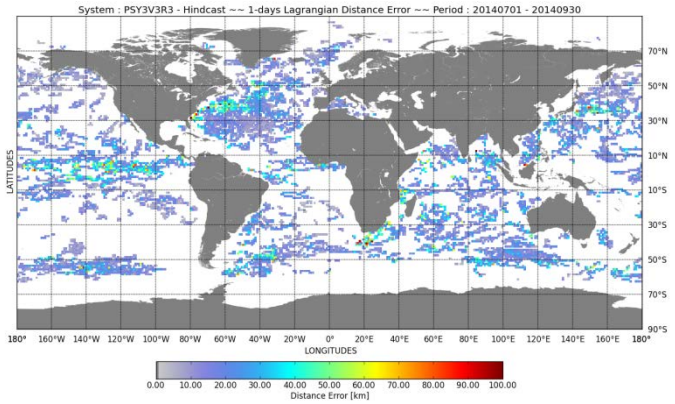

b)

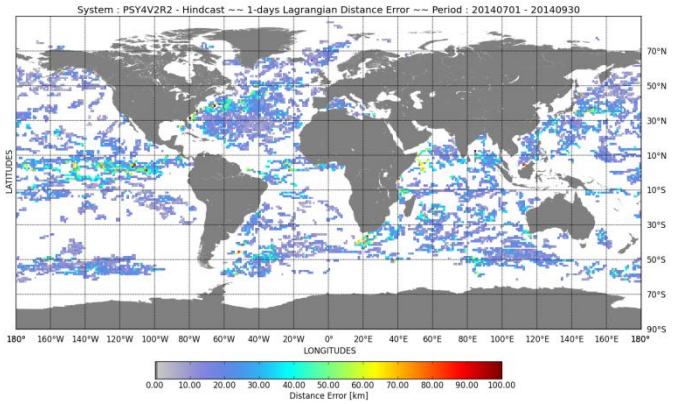

[5] http://stockage.univ-brest.fr/~grima/Ariane/

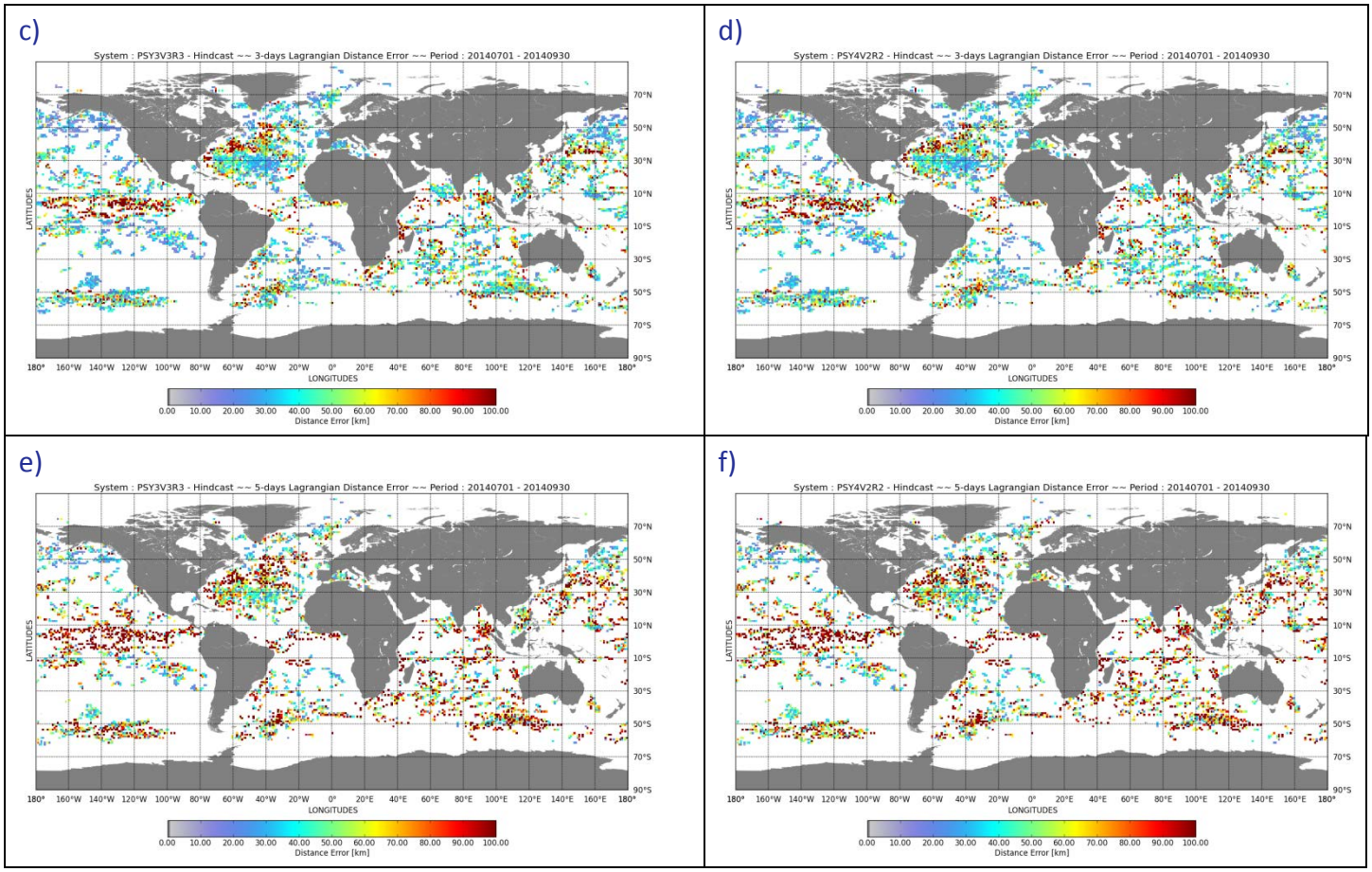

Figure 39: In JAS 2014, comparison of the mean distance error in 1°x1° boxes after a 1-day drift (a and b), after a 3-days drift (c and d), and after a 5-days drift (e and f).between AOML drifters' trajectories and PSY3V3R3 trajectories (a, c, and e) and between AOML drifters' trajectories and PSY4V2R2 (b,d, and f).

Few differences appear between the systems and most of the high velocity biases that are diagnosed in Figure 38 imply a large distance error (120 to 180km) after a few days drift in Figure 39. In the subtropical gyres and in the North Pacific, which are less turbulent regions, the errors rarely exceed 30 km after 5 days.

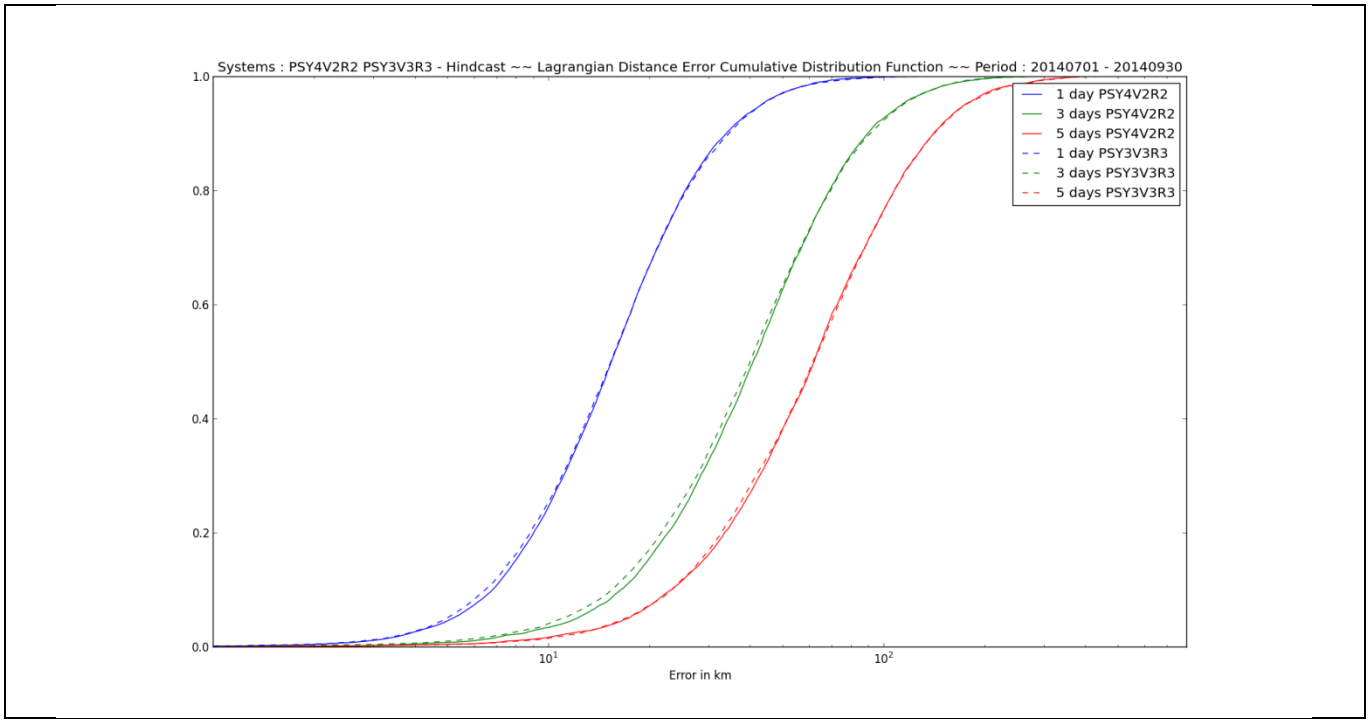

Figure 40: Cumulative Distribution Functions of the distance error (km, on the left) and the direction error (degrees, on the right panel) after 1 day (blue), 3 days (green) and 5 days (red), between PSY4V1R3 forecast trajectories and actual drifters trajectories.

Over the whole domain on a long period, cumulative distribution functions (Figure 40) show that in 80% of cases, PSY3 and PSY4 modelled drifters move away from the real drifters less than : 30km after 1 day, 70km after 3 days, and 100km after 5 days. As explained before, the remaining 20% generally correspond to ill positioned strong current structures in high variability regions. PSY4 currents seem to induce slightly more errors than PSY3 currents. This may not be systematic at the regional scale (under investigation).

V.2.4. Sea ice concentration

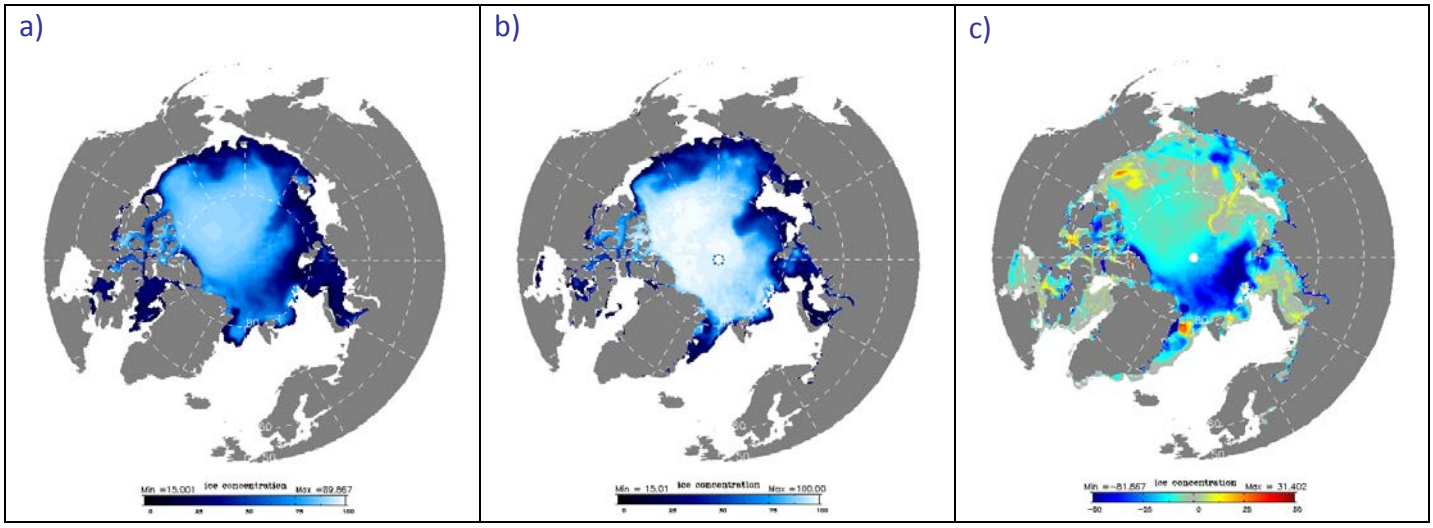

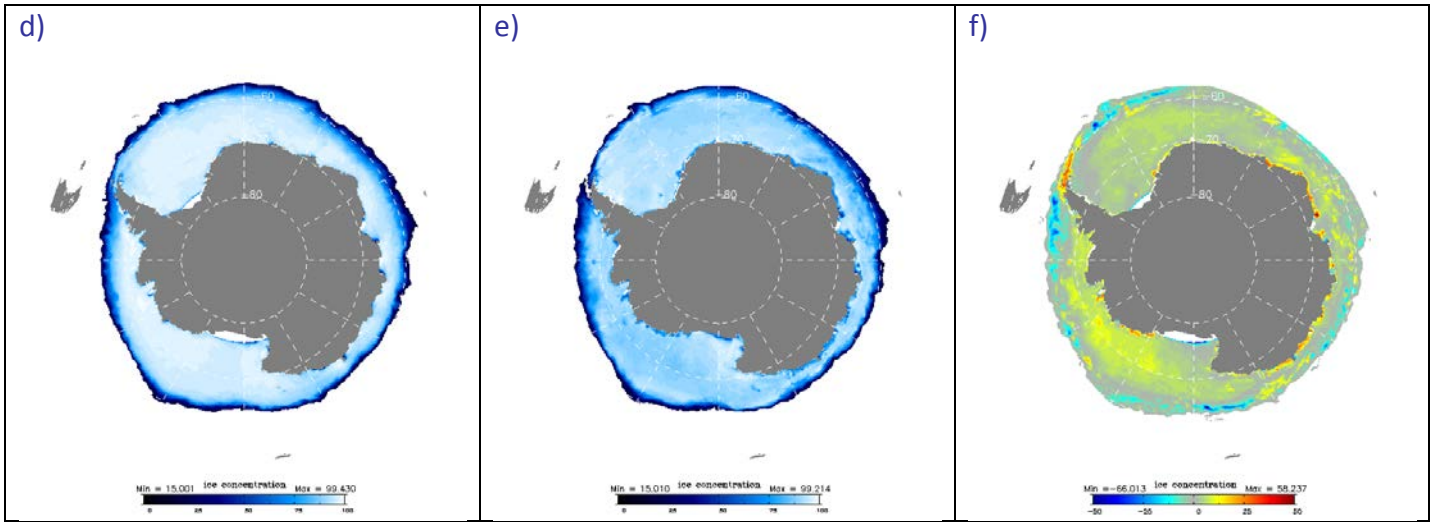

Figure 41: Arctic (a to c) and Antarctic (d to f) J 2014 Sea ice cover fraction in PSY3V3R3 (a and d), in CERSAT observations (b and e) and difference PSY3 – CERSAT (c and f).

On average over the JAS 2014 period, including the sea ice minimum of September, strong discrepancies with observed sea ice concentration appear between the centre of the Arctic and the Atlantic Ocean in PSY3 and PSY4 (Figure 41 and Figure 42) as sea ice observations are not yet assimilated by the systems. Both PSY3 and PSY4 are melting too much ice in summer, although differences are smaller in PSY4. The other small discrepancies that can be distinguished inside the sea ice pack will not be considered as significant as the sea ice concentration observations over 95% are not reliable. Differences with the observations remain significant in the marginal seas, for instance the sea ice melts too much in the Denmark Strait.

Model studies show that the overestimation in the Canadian Archipelago is first due to badly resolved sea ice circulation. The overestimation in the eastern part of the Labrador Sea is due to a weak extent of the West Greenland Current; similar behaviour in the East Greenland Current.

In the Antarctic the winter sea ice concentration is overestimated on average by both PSY3 and PSY4, for instance in the Weddell Sea. On the contrary it is underestimated along the sea ice edge.

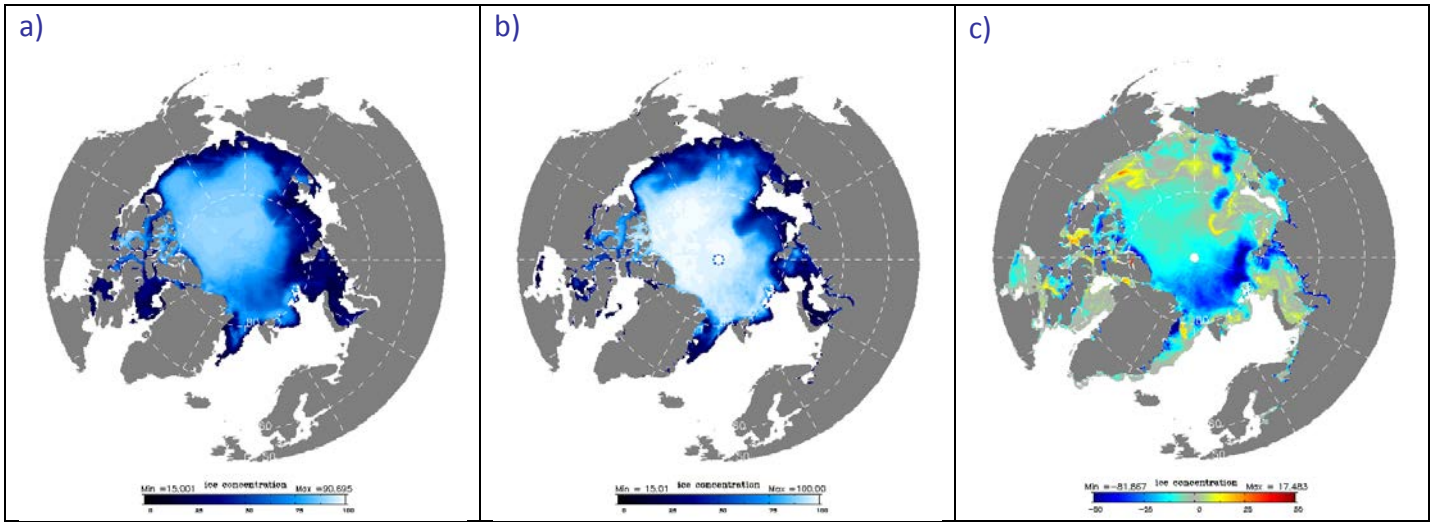

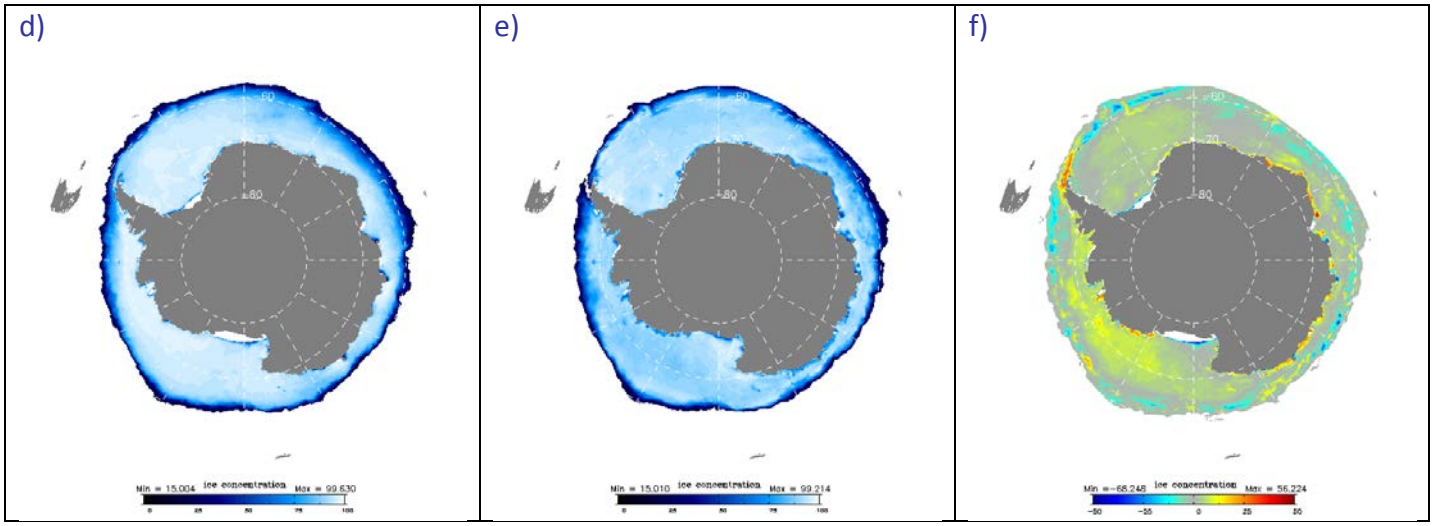

Figure 42: Arctic (a to c) and Antarctic (d to f) AMJ 2014 Sea ice cover fraction in PSY4V2R2 (a and d), in CERSAT observations (b and e) and difference PSY4 – CERSAT (c and f).

Figure 43 illustrates the fact that sea ice cover in JAS 2014 is less than the past years climatology, especially in the Nansen Basin (see also section IV).

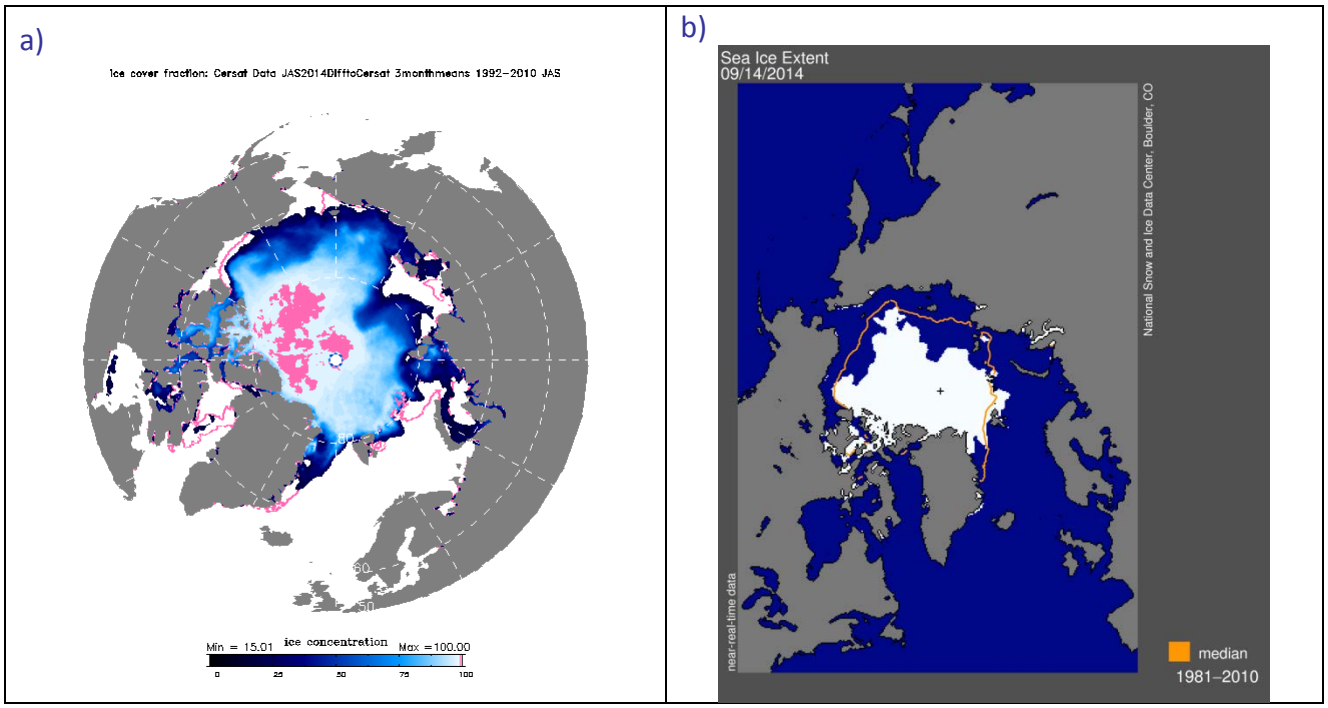

Figure 43: JAS 2014 Arctic sea ice extent in PSY4V2R2 with overimposed climatological AMJ 1992-2010 sea ice fraction (magenta line, > 15% ice concentration) (a) and NSIDC map of the sea ice extent in the Arctic for September 2014 in comparison with a 1981-2010 median extend (b).

V.2.5. Closer to the coast with the IBI36V2 system: multiple comparisons

V.2.5.1. Comparisons with SST from CMS

The bias, RMS error and correlation calculated from comparisons with SST measured by satellite in JAS 2014 (Météo-France CMS high resolution SST at 0.02°) are displayed in Figure 44. The bias patterns are similar to those observed in JAS 2013. The cold bias already noticed in the North Sea in AMJ 2014 is still present and extends to the Channel (except around the western part of Britanny) and the Irish Sea. A warm bias is present along the south Moroccan coast and Canary Islands, and along the Algerian coast. A warm bias is also present along the shelf slope between 46 and 50°N (where internal waves can be generated), and in the north of the British islands. In the English Channel and Celtic Sea, the biases are linked to tidal mixing. In the Mediterranean Sea, biases are associated to the Alboran gyre and the Algerian current. Away from the shelf, the bias is near zero and the RMS error is small (less than 0.5°C). The lower correlation is found western and eastern of the Gibraltar strait and in the northern part of the domain. The biases are lower along the west Iberian coast this summer JAS 2014 season with respect to the previous spring season. The correlation for PSY2 and PSY4 is almost the same than for IBI36. The bias along the shelf slope between 46 and 50°N is smaller in PSY2 and PSY4.
Note that the number of observations is very good for JAS 2014 except in the western part of the domain between 40°N and 50°N.

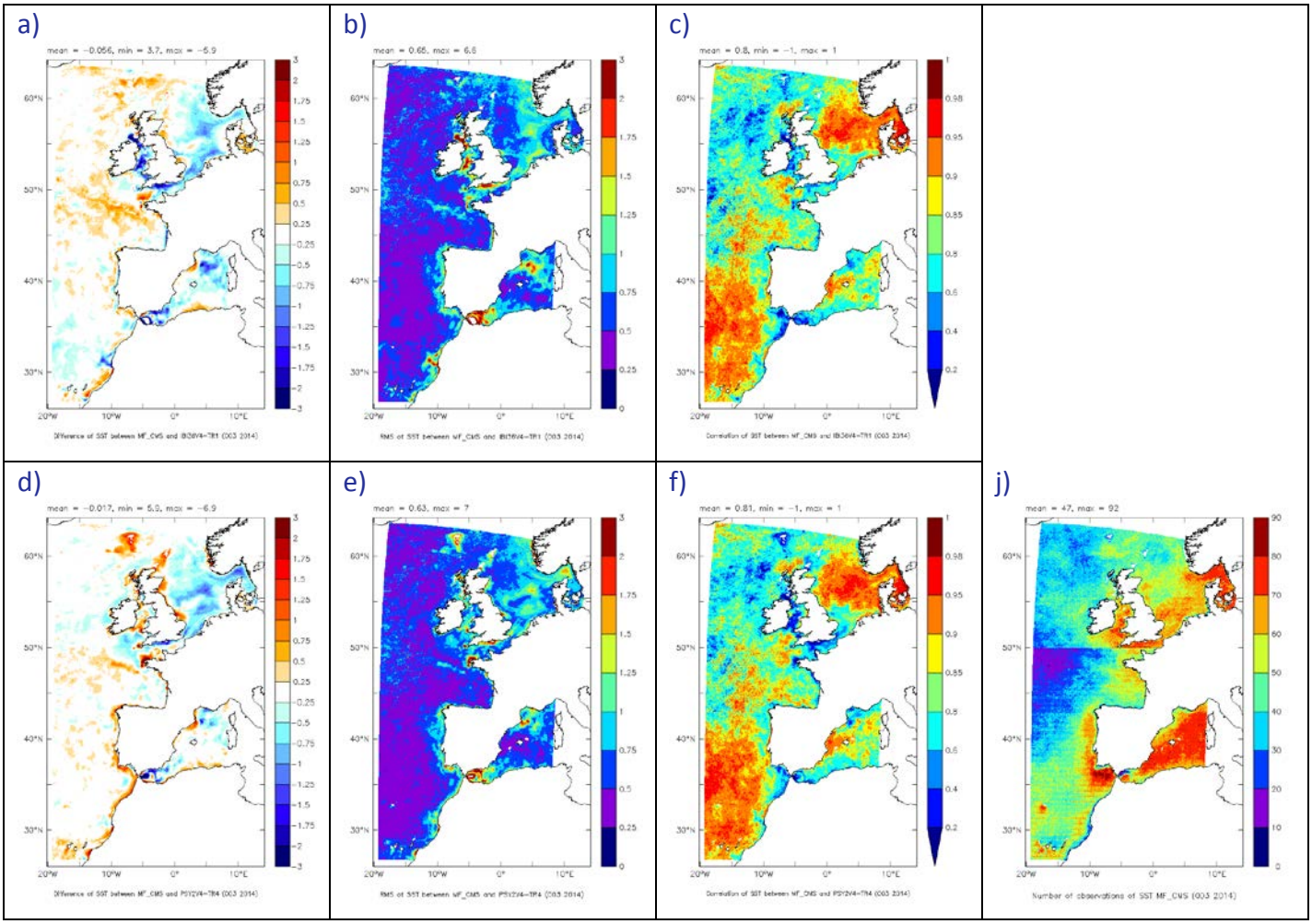

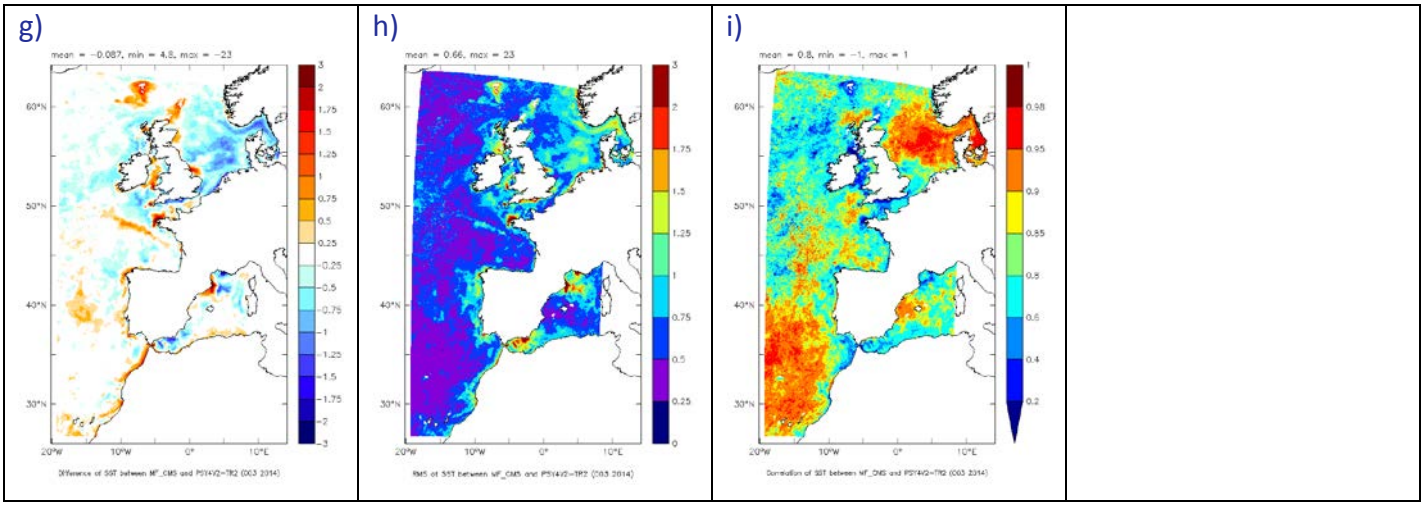

Figure 44 : Mean bias (model-observation) (a), RMS error (b), correlation (c) between IBI36V4 and analysed L3 SST from Météo-France CMS for the JAS 2014 quarter. Same diagnostics for PSY2V4R4 (d,e,f) and PSY4V2R2 (g,h,i). Number of Météo-France CMS observations for the JAS 2014 quarter (j).

V.2.5.2. Comparisons with in situ data from EN4/ENSEMBLE for JAS 2014

Averaged temperature profiles (Figure 49) show that the strongest mean bias and RMS error (more than 1.5°C) are observed between surface and 100 m depth, in the thermocline, and also around 500 m depth (more than 1°C, already present in AMJ 2014). The bias and RMS error in the thermocline are higher than in JAS 2013. Below 800 m depth, the mean bias is almost zero, and the strongest RMS is found at the Mediterranean Sea Water level. In the Bay of Biscay, the RMS error is similar to those of the domain average, except for the maximum around 500 m depth. As shown by the mean temperature profiles, IBI36 and PSY2 are very close.

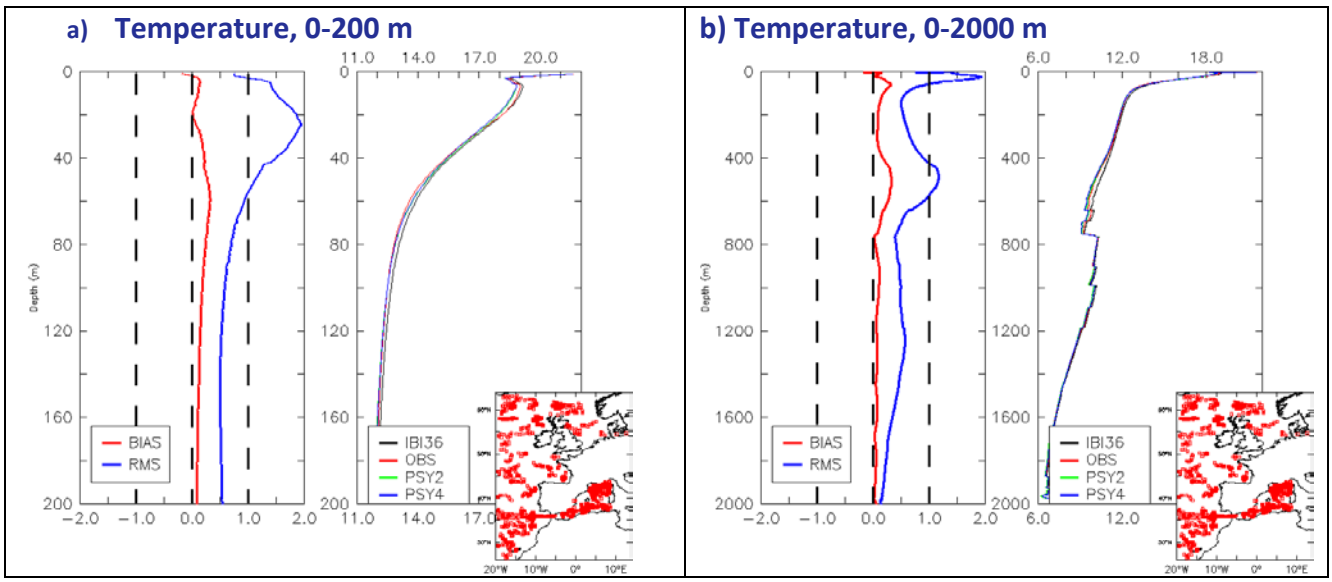

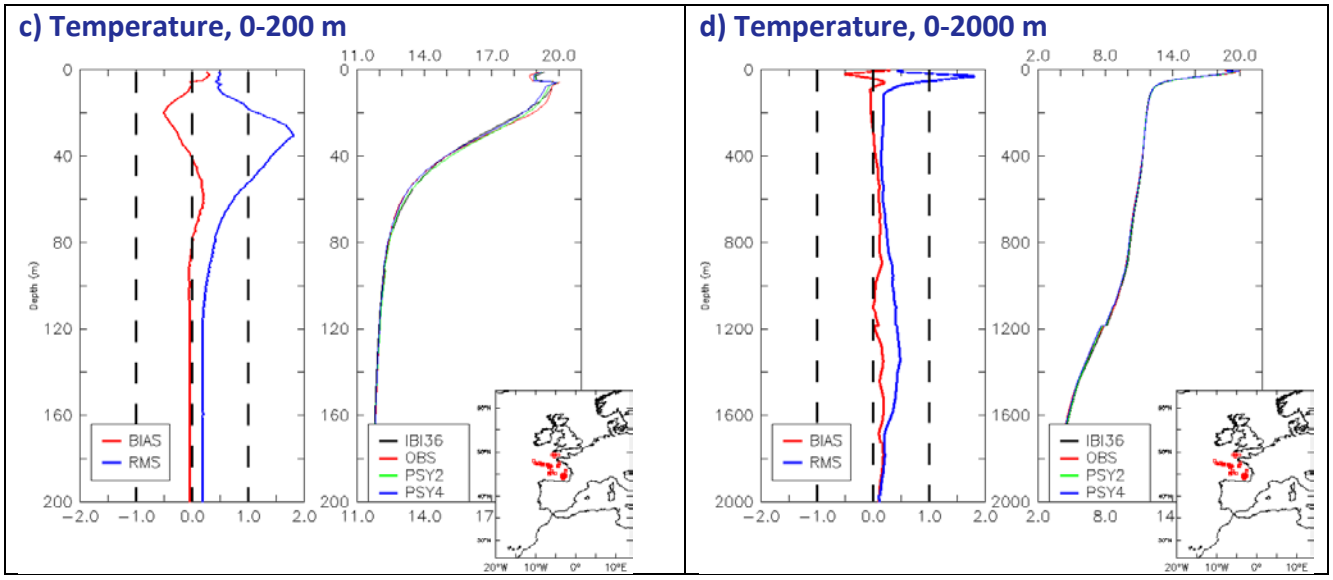

Figure 45 : Over the whole IBI36V4 domain (a and b) and over the Bay of Biscay (c and d): mean "IBI36V4 - observation" temperature (°C) bias (red) and RMS error (blue) in JAS 2014 (a and c), and mean profile from IBI36V4 (black), PSY2V4R4 (green) and from the observations (red) in JAS 2014 (b and d). In the lower right corner of each plot: position of the individual profiles.

The maximum salinity bias and RMS error (Figure 46) occur near the surface. The model is too fresh between the surface and 160 m depth, with PSY2 closer to the observations than IBI36. The RMS error is strong at the Mediterranean Sea Water level (as for temperature). In the Bay of Biscay the Mediterranean waters are slightly too fresh.
Note: averaged profiles are discontinuous because the number of observations varies with depth.

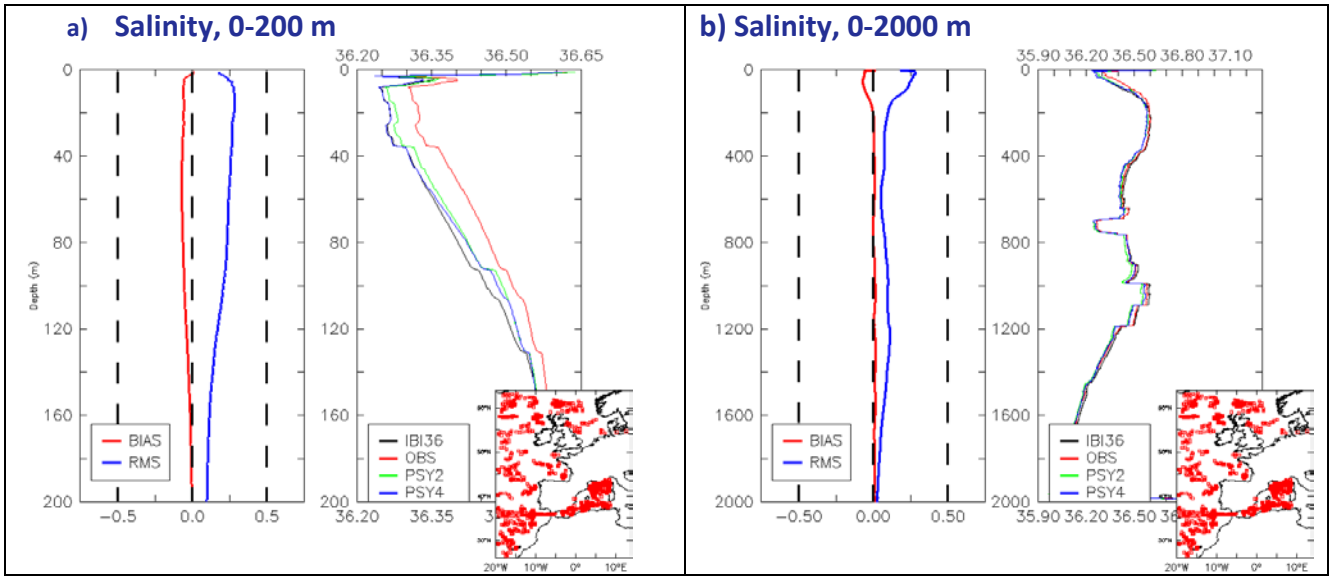

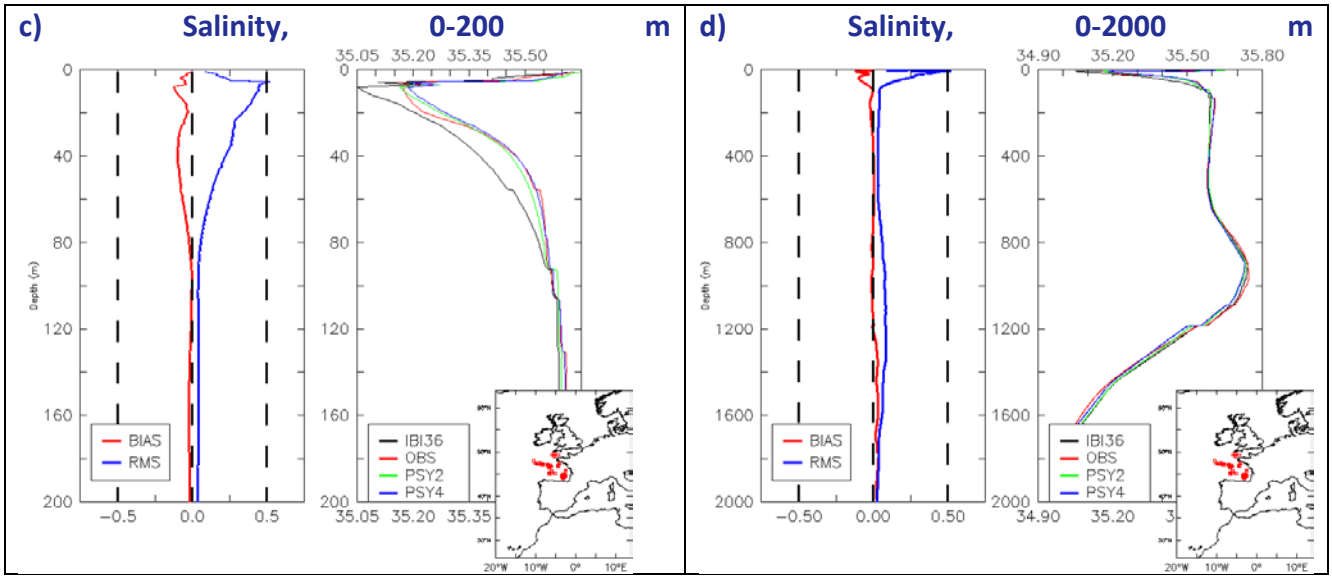

Figure 46: Over the whole IBI36V4 domain (a and b) and over the Bay of Biscay (c and d): mean "IBI36V4 - observation" salinity (psu) bias (red) and RMS error (blue) in JAS 2014 (a and c), and mean profile from IBI36V4 (black), PSY2V4R4 (green) and from the observations (red) in JAS 2014 (b and d). In the lower right corner of each plot: position of the individual profiles.

V.2.5.3. MLD Comparisons with in situ data

Figure 47 shows that the distribution of modeled mixed layer depths among the available profiles is comparable to the observed distribution for both PSY2 and IBI over the whole IBI domain. Values of the mixed layer depth between 5 m and 25 m occur too often in the systems compared with the observations (especially for PSY2), suggesting the mixed layer is too shallow in the systems. On the contrary, values between surface and 5 m are under-estimated by the systems. In the Bay of Biscay IBI36 is slightly closer to the observations than PSY2.

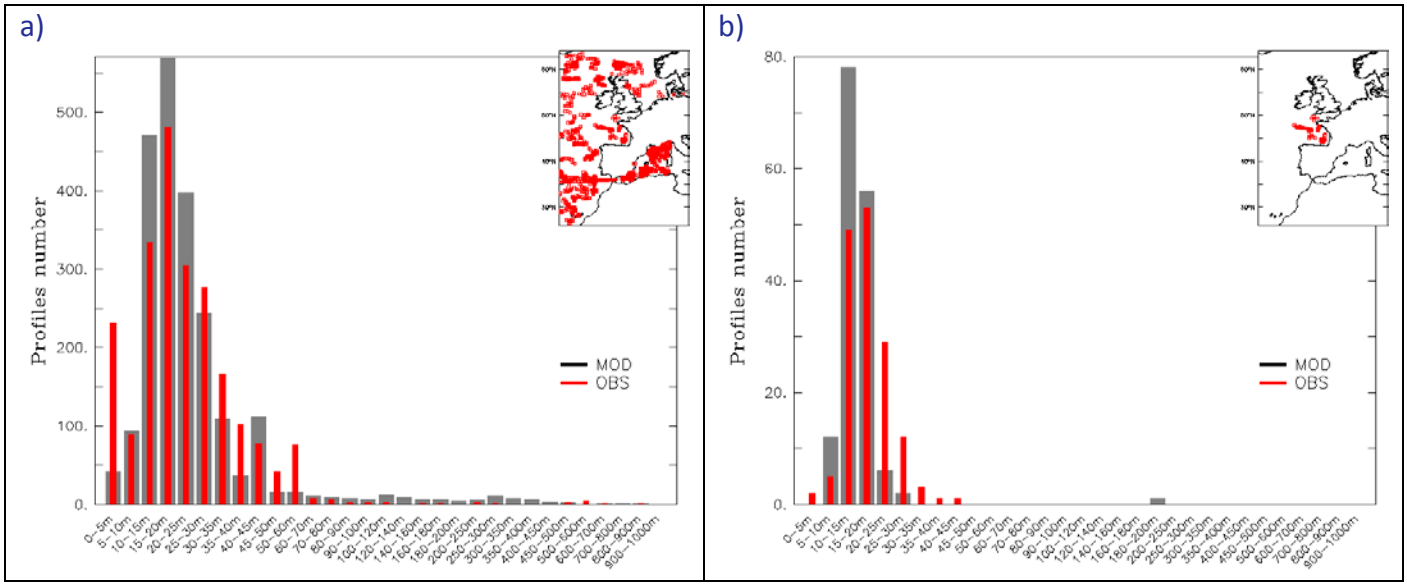

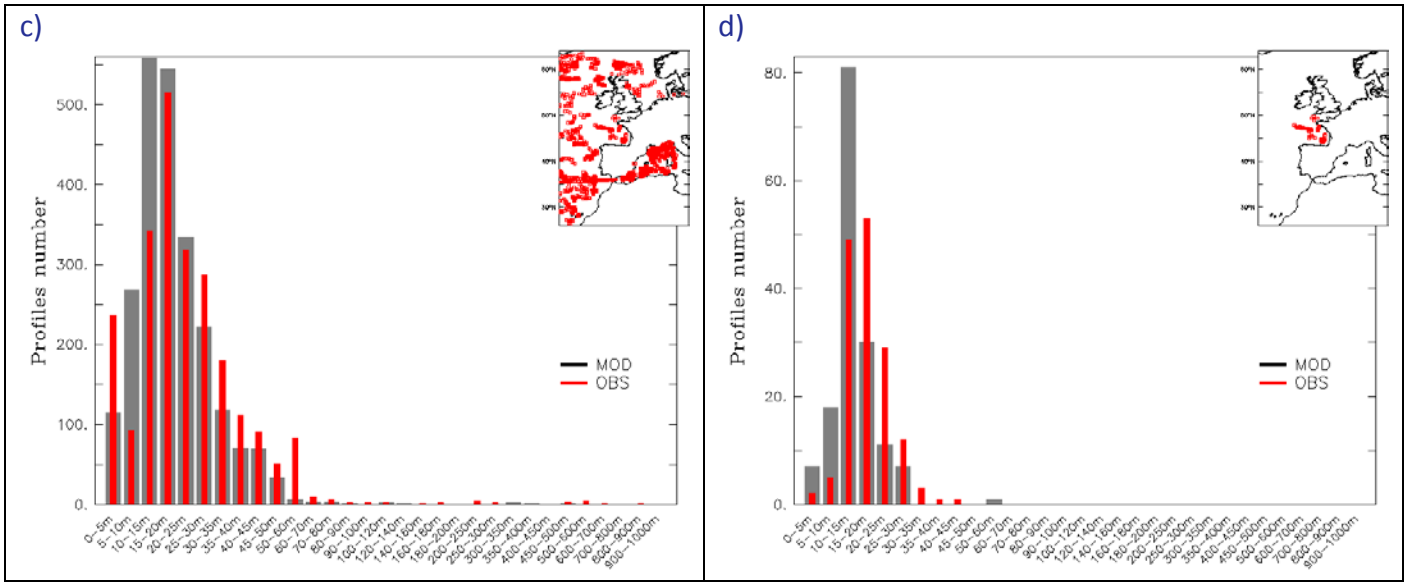

Figure 47 : Mixed Layer Depth distribution in JAS 2014 in IBI36V4 (a and b) and PSY2V4R4 (c and d), calculated from profiles with the temperature criteria (difference of 0.2°C with the surface); the models are in grey, the observations in red. a and c: classification for the whole IBI domain, b and d: classification for the Bay of Biscay.

V.2.5.4. Comparisons with moorings and tide gauges

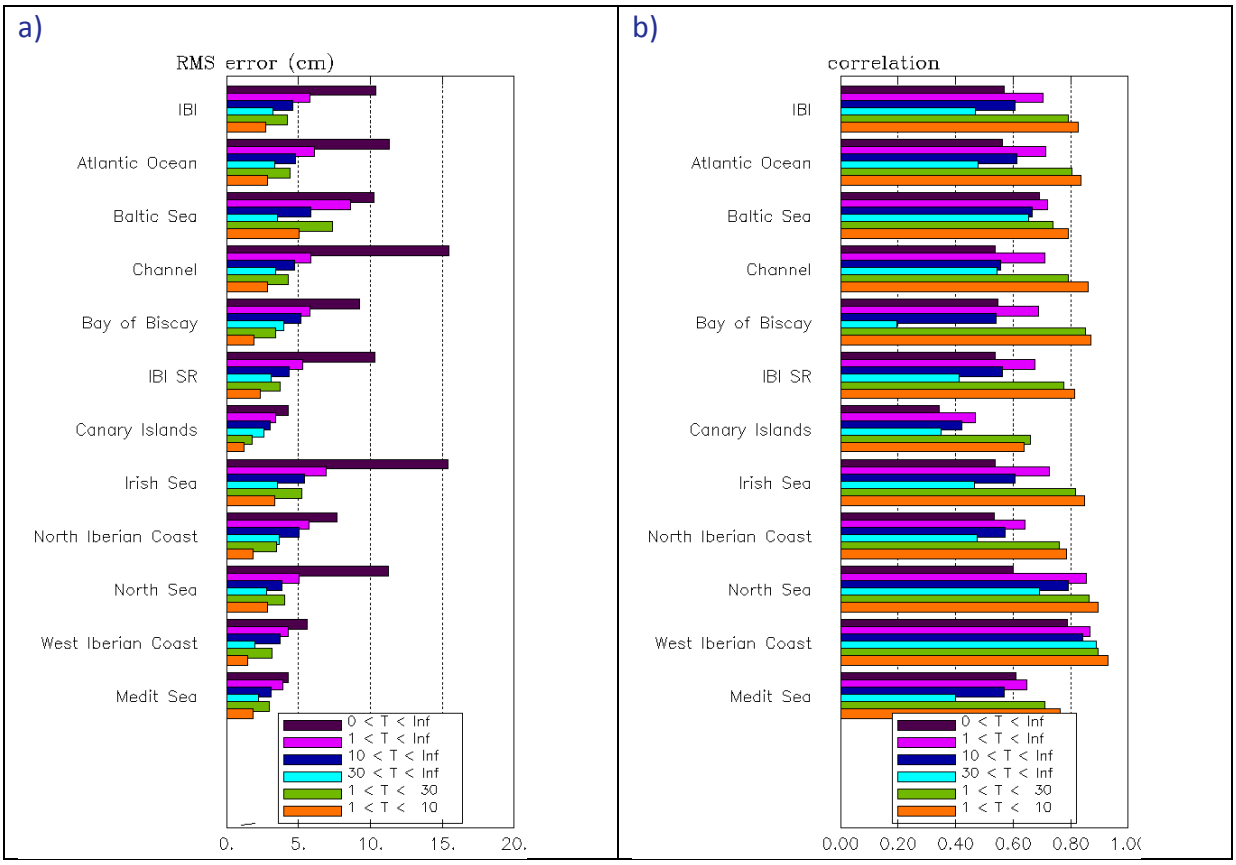

Figure 48 : For IBI36V4: RMS error (a, in cm) and correlation (b) for the non-tidal Sea Surface Elevation at tide gauges in JAS 2014, for different regions and frequencies.

The RMS error of the residual (non tidal) elevation of sea surface (Figure 51) computed with harmonic decomposition (Foreman 1977) and Loess low-pass filtering is between 4 and 16 cm. It is close to 5 cm in

the Canary Islands, Mediterranean Sea and Iberian Coast. The RMS decreases for some frequency bands, and the smallest values occur in the 1-10-day band. The correlation is significant at all frequencies, and reaches high values for periods lower than 30 days (at high frequencies).

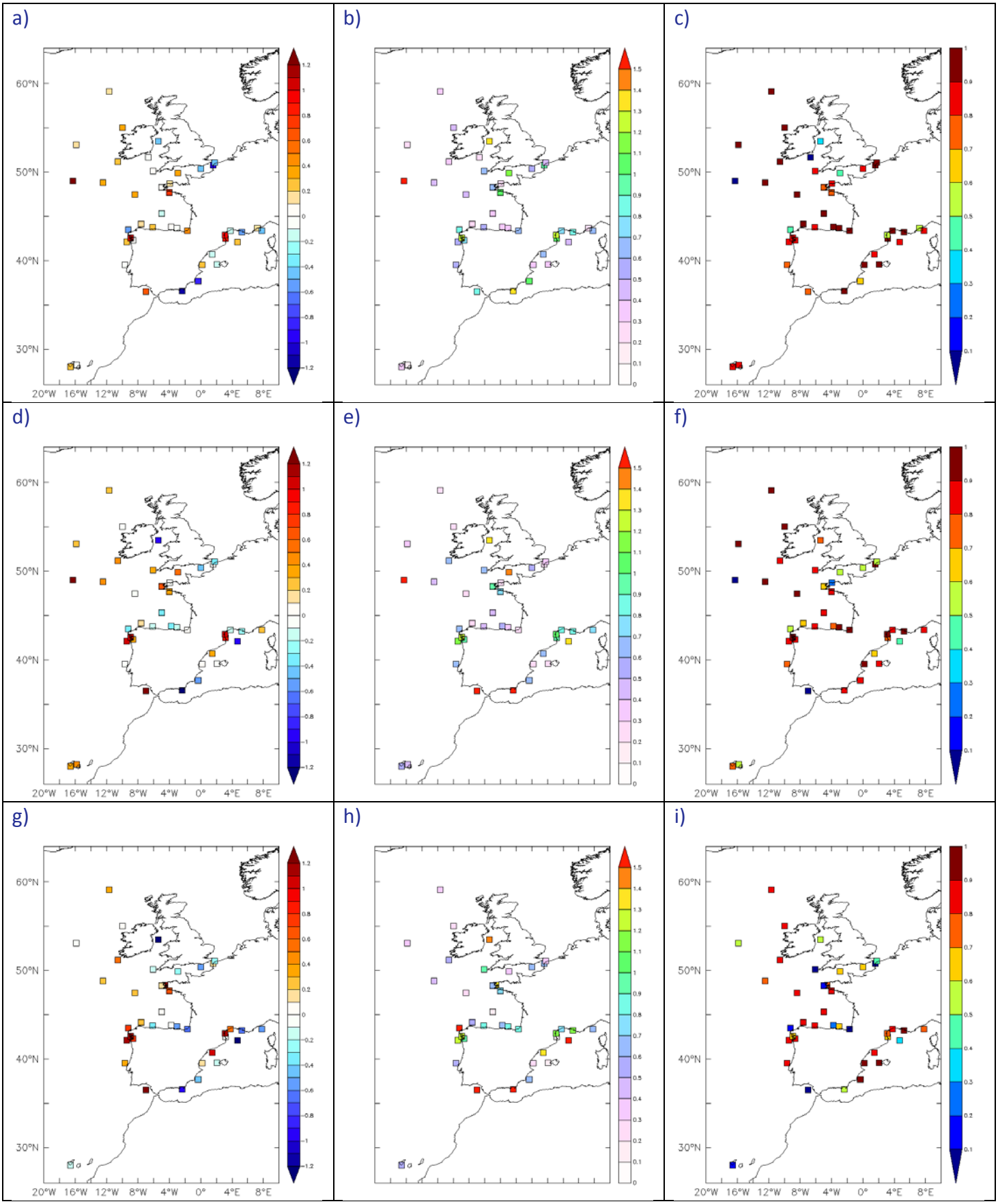

Figure 49 : For IBI36V4: Bias (observation-model) (a, d and g), RMS error (°C) (b, e and h) and correlation (c, f and i) of the Sea Surface Temperature between IBI36 and moorings measurements in July (a to c), August (d to f) and September 2014 (g to i).

In Figure 52 we can see that the SST correlations between the coastal moorings and the IBI model are generally good for the three months. Maximum values of correlation are reached in September. In the Irish Sea the bias is negative with low correlation, consistently with the L3 SST biases of Figure 44. At Villano Sisargas (north-west corner of Spain) the correlation is also weak.

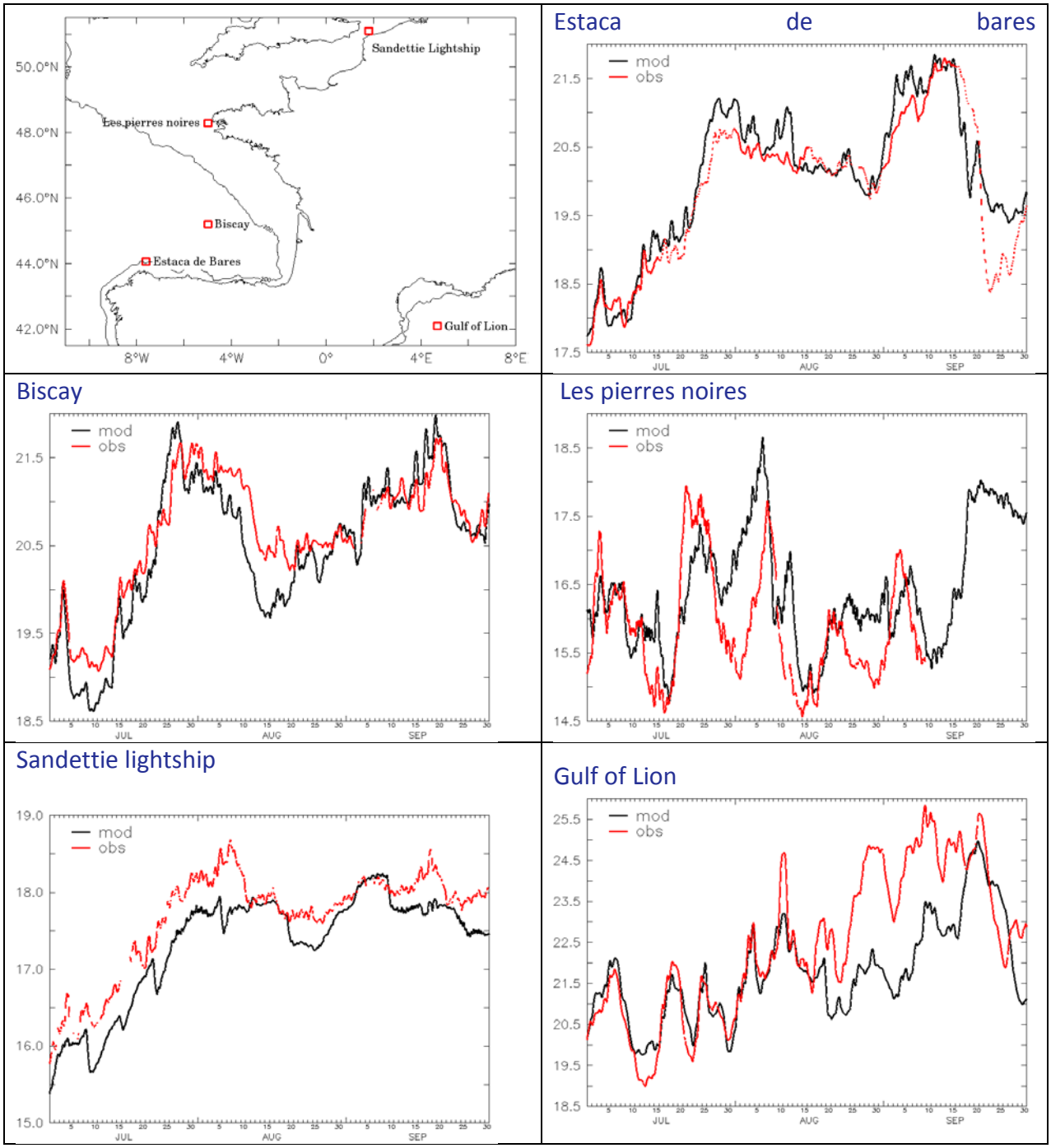

Figure 50: Surface temperature (°C) time series at a selection of moorings which locations are shown on the upper left panel (no observation for Gulf of Lion).

V.2.6. Biogeochemistry validation: ocean colour maps

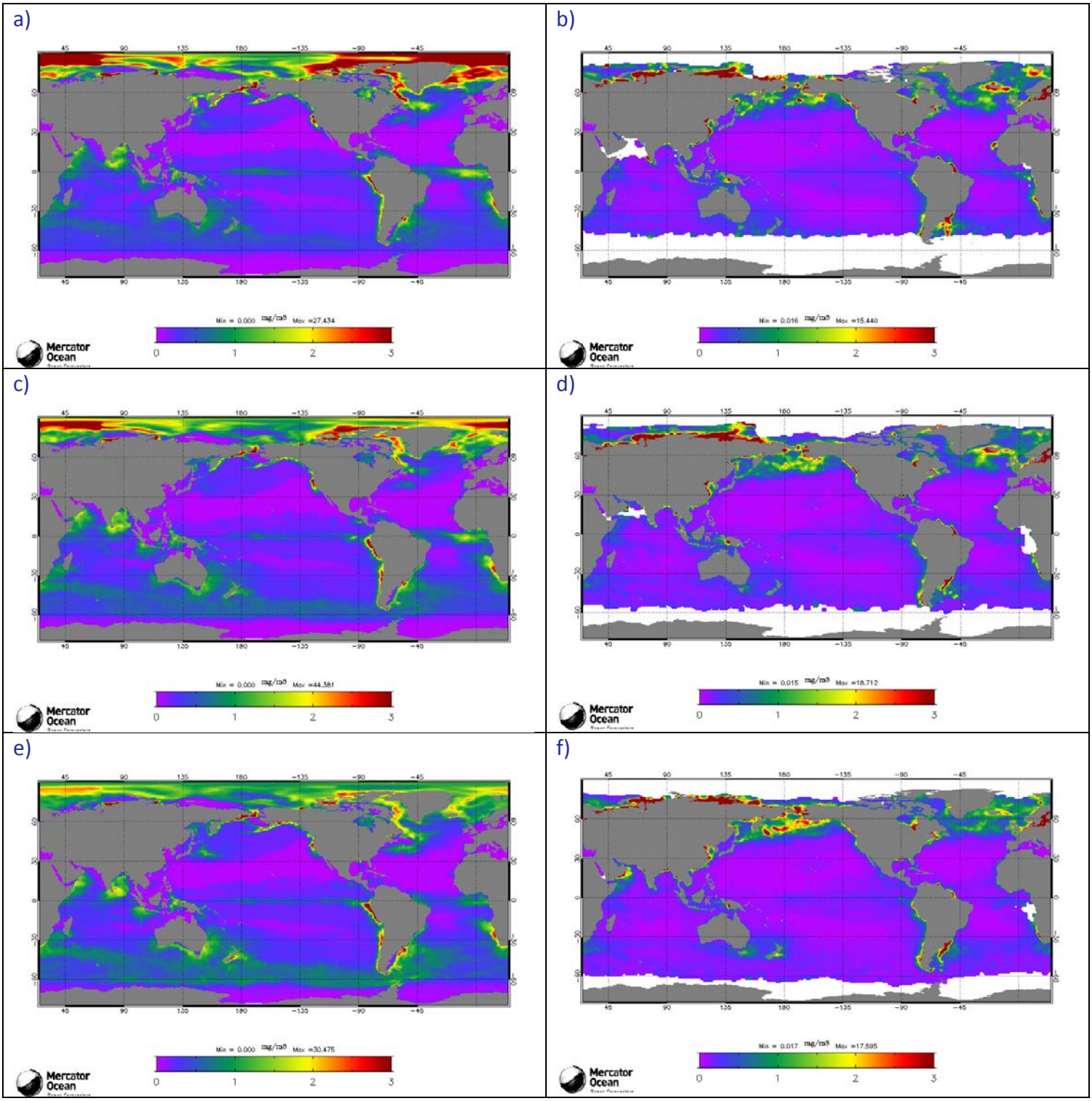

Figure 51 : Chlorophyll-a concentration (mg/m^3) in July (a and b), August (c and d) and September 2014 (e and f) for the Mercator system BIOMER1 (a, c, and e) and Chlorophyll-a concentration from Globcolour (b, d and f).

As can be seen in Figure 51 the surface chlorophyll-a concentration is overestimated by BIOMER1 on average over the globe. The production is especially overestimated in the Pacific and Atlantic tropical band. Blooms are observed in the northern hemisphere subpolar gyres. In the Atlantic it is slightly decaying from

July to September. In BIOMER1, the blooms have already disappeared before the beginning of the JAS quarter. Some coastal regions or semi enclosed seas like the North and Baltic seas or the China Seas do not display local enrichments that can be detected in the observations. On the contrary, BIOMER1 displays unobserved enrichments in the upwelling of Peru and Benguela, as well as in regions of high variability sugh as the Zapiola eddy or the Somali Gyre. Figure 52 shows the PDF of the Chl-a bias in North Atlantic. The positive values between 1 and 3 mg/m3 correspond mainly to the high values of the bloom in Globcolour that are not reproduced by BIOMER1. The highest positive biases are observed in September.

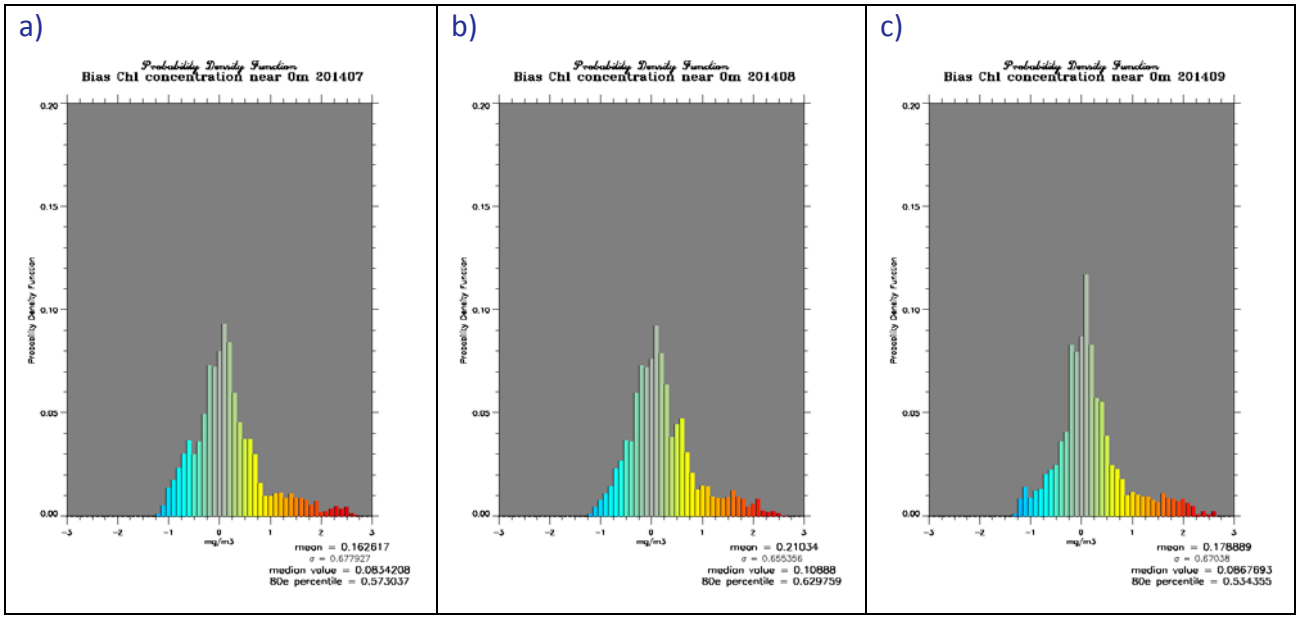

Figure 52 : Probability Density Function (PDF) of Chl-a bias in log scale (log10(obs)-log10(model)) in the North Atlantic (30-70N; 80W:20E) for July (a), August (b) and September (c) 2014.

The discrepancies at the global scale appear in the RMS differences for the mean JAS 2014 season (Figure 53).

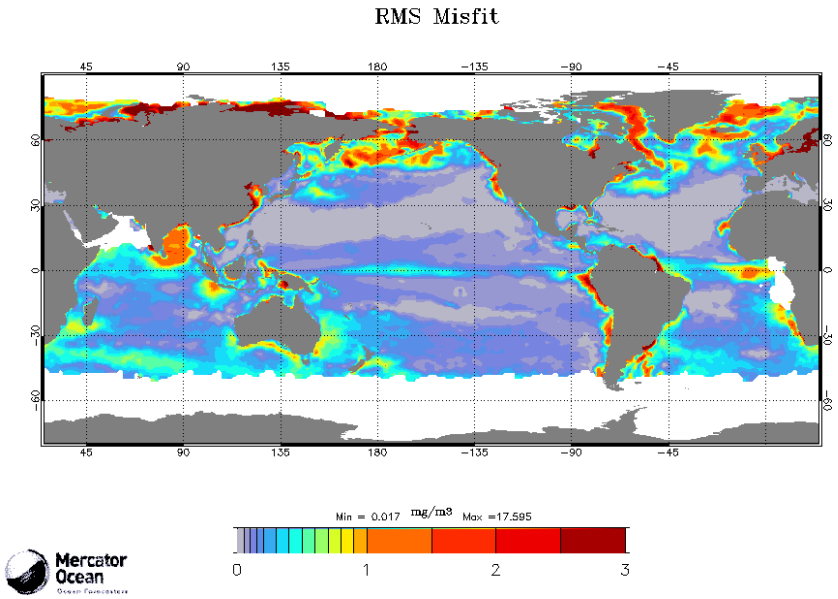

Figure 53 : RMS difference between BIOMER1 and Globcolour Chl-a concentrations (mg/m^3) in JAS 2014.

VI Forecast error statistics

VI.1. General considerations

The daily forecasts (with updated atmospheric forcings) are validated in collaboration with SHOM/CFUD. This collaboration has been leading us to observe the degradation of the forecast quality depending on the forecast range. When the forecast range increases the quality of the ocean forecast decreases as the initialization errors propagate and the quality of the atmospheric forcing decreases. Additionally the atmospheric forcing frequency also changes (see Figure 54). The 5-day forecast quality is optimal; starting from the 6th day a drop in quality can be observed which is linked with the use of 6-hourly atmospheric fields instead of 3-hourly; and starting from the 10th day the quality is strongly degraded due to the use of persisting atmospheric forcings (but not constant from the 10th to the 14th day as they are relaxed towards a 10-day running mean).

Figure 54: Schematic of the change in atmospheric forcings applied along the 14-day ocean forecast.

VI.2. Forecast accuracy: comparisons with T and S observations when and where available

VI.2.1. North Atlantic region

As can be seen in Figure 55 the PSY2 temperature products have a better accuracy than the climatology in the North Atlantic region in JAS 2014 (note that in the 2000-5000m layer, the statistics are performed on a very small sample of observations, and thus are not really representative of the region or layer), except for the surface salinity.
In general the analysis is more accurate than the 3-day and 6-day forecast for both temperature and salinity. The RMS error thus increases with the forecast range (shown for NAT region Figure 55 and MED region Figure 56). The biases in temperature are generally small compared to the climatology's biases while the salinity biases are significant (0.12 psu at the surface while the climatology bias is only 0.08 psu). The surface salinity is biased (~0.1 psu) towards saltier waters than observed.

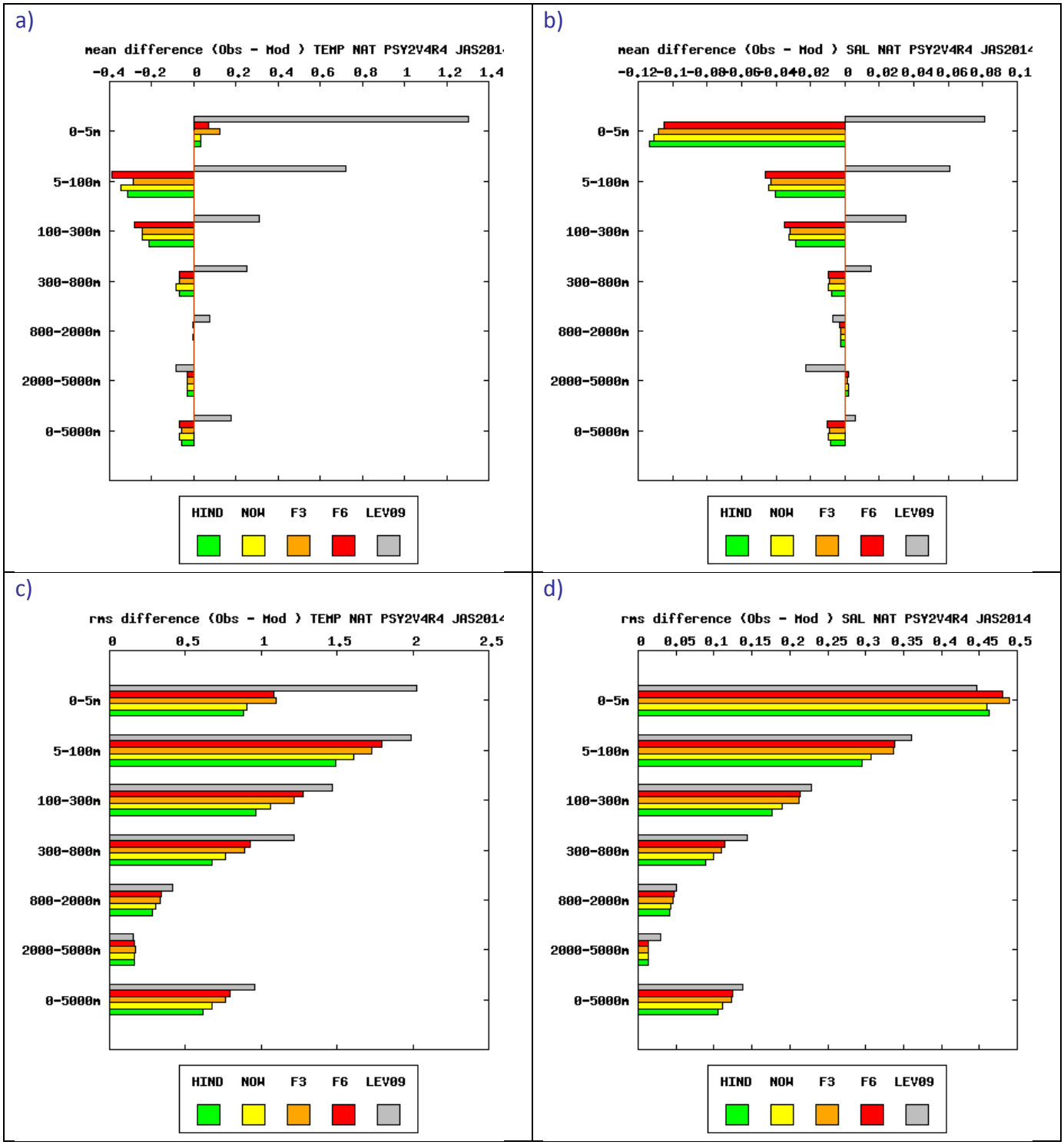

Figure 55: Accuracy intercomparison in the North Atlantic region for PSY2V4R4 in temperature (a and c) and salinity (b and dl) between hindcast (green), nowcast (yellow), 3-day (orange) and 6-day (red) forecast and WO09 climatology (grey). Accuracy is measured by a mean difference (a and b) and by a rms difference (c and d) of temperature and salinity with respect to all available observations from the CORIOLIS database averaged in 6 consecutive layers from 0 to 5000m. All statistics are performed for the JAS 2014 period. NB: average on model levels is performed as an intermediate step which reduces the artefacts of inhomogeneous density of observations on the vertical.

VI.2.2. Mediterranean Sea

In the Mediterranean Sea in JAS 2014 (Figure 56) the PSY2 products are more accurate than the climatology on average. PSY2 is less biased in temperature than in the North Atlantic (not at surface) and PSY2's salinity RMS error is smaller than the climatology's. Between surface and 800m the system is generally too fresh.

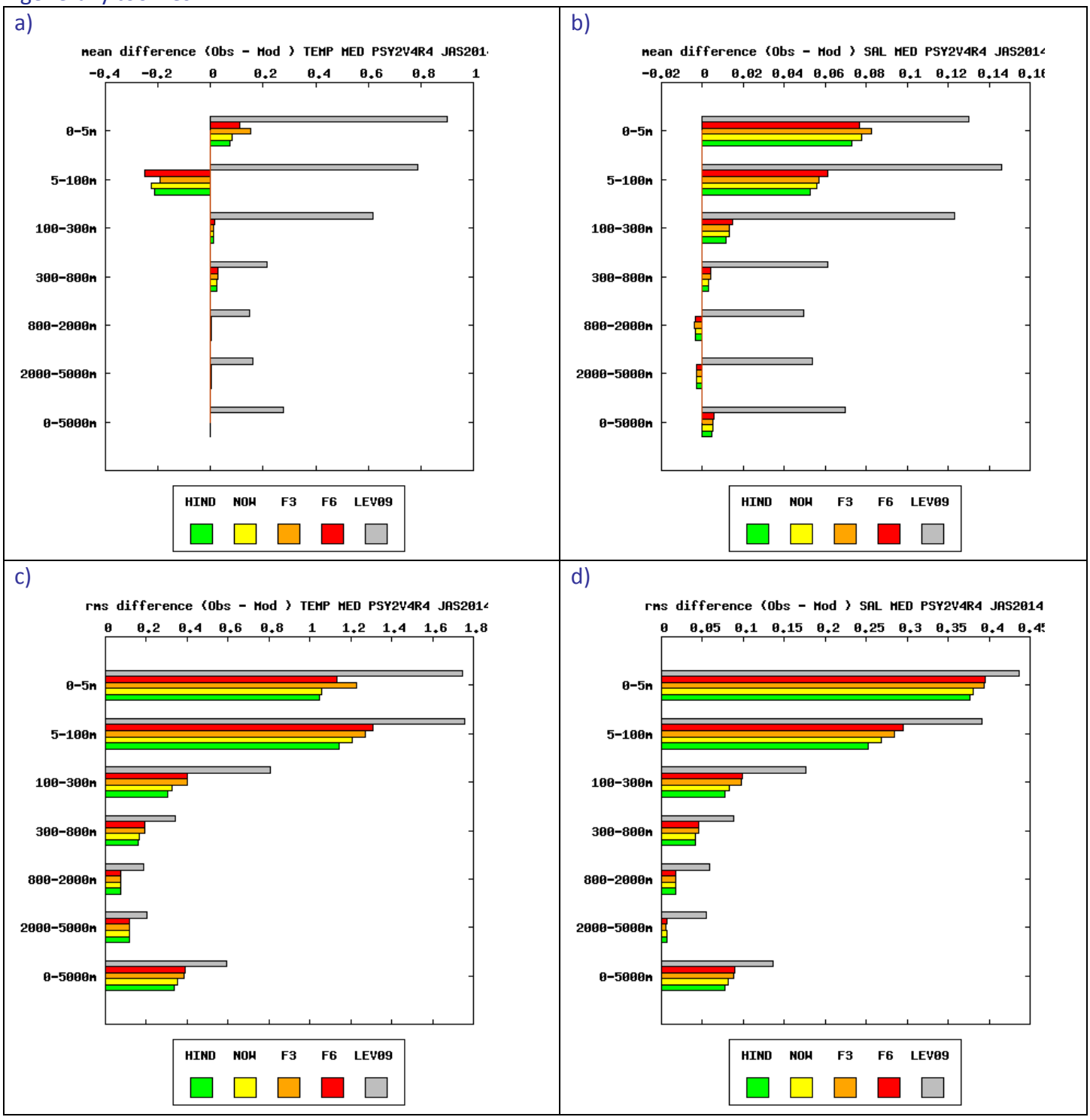

Figure 56: Accuracy intercomparison in the Mediterranean Sea region for PSY2V4R4 in temperature (°C, a and c) and salinity (psu, b and d) between hindcast, nowcast, 3-day and 6-day forecast and WO09 climatology. Accuracy is measured by a rms difference (c and d) and by a mean difference (a and b) with respect to all available observations from the CORIOLIS database averaged in 6 consecutive layers from 0 to 5000m. All statistics are performed for the JAS 2014 period. NB: average on model levels is performed as an intermediate step which reduces the artefacts of inhomogeneous density of observations on the vertical.

VI.2.3. Tropical Oceans and global

Results already described in previous sections are confirmed by the profiles shown in Figure 58. PSY4 is usually warmer (less cold) than PSY3 in common regions. PSY2 and PSY4 suffer from a fresh bias in the Tropical oceans, especially in the Tropical Atlantic. In the other tropical basins PSY3 is less biased than PSY4 in terms of salinity in surface layer.

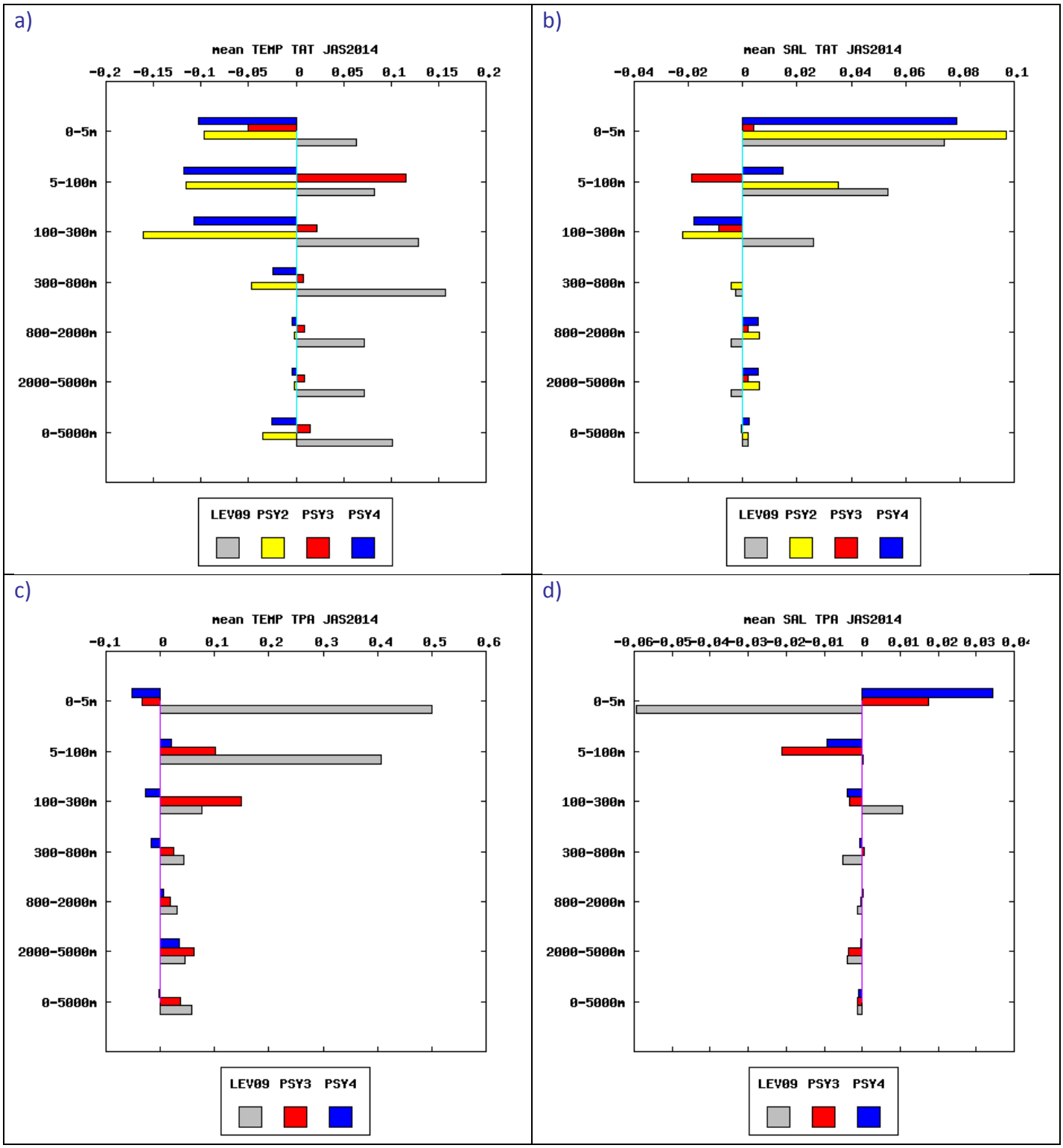

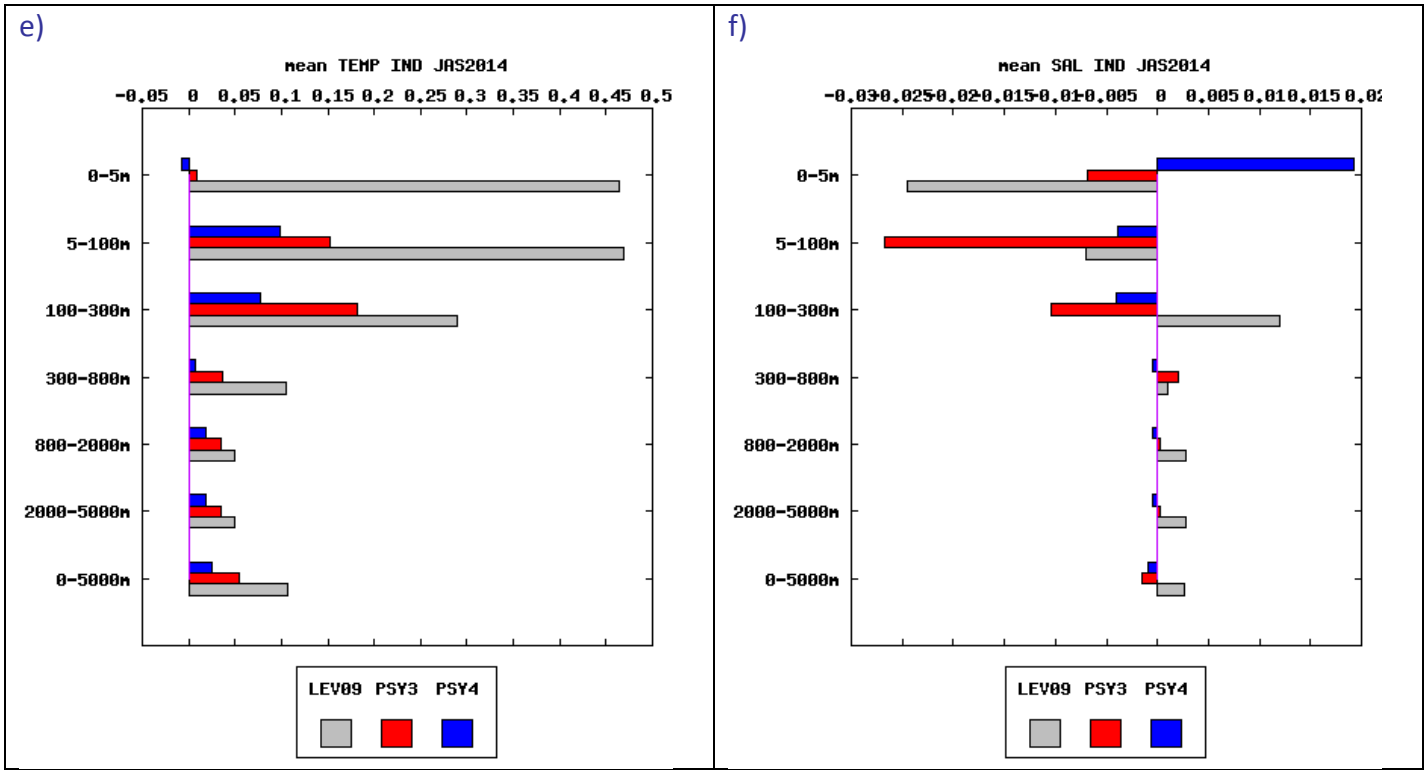

Figure 57: (Obs-model) mean differences in temperature (°C, a, c, and e) and salinity (psu, b, d, and f) for PSY3V3R3 (red), PSY2V4R4 (yellow) and PSY4V2R2 (blue) systems in the Tropical Atlantic (a and b), the Tropical Pacific (c and d) and the Indian Ocean (e and f) in JAS 2014.

PSY3, PSY4 and PSY2 display similar accuracy levels in terms of temperature RMS error in the Tropical Oceans. PSY3's salinity slightly outperforms PSY4 on average over the globe. RMS error increases with forecast range (shown here for PSY3), as could be expected, and that the 6-day forecast always beats the climatology (except for global mean salinity).

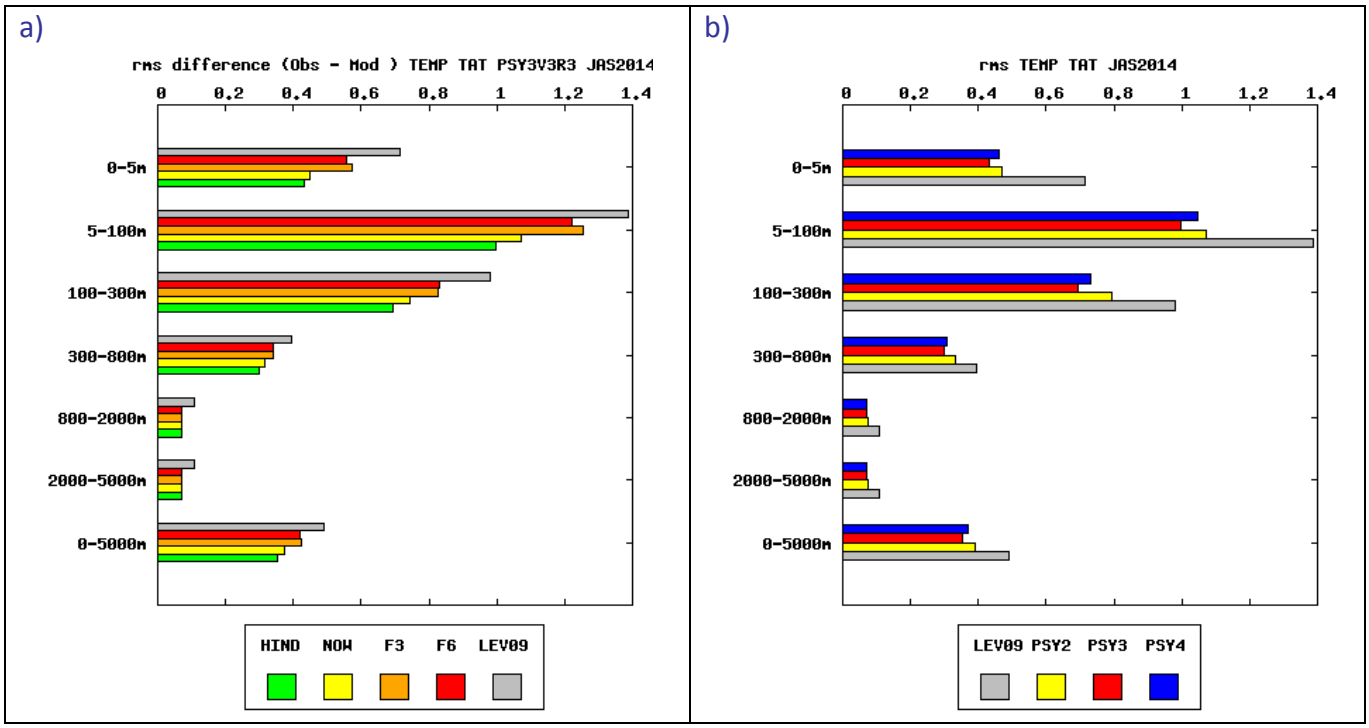

c)

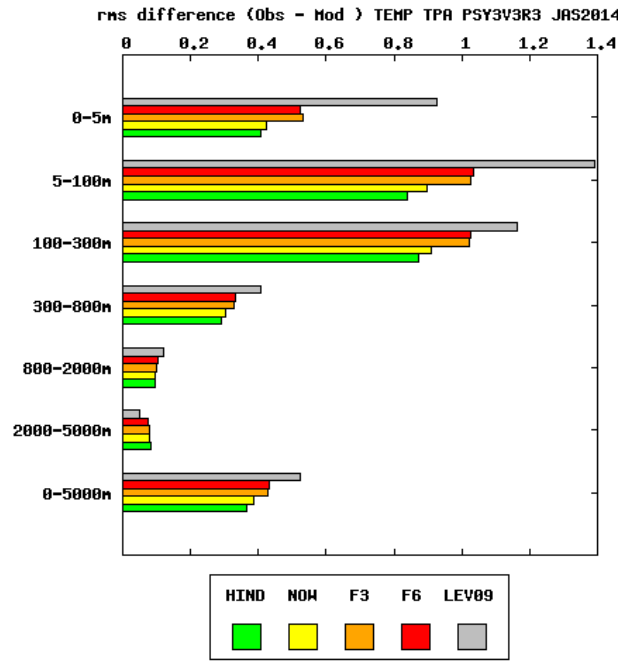
rms difference (Obs - Mod) TEMP TPA PSY3V3R3 JAS2014
0 0.2 0.4 0.6 0.8 1 1.2 1.4
0-5m
5-100m
100-300m
300-800m
800-2000m
2000-5000m
0-5000m
HIND NOW F3 F6 LEV09

d)

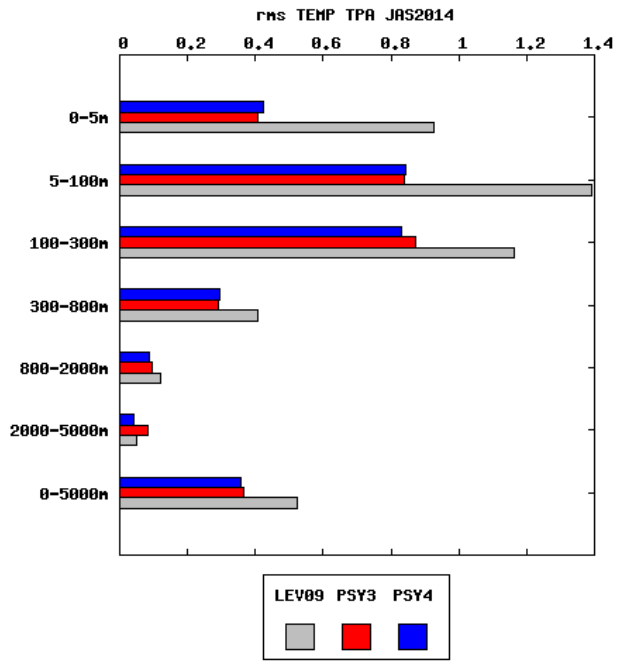
rms TEMP TPA JAS2014
0 0.2 0.4 0.6 0.8 1 1.2 1.4
0-5m
5-100m
100-300m
300-800m
800-2000m
2000-5000m
0-5000m
LEV09 PSY3 PSY4

e)

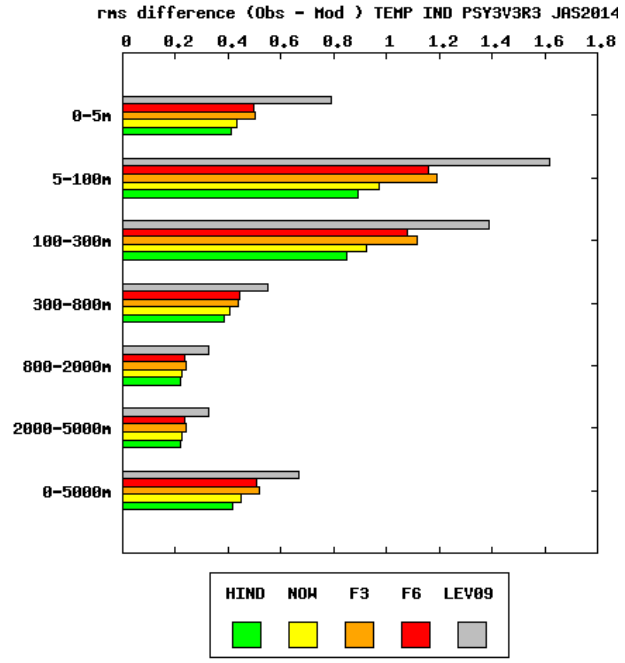
rms difference (Obs - Mod) TEMP IND PSY3V3R3 JAS2014
0 0.2 0.4 0.6 0.8 1 1.2 1.4 1.6 1.8
0-5m
5-100m
100-300m
300-800m
800-2000m
2000-5000m
0-5000m
HIND NOW F3 F6 LEV09

f)

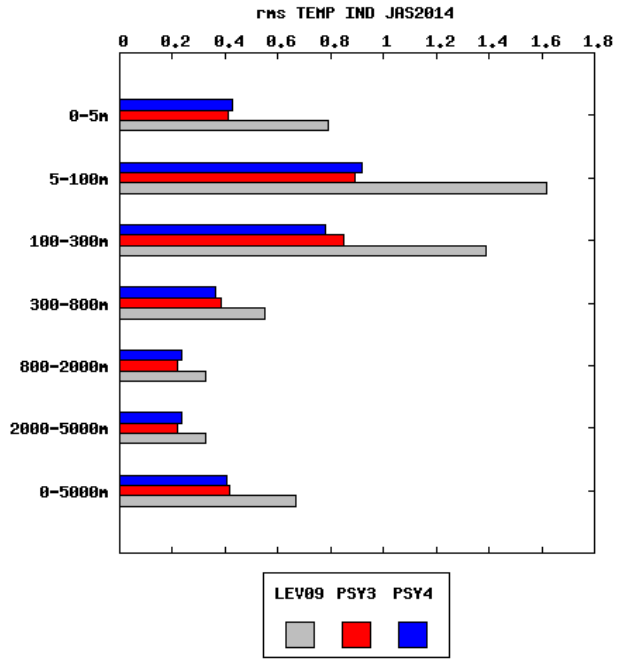
rms TEMP IND JAS2014
0 0.2 0.4 0.6 0.8 1 1.2 1.4 1.6 1.8
0-5m
5-100m
100-300m
300-800m
800-2000m
2000-5000m
0-5000m
LEV09 PSY3 PSY4

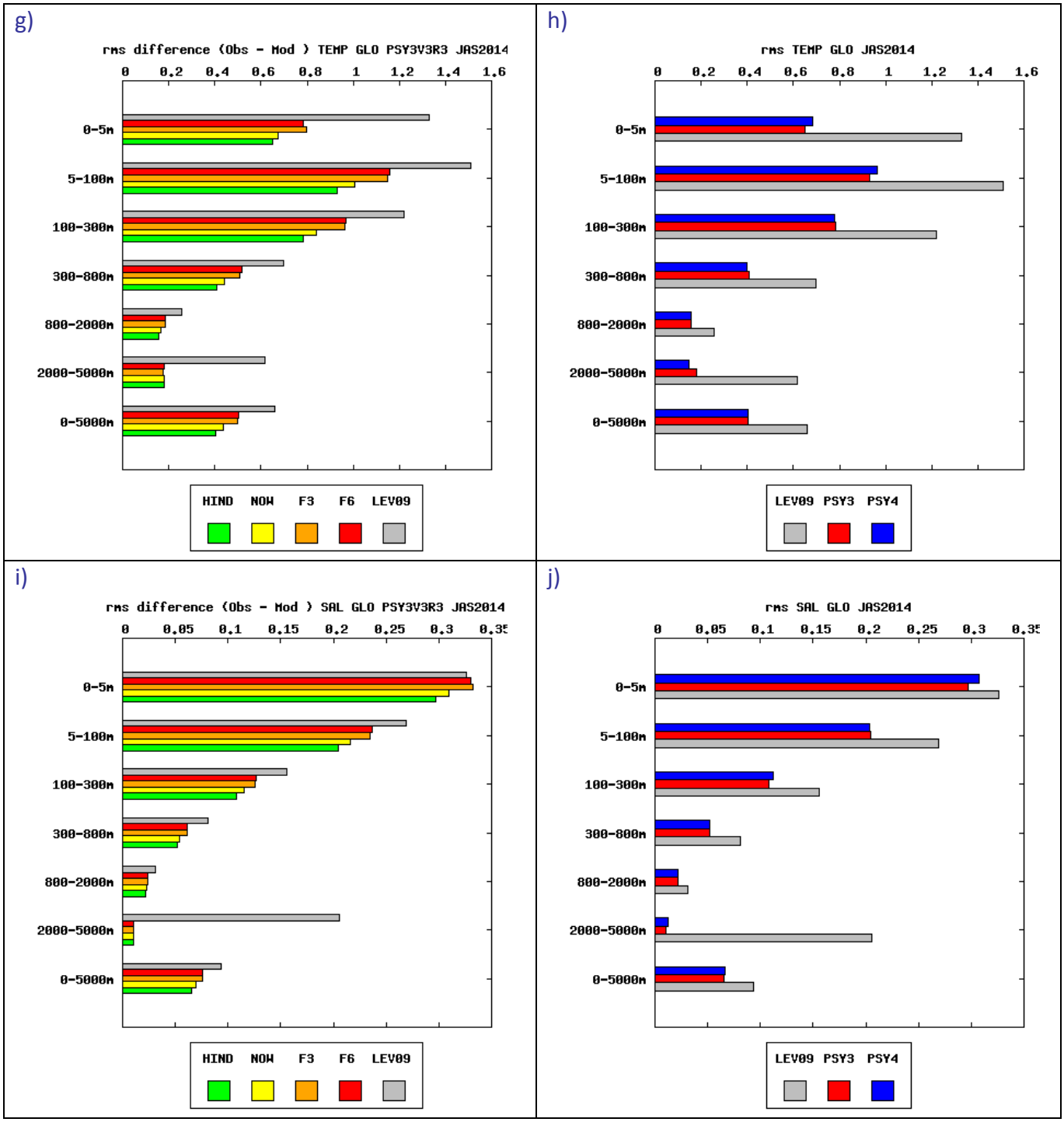

Figure 58: same as Figure 55 but for RMS statistics and for temperature (°C), PSY3V3R3 and PSY4V2R2 systems and the Tropical Atlantic (a and b), the Tropical Pacific (c and d) and the Indian Ocean (e and f). The global statistics are also shown for temperature (°C, g and h) and salinity (psu, I and j). The right column compares the analysis of the global ¼° PSY3V3R3 (red) with the analysis of the global 1/12° PSY4V2R2 (blue).

VI.3. Forecast accuracy: skill scores for T and S

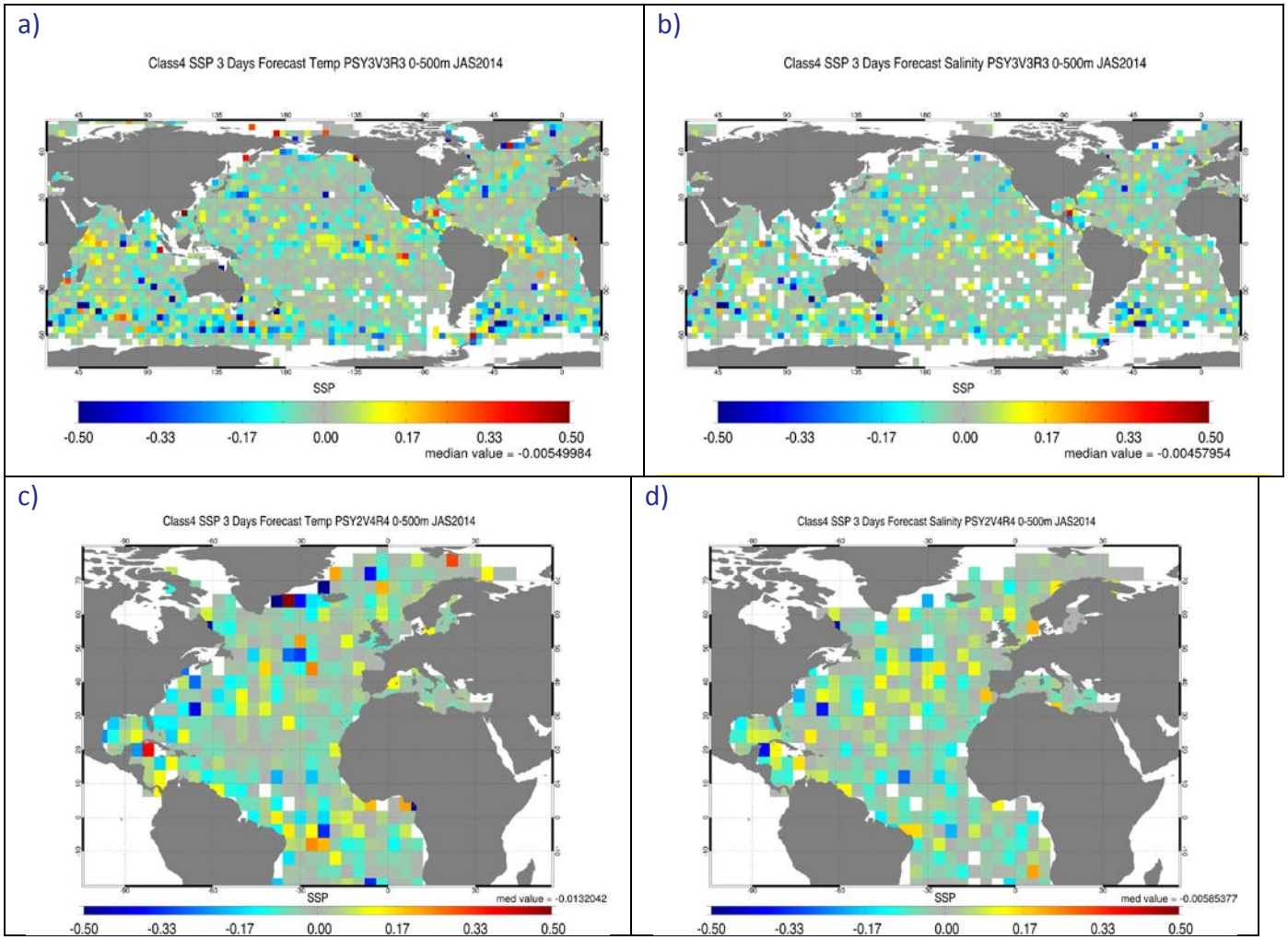

Figure 59: Temperature (left) and salinity (right) skill scores in 4°x4° bins and in the 0-500m layer in JAS 2014 in PSY3V3R3 (a and b) and PSY2V4R4 (c and d). The skill illustrates the ability of the 3-days forecast to be closer to in situ observations than the persistence of the analysis, see Equation 1. Yellow to red values indicate that the forecast is more accurate than the persistence.

The Murphy Skill Score (see Equation 1) is described by Wilks, *Statistical Methods in the Atmospheric Sciences*, Academic Press, 2006. This score is close to 0 if the forecast is equivalent to the reference. It is positive and aims towards 1 if the forecast is more accurate than the reference.

$$SS = 1 - \frac{\sum_{k=1}^{n}\left[\frac{1}{M}\sum_{m=1}^{M}\left(Forecast_m - Obs_m\right)^2\right]}{\sum_{k=1}^{n}\left[\frac{1}{M}\sum_{m=1}^{M}\left(Ref_m - Obs_m\right)^2\right]}$$

Equation 1

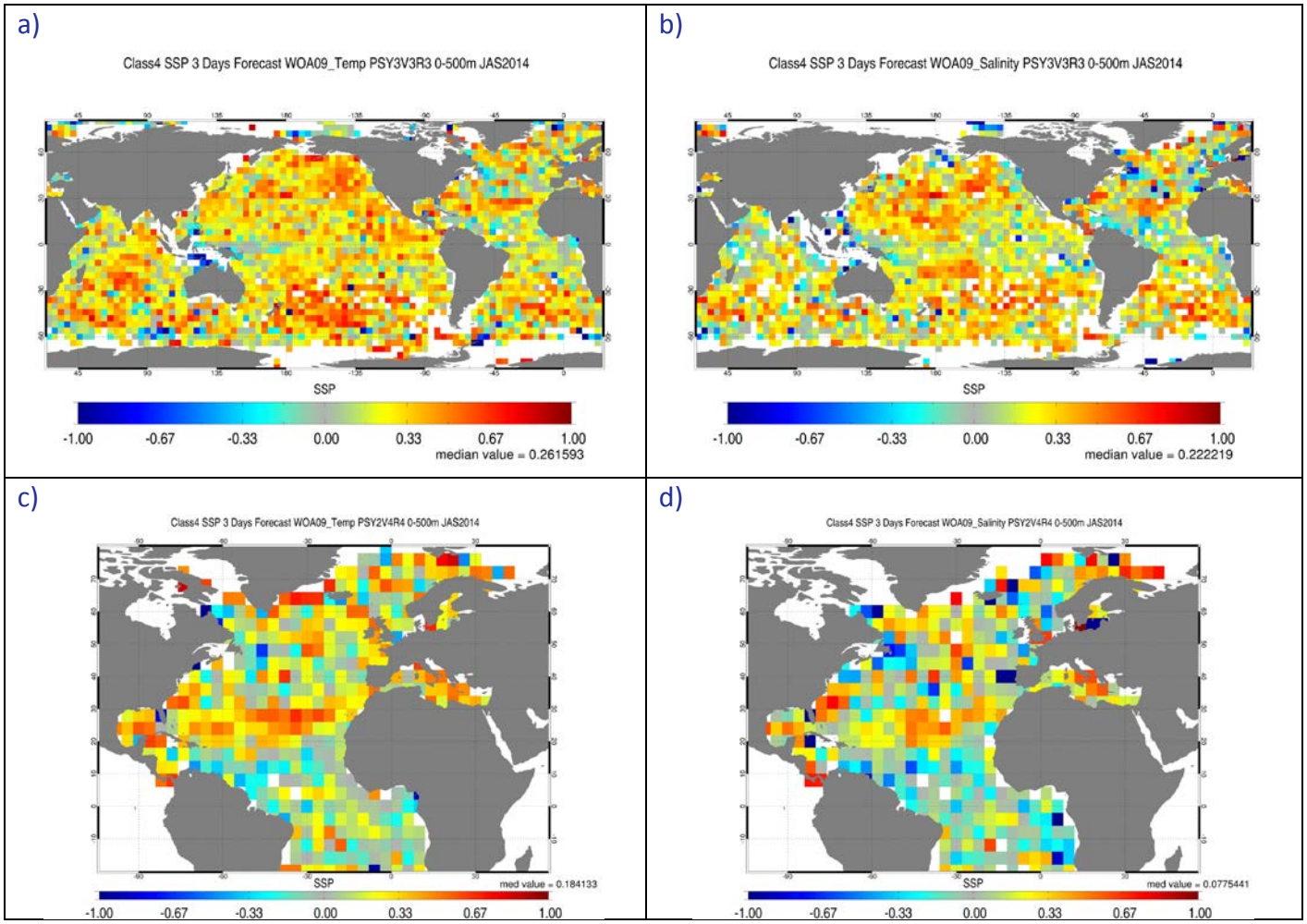

Figure 60 : As Figure 59 but the reference is the WOA 2009 climatology. Temperature (a and c) and salinity (b and d) skill scores are displayed for JAS 2014, for PSY3V3R3 (a and b) and for PSY2V4R4 (c and d). The skill illustrates the ability of the 3-days forecast to be closer to in situ observations than the climatology, see Equation 1. Yellow to red values indicate that the forecast is more accurate than the climatology.

The Skill Scores displayed on Figure 59 and Figure 60 show the added value of the PSY3 forecast with respect to the persistence of the analysis (Figure 59) and to climatology (Figure 60). All Mercator Ocean systems have a very good level of performance with respect to the climatology (see previous section). When the reference is the persistence of the last analysis, the result is noisier and the systems 3-day forecast seems to have skill in some regions in particular: North East Atlantic, eastern pacific, western tropical Atlantic, western Indian basin. In some regions of high variability (for instance in the Antarctic, Gulf Stream, Agulhas Current, Zapiola) the persistence of the previous analysis is locally more accurate than the forecast.

VI.4. Forecast verification: comparison with analysis everywhere

Not available this quarter.

VII Monitoring of ocean and sea ice physics

VII.1. Global mean SST and SSS

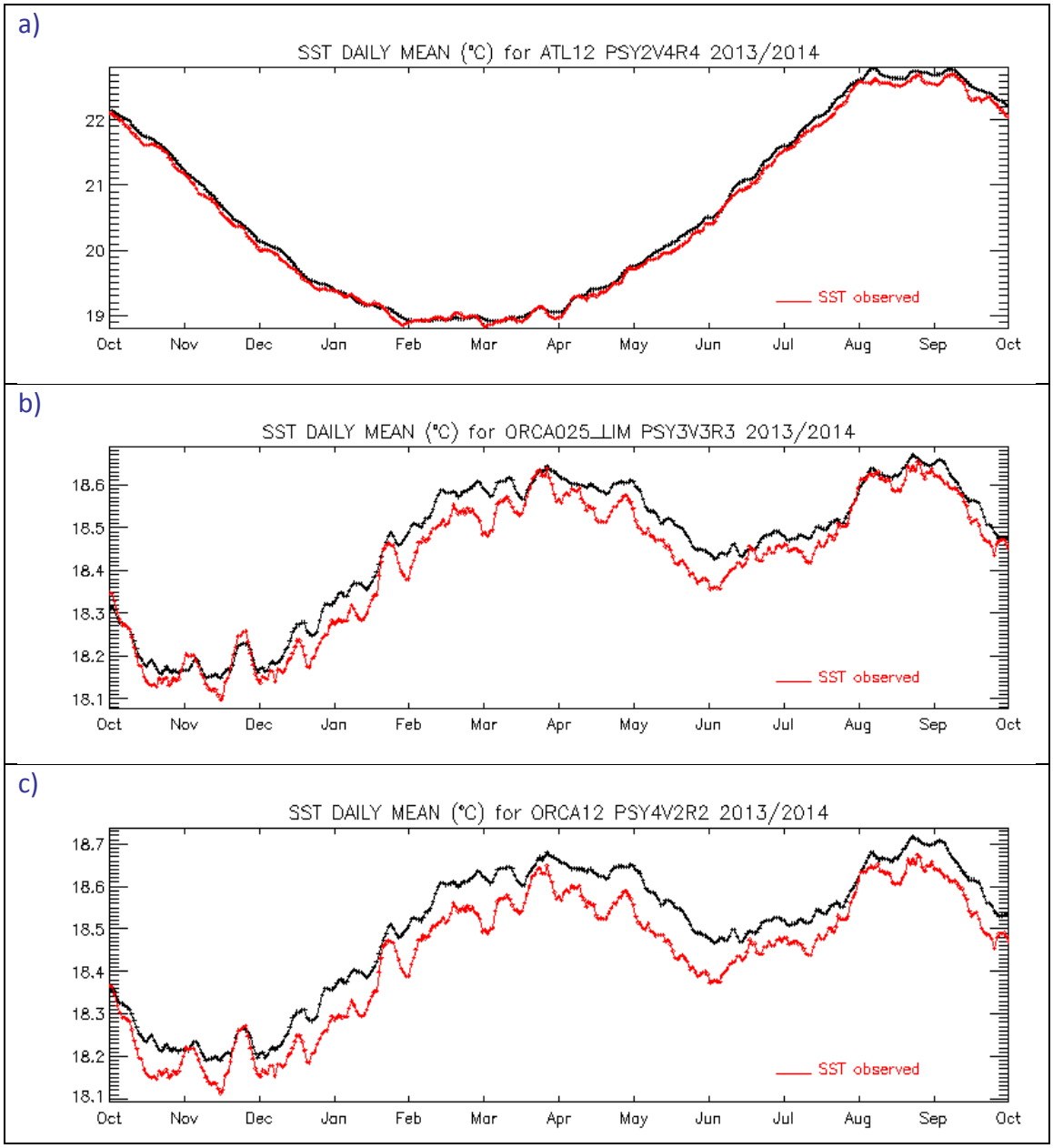

Figure 61: daily SST (°C) spatial mean for a one year period ending in JAS 2014 for PSY2V4R4 (a), PSY3V3R3 (b), and PSY4V2R2 (c). Mercator Ocean systems are in black and Reynolds AVHRR ¼° analysis in red.

The spatial mean of SST is computed for each day of the year, for PSY2, PSY3 and PSY4. The mean SST is compared to the mean of Reynolds AVHRR SST on the same domain (Figure 61).
The main feature is the good agreement of the systems with the observations all year long and on global average. A warm bias can be diagnosed in all the systems (stronger in PSY4 than in PSY3) with respect to the observations. The bias disappears in winter for PSY2.

VII.2. Surface EKE

Regions of high mesoscale activity are diagnosed in Figure 62: Kuroshio, Gulf Stream, Niño 3 region in the eastern Equatorial pacific, Zapiola eddy, Agulhas current. PSY3 at ¼° and PSY4 at 1/12° are in very good agreement. EKE is generally higher in the high resolution PSY4 system, for instance this quarter at the Equator near 120°W. Compared to JAS 2013 (not shown), the EKE is higher in PSY4 along the equator in the Atlantic and Pacific oceans.

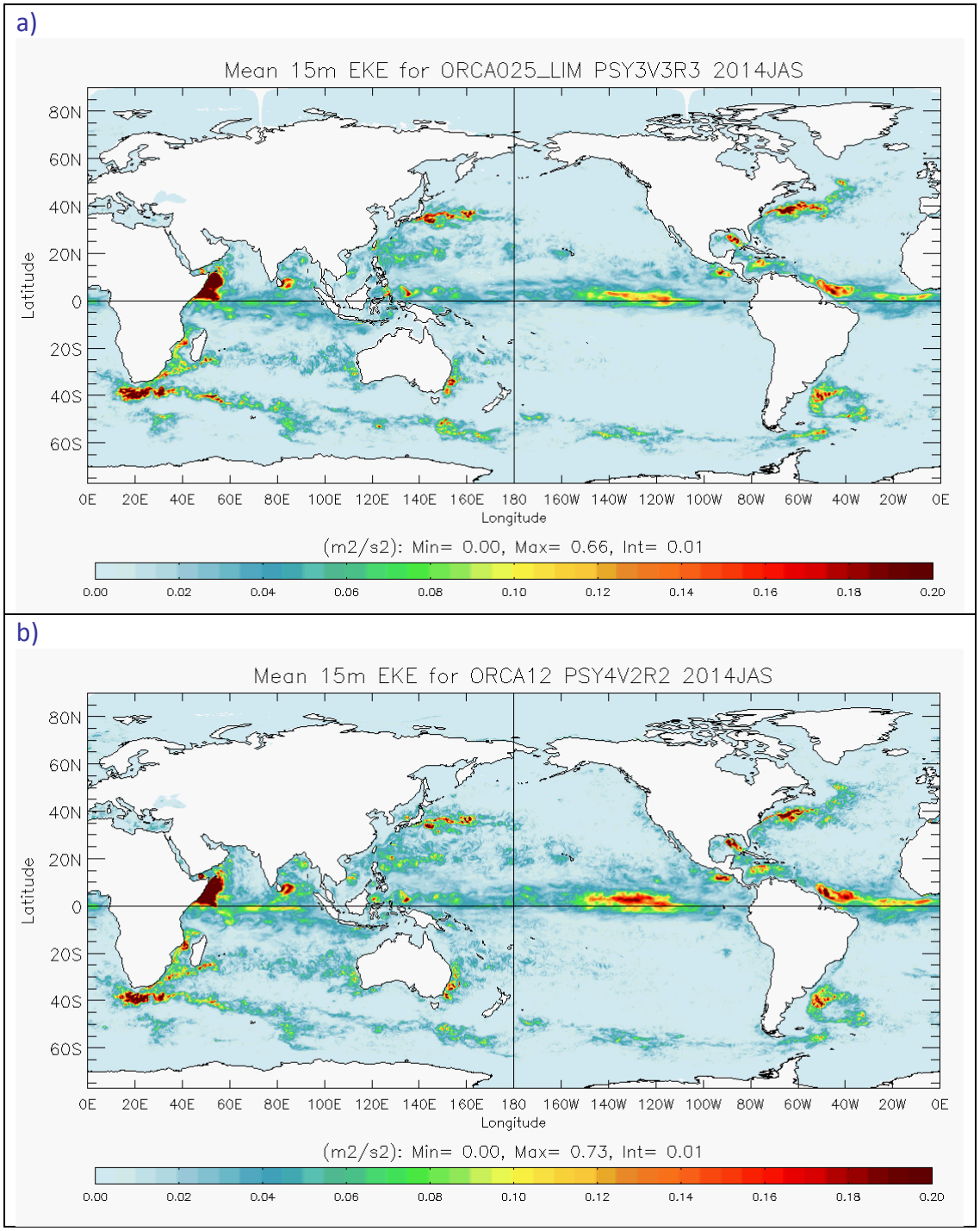

Figure 62: surface eddy kinetic energy EKE (m^2/s^2) for PSY3V3R3 (a) and PSY4V2R2 (b) for JAS 2014.

VII.3. Mediterranean outflow

The Mediterranean outflow displayed in Figure 63 is more diffuse in all systems than in the climatology of the Gulf of Cadiz. All systems now display similar vertical structure in the region, with PSY2 closer to the climatology than PSY3 and PSY4. Compared to the climatology, the systems are too salty between 300 and 500m depth, and too fresh deeper than 1100m depth.

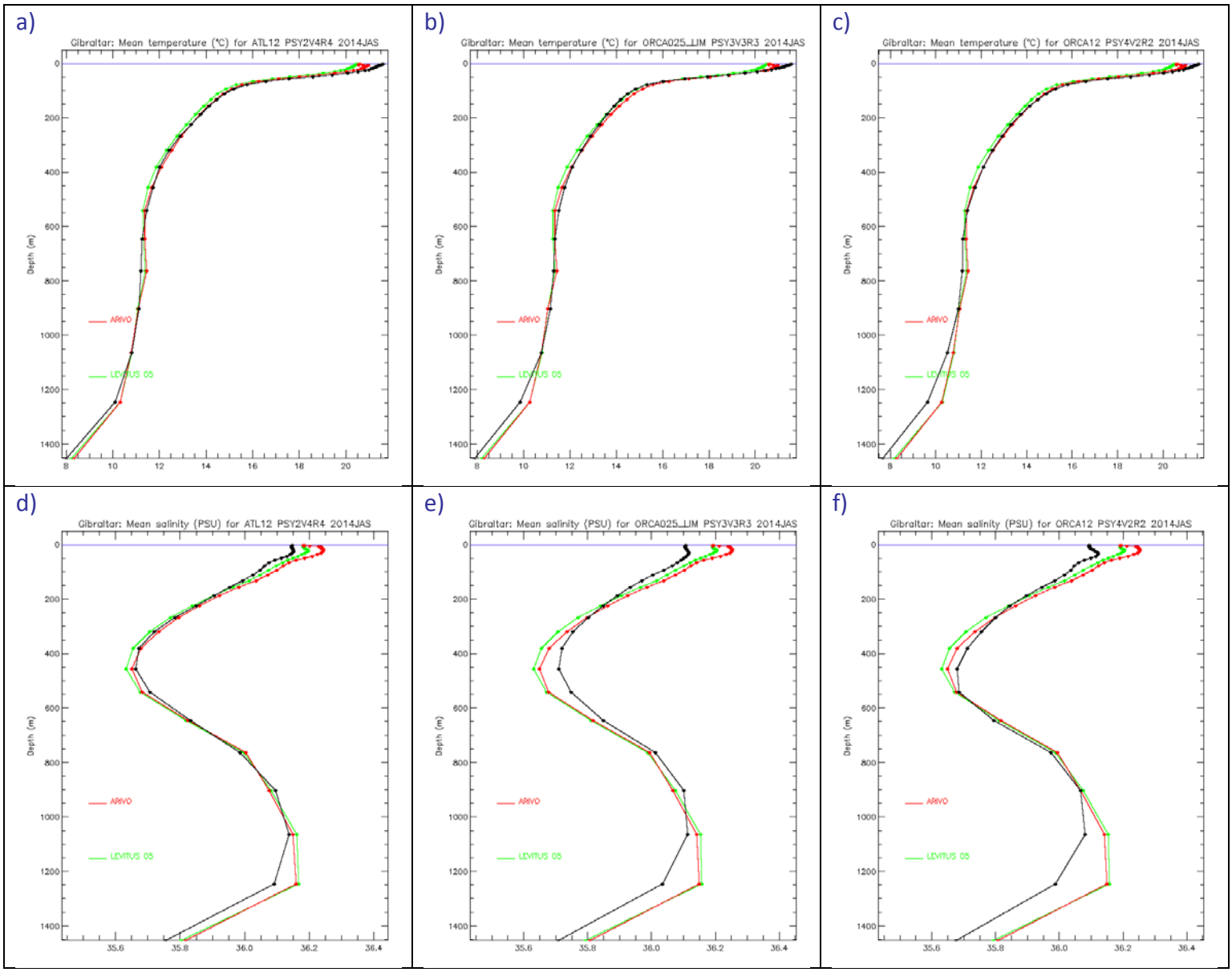

Figure 63: Comparisons between JAS 2014 mean temperature (°C, a to c) and salinity (psu, d to f) profiles in Mercator systems (black): PSY2V4R4 (a and d), PSY3V3R3 (b and e) and PSY4V2R2 (c and f), and in the Levitus WOA05 (green) and ARIVO (red) monthly climatologies.

VII.4. Sea Ice extent and area

The time series of monthly means of sea ice area and sea ice extent (area of ocean with at least 15% sea ice) are displayed in Figure 64 and compared to SSM/I microwave observations. Both ice extent and area include the area near the pole not imaged by the sensor. NSIDC web site specifies that it is assumed to be entirely ice covered with at least 15% concentration. This area is 0.31 million square kilometres for SSM/I.

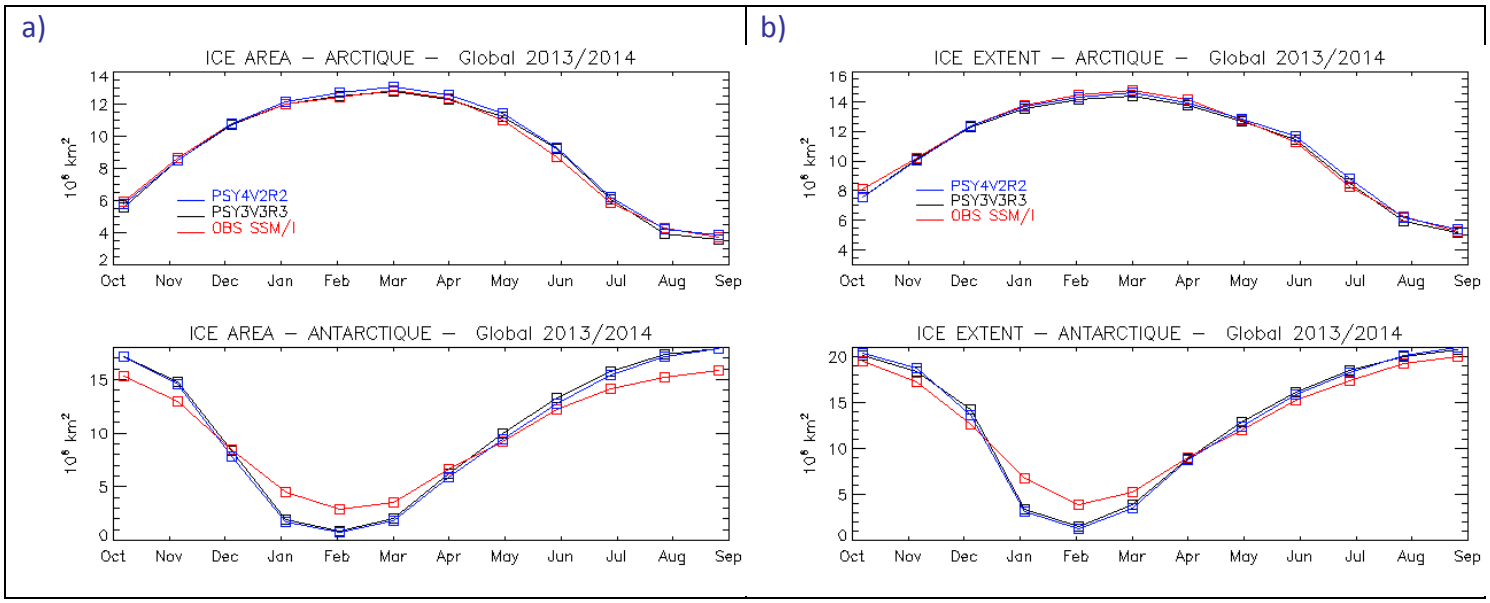

Figure 64: Sea ice area (a, 10^6 km2) and extent (b, 10^6 km2) in PSY3V3R3 (blue line), PSY4V2R2 (black line) and SSM/I observations (red line) for a one year period ending in JAS 2014, in the Arctic (upper panel) and Antarctic (lower panel).

These time series indicate that sea ice products from PSY4 and PSY3 are very similar on average over the polar domains. In the Arctic both systems perform very well in terms of average quantities. In the Antarctic the seasonal cycle of the sea ice area is overestimated, with an overestimated sea ice area this austral winter in both systems (while the extent is better captured), and too much melting in summer for both systems.

VIII Comparison between BIOMER1 and BIOMER4

VIII.1.1. Description of BIOMER4

The BIOMER4 system has been operated since July 2014 and is disseminated to users since September 2014. Starting from the next issue of the "*QuO Va Dis?*" BIOMER4 products will be evaluated, and will replace BIOMER1 products.

The biogeochemical model used in BIOMER1 and BIOMER4 is PISCES (Aumont, in prep). It is a model of intermediate complexity designed for global ocean applications (Aumont and Bopp, 2006) and is part of NEMO modeling platform. **In BIOMER4 the version of NEMO is upgraded to NEMO3.2, while NEMO2.3 was used in BIOMER1.** PISCES has 24 prognostic variables and simulates biogeochemical cycles of oxygen, carbon and the main nutrients controlling phytoplankton growth (nitrate, ammonium, phosphate, silicic acid and iron). The model distinguishes four plankton functional types based on size: two phytoplankton groups (small = nanophytoplankton and large = diatoms) and two zooplankton groups (small = microzooplankton and large = mesozooplankton). Prognostic variables of phytoplankton are total biomass

in C, Fe, Si (for diatoms) and chlorophyll and hence the Fe/C, Si/C, Chl/C ratios are variable. For zooplankton, all these ratios are constant and total biomass in C is the only prognostic variable. The bacterial pool is not modeled explicitly. PISCES distinguishes three non-living pools for organic carbon: small particulate organic carbon, big particulate organic carbon and semi-labile dissolved organic carbon. While the C/N/P composition of dissolved and particulate matter is tied to Redfield stoichiometry, the iron, silicon and carbonate contents of the particles are computed prognostically. Next to the three organic detrital pools, carbonate and biogenic siliceous particles are modeled. Besides, the model simulates dissolved inorganic carbon and total alkalinity. In PISCES, phosphate and nitrate + ammonium are linked by constant Redfield ratio (C/N/P = 122/16/1), but cycles of phosphorus and nitrogen are decoupled by nitrogen fixation and denitrification.
The distinction of two phytoplankton size classes, along with the description of multiple nutrient co-limitations allows the model to represent ocean productivity and biogeochemical cycles across major biogeographic ocean provinces (Longhurst, 1998). PISCES has been successfully used in a variety of biogeochemical studies (e.g. Bopp et al. 2005; Gehlen et al. 2006; 2007; Schneider et al. 2008; Steinacher et al. 2010; Tagliabue et al. 2010, Séférian et al, 2013). The biogeochemical model is initialized with World Ocean Atlas 2001 for nitrate, phosphate, oxygen and silicate (Conkright et al. 2002), with GLODAP climatology including anthropogenic CO2 for Dissolved Inorganic Carbon and Alkalinity (Key et al. 2004) and, in the absence of corresponding data products, with model fields for dissolved iron and dissolved organic carbon. Boundary fluxes account for nutrient supply from three different sources: atmospheric deposition (Aumont et al., 2008), rivers for nutrients, dissolved inorganic carbon and alkalinity (Ludwig et al., 1996) and inputs of Fe from marine sediments.

VIII.1.2. Validation summary

The 3D physical forcing of PISCES comes from PSY3R3V3 at ¼° resolution (Lellouche et al., 2013). **PISCES is forced offline by daily fields in BIOMER4, while BIOMER1 was forced by weekly averages**. A special treatment is done on vertical diffusivity coefficient (Kz): the daily mean is done on Log10(Kz) after a filtering of enhanced convection (Kz increased artificially to 10 $m^2.s^{-1}$ when the water column is unstable). The purpose of this Log10 is to average the orders of magnitudes and to give more weight to small values of vertical diffusivity.
In BIOMER4, the grid of PISCES is the same as for PSY3V3R3, it is the standard ORCA025 tri-polar grid (1440 x 1021 grid points on the horizontal). The three poles are located over Antarctic, Central Asia and North Canada. The vertical grid has 50 levels, with a resolution of 1 meter near the surface and 500 meters in the deep ocean. **BIOMER1's grid was ORCA1 with a 1° horizontal resolution.**
The biogeochemical simulation starts in January 2007. Outputs are interpolated on a standard collocated grid at 1/2 degree.

The quality of the global biogeochemical system has been assessed using a seven-year hindcast (years 2007-2013). The headline results for each of the variables assessed are as follows:
Chlorophyll: At sea surface, modelled chlorophyll fields are in good agreement with satellite data. The large-scale structures corresponding to specific biogeographic regions (double-gyres, Antarctic Circumpolar Current, etc.) are well reproduced (not shown). However, concentrations are still too high in the tropical band. Concerning the temporal monitoring, our model succeeds well in reproducing the seasonal cycle at mid- and high- latitudes (spring bloom), but the timing of the bloom is not yet in phase with observations (one or two-month lag). On the global ocean, the model has a correlation of 0.59 in log10(chlorophyll) at sea surface in comparison with satellite chlorophyll observations (see Figure 65).

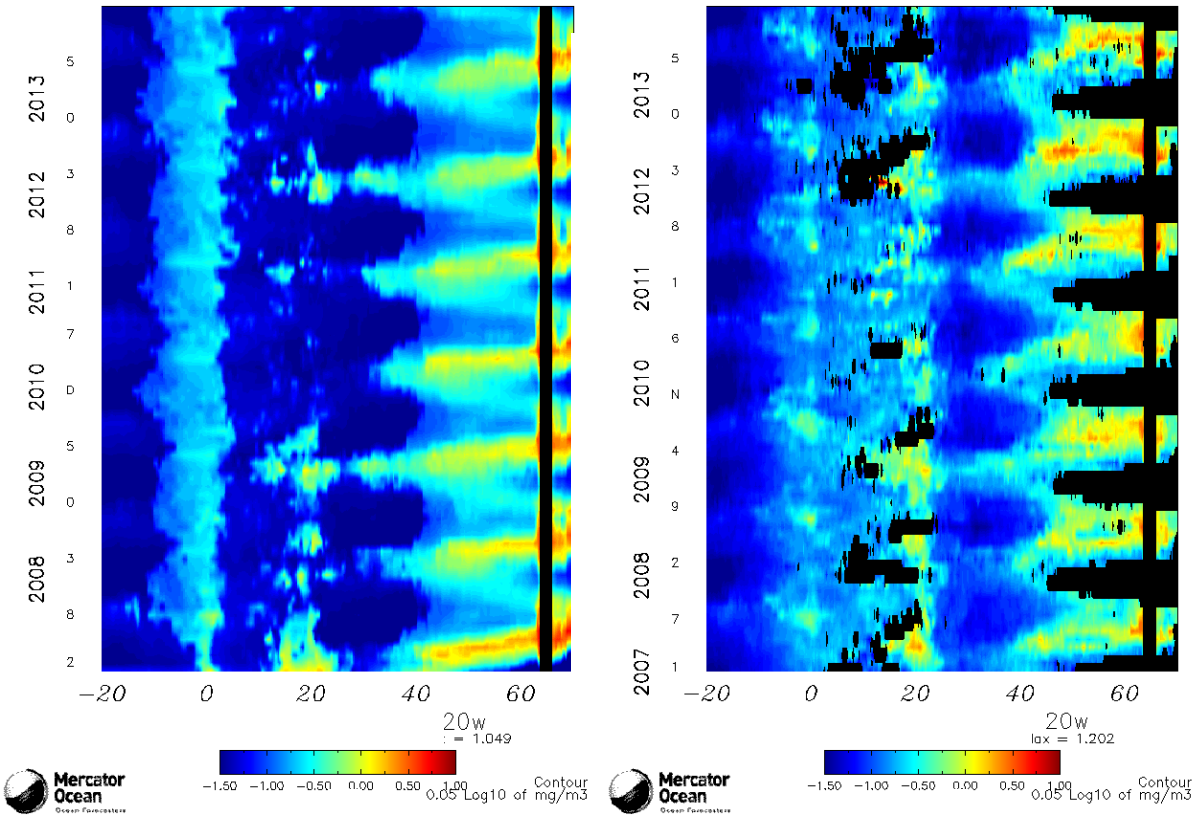

Figure 65: Hovmöller diagram of Log10(chlorophyll) between 2007 and 2013 at 20°W in North Atlantic (20°S:70°N); (left) model; (right) Globcolour data.

Nutrients (NO3, PO4, Si): They display a good agreement with World Ocean Atlas Climatology at global scale (correlation > 0.9, not shown). The concentrations of nutrients are globally too high at sea surface (negative mean bias). This is mainly due to the tropical band where the model overestimates the nutrient concentrations.

Dissolved Oxygen: Oxygen presents very good scores at sea surface (correlation > 0.9; in comparison with World Ocean Atlas climatology, not shown). This is due to the intrinsic link between O2 concentration and temperature (and especially at sea surface). Dissolved oxygen benefits of the data assimilation via the temperature. In subsurface and deep layers, the model is able to reproduce OMZs (oxygen minimum zone).

Illustrations of the validation results and further information (Quality Information Document, or QUID) are available online on the MyOcean website, at http://www.myocean.eu/documents/QUID/MYOF-GLO-QUID-001-014-V2.2.pdf.

VIII.1.3. Comparison over the JAS 2014 quarter

In the following, we compare the outputs of both systems BIOMER1 and BIOMER4 on the JAS 2014 quarter, in order to document the main improvements, and describe the main strengths and weaknesses of the new release of BIOMER.

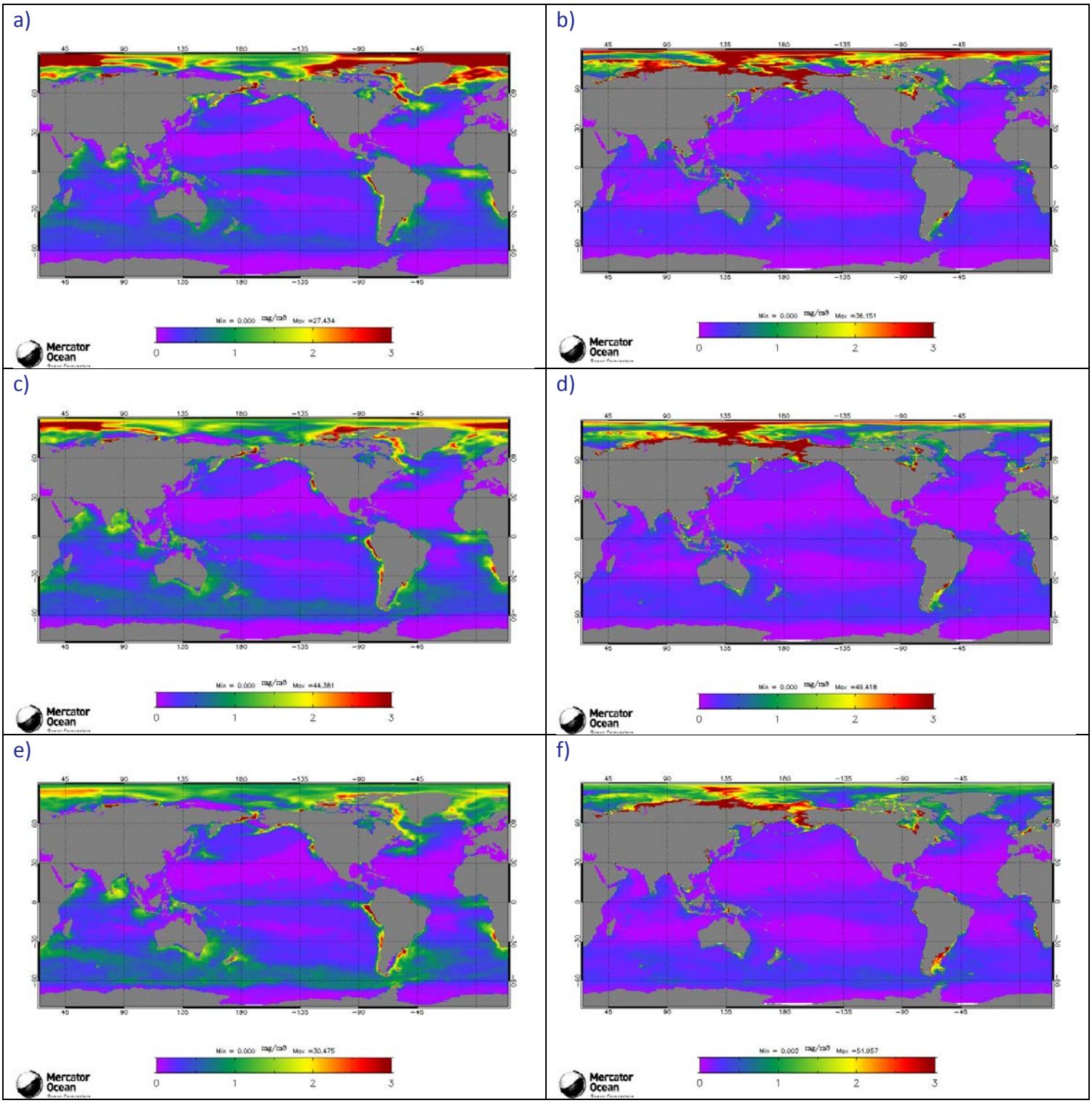

Figure 66 : Chlorophyll-a concentration (mg/m^3) in July (a and b), August (c and d) and September 2014 (e and f) for the Mercator systems BIOMER1 (a, c, and e) and BIOMER4 (b, d and f).

Using the "*QuO Va Dis?"* diagnostics based on comparison with ocean colour observations of Chlorophyll-a concentration, the new BIOMER4 system performs better than BIOMER1. The global overestimation of BIOMER1 is corrected in BIOMER4, and BIOMER4 is closer to the observations than the old system (Figure 66, Figure 67 and Figure 68). Discrepancies remain anyway, like along the Argentina's coast, or in the subpolar gyres.

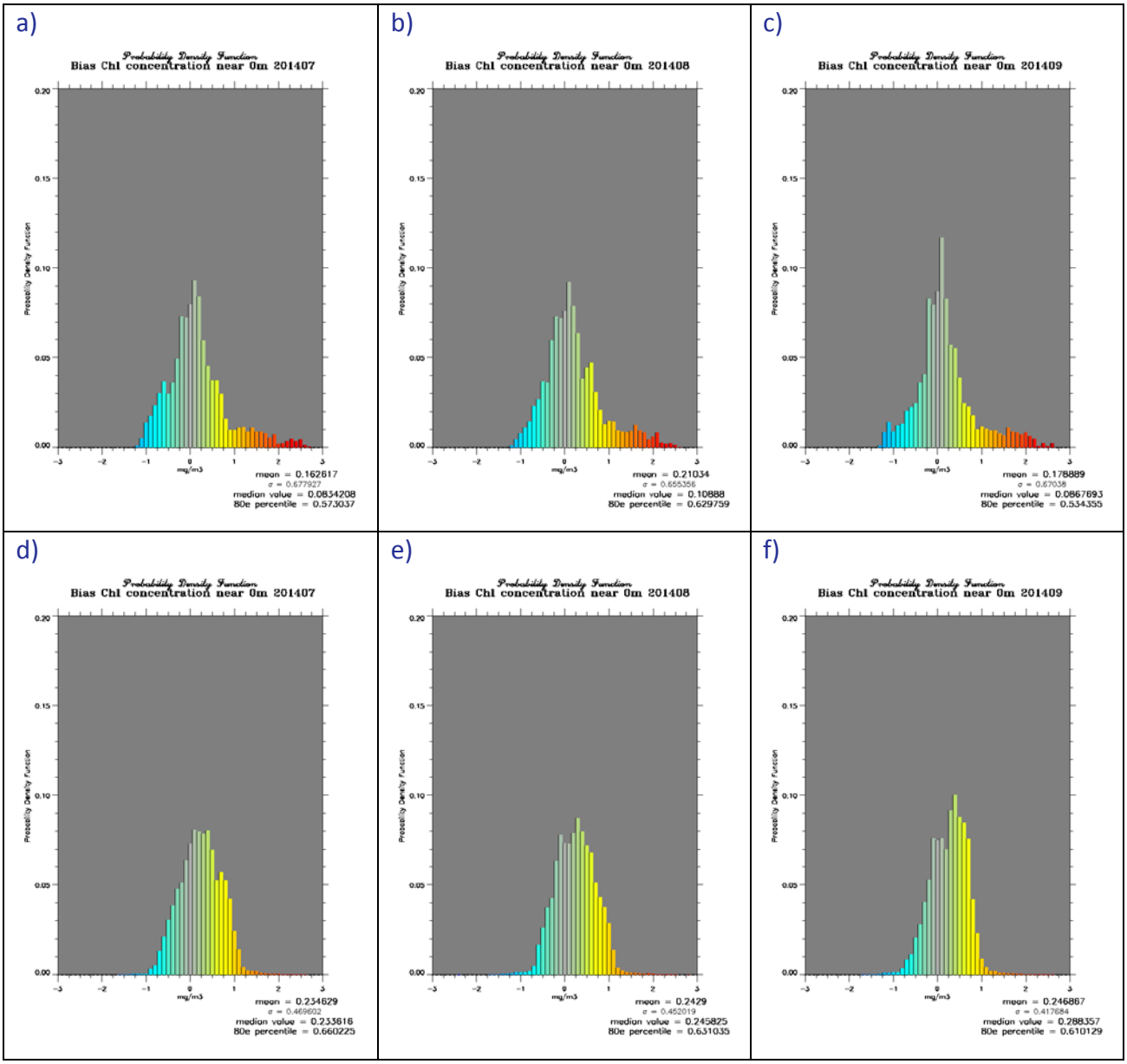

Figure 67 : Probability Density Function (PDF) of Chl-a bias in log scale (log10(obs)-log10(model)) in the North Atlantic (30-70N; 80W:20E) for BIOMER1 for July (a), August (b) and September (c) 2014. The same for BIOMER4 for July (d), August (e) and September (f) 2014.

As can be seen in the distribution of Chlorophyll-a concentration errors in Figure 67, the shape of BIOMER4's distribution is much more Gaussian than that of BIOMER1. BIOMER4 displays less very high departures from observations than BIOMER1, but a slightly larger mean bias. The highest overestimation errors have thus been reduced.

Some of these strong biases were located in the Equatorial band, in the upwelling regions, or in regions of high mesoscale variability (for instance around Australia, or in the Somali Gyre). A spurious enrichment which happened in the Gulf of Bengal in BIOMER1 disappears in BIOMER4.

The RMS error with respect to ocean colour observations is strongly reduced in BIOMER4 with respect to BIOMER1 (Figure 68). In the northern hemisphere in regions of seasonal blooms, the timing of the bloom is still not in phase with the observations, giving rise to high RMS errors in BIOMER4 as in BIOMER1.

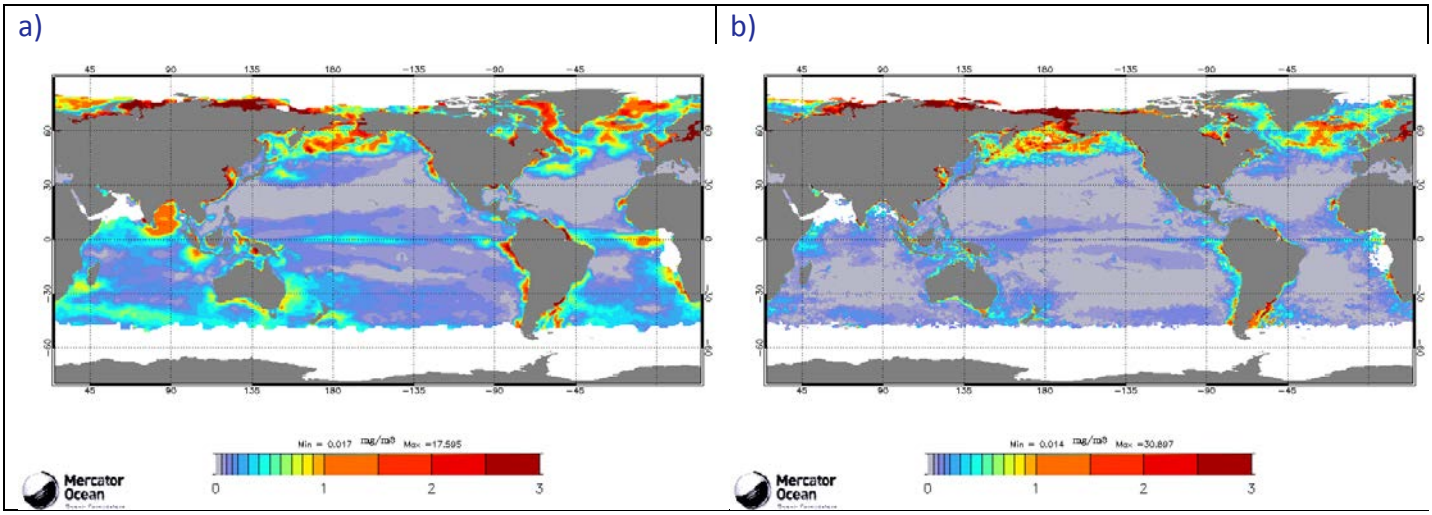

Figure 68 : RMS difference between BIOMER1 and Globcolour Chl-a concentrations (mg/m^3) in JAS 2014 (a). The same for BIOMER4 (b).

VIII.1.4. Conclusion

As a conclusion, even if there is still room for improvement of the biogeochemical system, the update of the BIOMER system to BIOMER4 allows a significantly better representation of the surface Chlorophyll-a concentration. Some limitations of the system are still present, such as the wrong timing of the North Pacific and North Atlantic blooms.

I Annex A

I.1. Table of figures

II Annex B

II.1. Maps of regions for data assimilation statistics

II.1.1. Tropical and North Atlantic

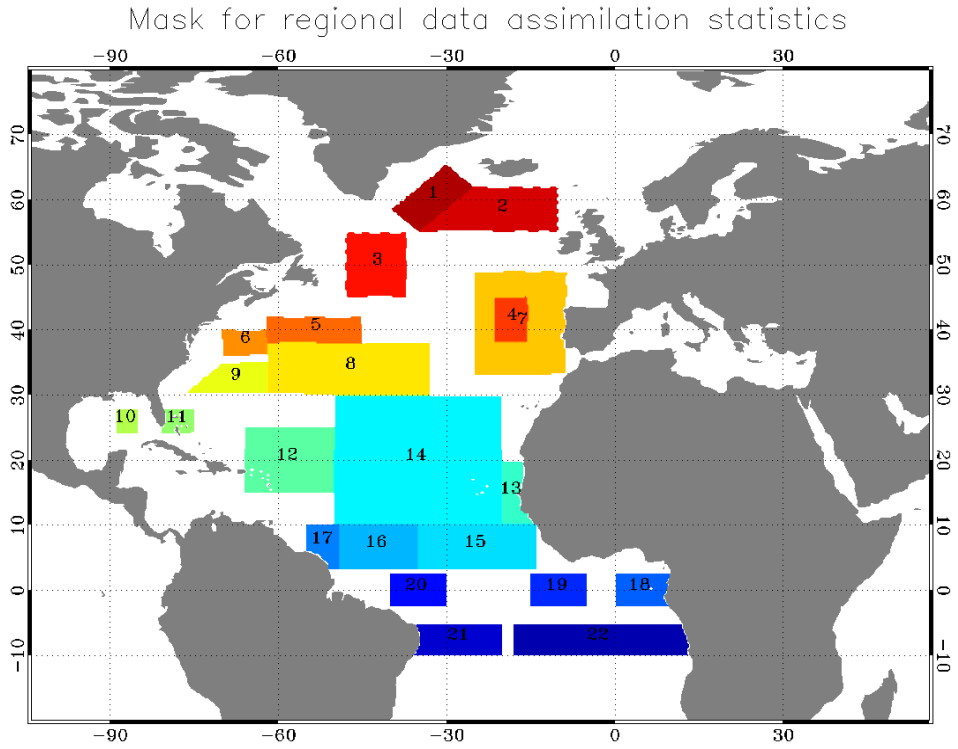

1	Irminger Sea	12	Puerto Rico XBT
2	Iceland Basin	13	Dakar
3	Newfoundland-Iceland	14	Cape Verde XBT
4	Yoyo Pomme	15	Rio-La Coruna Woce
5	Gulf Stream2	16	Belem XBT
6	Gulf Stream1 XBT	17	Cayenne tide
7	North Medeira XBT	18	Sao Tome tide
8	Charleston tide	19	XBT - central SEC
9	Bermuda tide	20	Pirata
10	Gulf of Mexico	21	Rio-La Coruna
11	Florida Straits XBT	22	Ascension tide

II.1.2. Mediterranean Sea

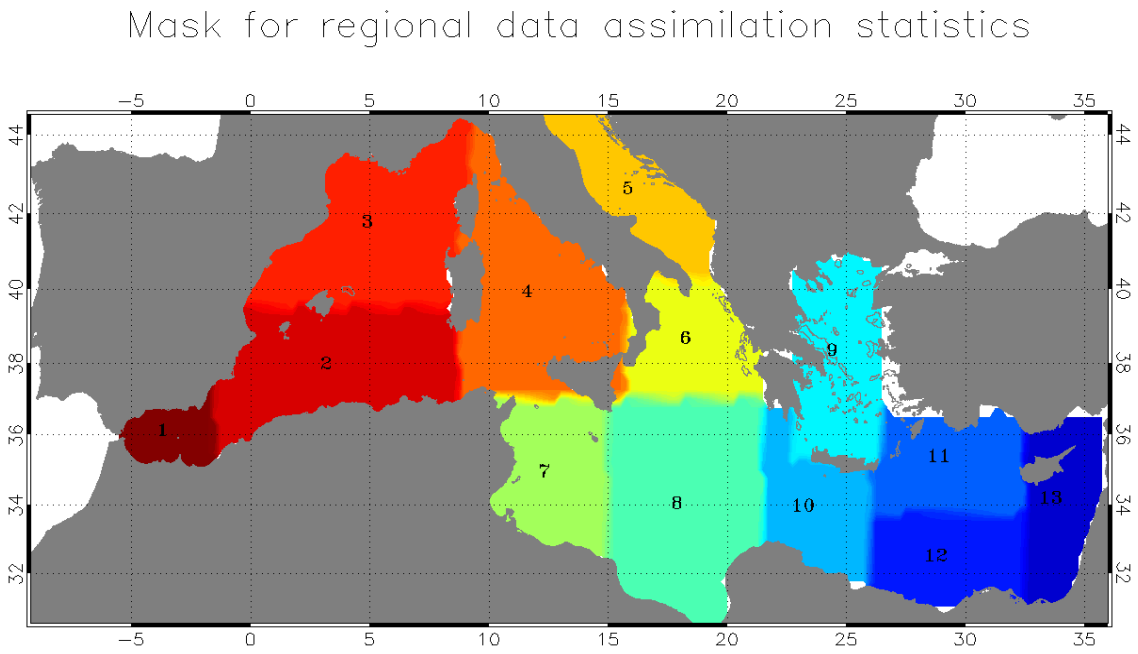

1	Alboran	8	Ionian
2	Algerian	9	Egee
3	Lyon	10	Ierepetra
4	Thyrrhenian	11	Rhodes
5	Adriatic	12	MersaMatruh
6	Otranto	13	Asia Minor
7	Sicily		

II.1.3. Global ocean

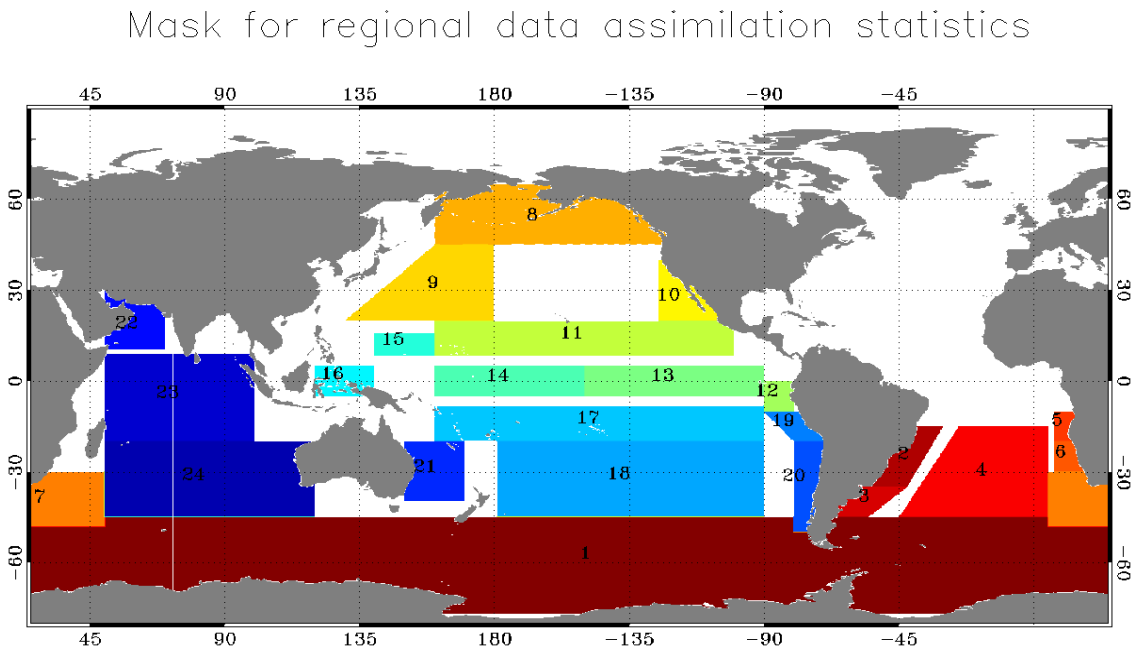

1	Antarctic Circumpolar Current	13	Nino3
2	South Atlantic	14	Nino4
3	Falkland current	15	Nino6
4	South Atl. gyre	16	Nino5
5	Angola	17	South tropical Pacific
6	Benguela current	18	South Pacific Gyre
7	Agulhas region	19	Peru coast
8	Pacific Region	20	Chile coast
9	North Pacific gyre	21	Eastern Australia
10	California current	22	Indian Ocean
11	North Tropical Pacific	23	Tropical indian ocean
12	Nino1+2	24	South indian ocean

III Annex C

III.1. Quality control algorithm for the Mercator Océan drifter data correction (Eric Greiner)

Before estimating the bias, it is essential to conduct a quality control. We must consider an individual monitoring of buoys, and a comparison with the geostrophy and windage. In real time, this is not possible, and I propose below a simple test developed by position (date by date) which involves only the mean wind (2 days) and the buoy drift. Basically, we found drifters where drift is close to argue between 0.2 and 3% of the wind (almost the same direction with a drag corresponding to a loss of drogue). For these buoys, if the contamination is real, then the error due to the wind is important with respect to current real at 15m depth. We test different values of windage (wind effect for a fraction of a given wind between 0.2% and 3%). If a questionable observation is found for a given windage, we estimate a correction. We apply at the end an average correction QC (windage among all acceptable). We although increase the error of observation. Note that in delayed time, we could correct all the data from the buoy, at least in a 10-day window. **Note however that a buoy that has lost its drogue can give a good measure if the wind is low**

- **No anomaly : slippage correction of 0.07% of the 10m wind speed**
- **Windage > 0.2% or < 3% correction of 1% of windage**

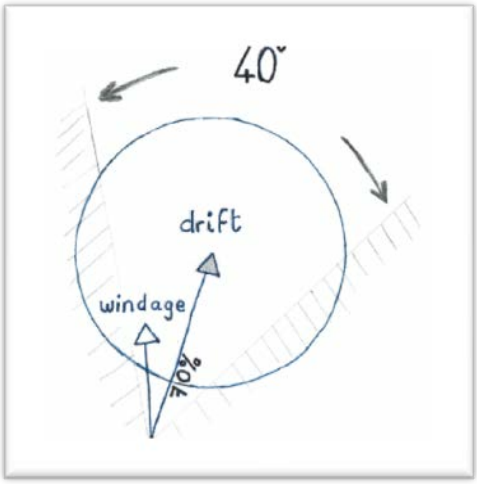

Figure 69 : illustration of QC: Quality test example chosen for windage (eg. 1%) we reject or correct a drift that differs little from the windage (less than 70% of the drift angle <40 °)

Note that a correction of more than 3% is not normally possible (construction of the buoy). This may correspond to breaking waves and swell. Between 2% and 3%, there is ambiguity between Stokes and windage. In other words, it is likely that beyond 2%, we eliminate all or part of the effect of waves and swell. If waves and swell are not aligned with the mean wind (swell remote for example), then the correction will be approximate. Ideally, you should use the Stokes drift from a wave model like Wavewatch3.

When calculating the equivalent models with AOML positions, which were filtered to remove 36h gravity waves and reduce positioning errors, we must :

- **add 0.07% wind averaged over 48h 10m : slippage correction**
- **windage correction and modify the error**

III.2. Algorithm of the Lagrangian verification of the Mercator Océan surface currents forecast.

Algorithm of the Lagrangian verification of the Mercator Océan surface currents forecast. The Mercator Océan surface currents quality control now combines two methods based on Eulerian and Lagrangian approaches using the AOML drifters network.
The Lagrangian approach is slightly different from the Eulerian approach. In the Eulerian approach, the consecutive positions of a drifter are considered as independent buoys recording velocity observations. Then, these observations are compared to the modeled velocity.

We aim here at studying the trajectory of the buoy along with the trajectory of a modeled buoy which would drift from the same starting point. The computation of the trajectory of the modeled drifter is made possible by ARIANE (see ref 1 above)
The algorithm aims at producing the maps on Figure 70. It shows the mean 1-to-5-days distance error –that is the distance between the modeled trajectory and the observed trajectory- in 1°x1° boxes. The mean D-days distance error is computed by averaging the D-days distance errors computed for all the drifters that crossed the box.
The individual points of a trajectory are not independent, merely because the location of a drifter is to a large extent determined by its former location.

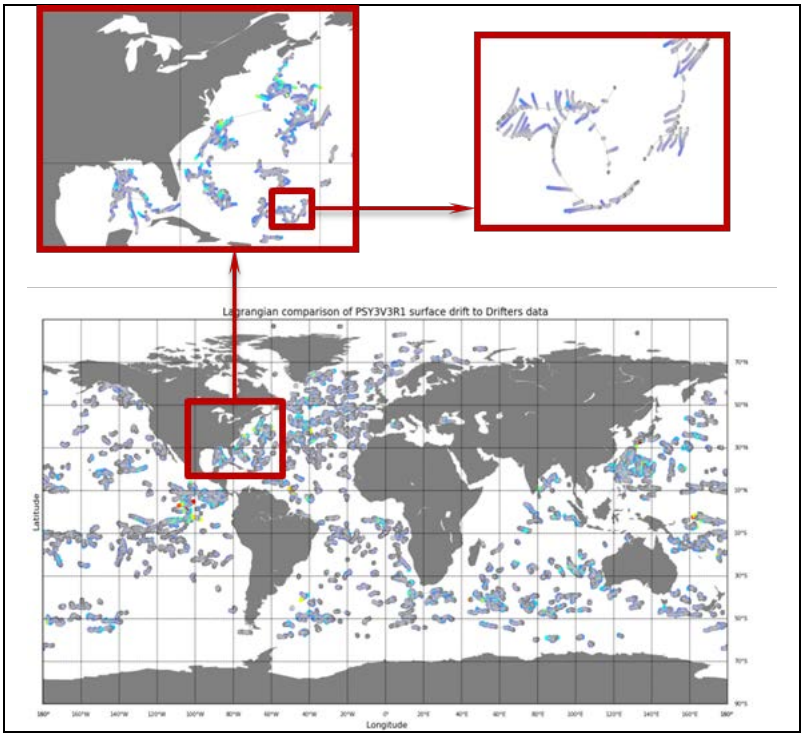

Figure 70: Example of the surface currents Lagrangian quality control algorithm on a global map (bottom panel) and zooms (upper panels).

Let us consider the example above (Figure 71). The thin grey line represents the trajectory of the drifter on a daily frequency. The thick ones represent the system drifting, starting from an observed point. Their colors show the distance to the corresponding point in the observed trajectory after D-days. Considering only this drifter, if we compute the D-days distance error starting from the t=0 observed point (01/02/2013 in the example), we may compute it again only from the observed point t=D days. This way we may reasonably assume the two distance errors are uncorrelated and use most of the data (see ref 2 above).

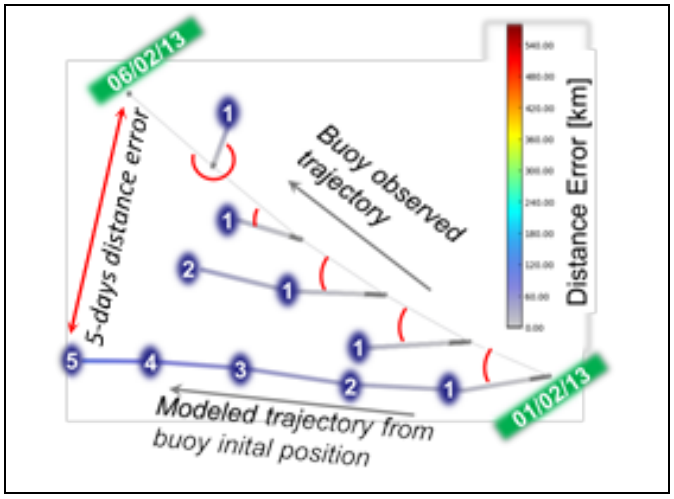

Figure 71: Illustration of the surface currents Lagrangian quality control algorithm.

References:

1- Ariane : utility developed at LPO (http://wwz.ifremer.fr/lpo_eng/Produits/Logiciels/ARIANE)
2- Scott, R. B., N. Ferry, M. Drevillon, C. N. Barron, N. C. Jourdain, J.-M. Lellouche, E. J. Metzger, M.-H. Rio, and O. M. Smedstad, Estimates of surface drifter trajectories in the equatorial Atlantic: A multi-model ensemble approach, Ocean Dynamics, 62, 1091-1109, 2012, doi:10.1007/s10236-012-0548-2.